# AN ABSTRACT OF THE THESIS OF

Emily Von Blon for the degree of Master of Science in Sustainable Forest Management presented on September 20, 2022.

Title: Variation in Productivity, Growing Season Phenology, and Wood Properties of 11 Conifer Species Across a Water Deficit Gradient in Western Oregon.

Abstract approved:

_____

Carlos A. Gonzalez-Benecke and Matthew Powers

Understanding the growth sensitivity of commercially and ecologically valuable species to water balance deficits can help to guide management decisions to enhance stand resistance and resilience to climate change. We utilized a species trial study that was implemented in 1996 on three sites in western Oregon, USA with varying levels of rainfall and evaporative demand in order to compare the growth, phenology, and wood properties of 11 species across a water deficit gradient. The species include *Abies grandis, Pinus ponderosa, Pinus monticola, Pseudotsuga menziesii, Tsuga heterophylla, Thuja plicata, Chamaecyparis lawsoniana,* × *Cupressocyparis leylandii, Picea sitchensis*, a weevil resistant variety of *Picea sitchensis,* and *Sequoiadendron giganteum*. The goal of this study is to contribute to knowledge of projected species distribution shifts under climate change and to inform species selection for reforestation efforts. Specific objectives included: (1) compare the cumulative, annual, and intra-annual growth rates of the 11 species across the water deficit gradient; (2) determine how the timing of radial growth initiation and cessation, as well as the growing season length, differs between species across the gradient; and (3) determine how each species' growth responded to seasonal climate variability across the gradient through the analysis of wood properties. Research methods included measuring tree volume and survival, measuring monthly change in

radial growth, and extracting increment cores to measure tree ring widths, latewood percentage, and wood basic density. Climate data from on-site weather stations and the PRISM Climate Group was used to evaluate climate interactions with measured growth and wood property data. While a few species had a slight decline in productivity under progressively high levels of water deficit and were therefore less sensitive to climate differences, many species had a dramatic decline in productivity under progressively high levels of water deficit, suggesting higher growth sensitivity to water deficit. An exception included *P. Ponderosa*, which had reduced productivity under the lowest level of water deficit.

# Variation in Productivity, Growing Season Phenology, and Wood Properties of 11 Conifer Species Across a Water Deficit Gradient in Western Oregon

by
Emily Von Blon

A THESIS

submitted to

Oregon State University

in partial fulfillment of
the requirements for the
degree of

Master of Science

Presented September 20, 2022
Commencement June 2023

Master of Science thesis of Emily Von Blon presented on September 20, 2022

APPROVED:

Major Professor, representing Sustainable Forest Management

Co-Major Professor, representing Sustainable Forest Management

Head of the Department of Forest Engineering, Resources, and Management

Dean of the Graduate School

I understand that my thesis will become part of the permanent collection of Oregon State University libraries. My signature below authorizes release of my thesis to any reader upon request.

Emily Von Blon, Author

# ACKNOWLEDGEMENTS

I would like to express my gratitude to my advisors, Dr. Carlos Gonzalez-Benecke and Dr. Matthew Powers, for their mentorship and commitment in supporting me in any way they could throughout the process of developing my thesis project. I am grateful to them for providing me with the foundation and opportunities to grow as an aspiring researcher.

I am also appreciative of the Vegetation Management Research Cooperative (VMRC) for their significant contributions and providing me with the resources needed to successfully complete this project. I would like to sincerely thank all those who have helped in the data collection process, and specifically thank Maxwell Wightman for his support with this study and for encouraging me to become involved in other research projects, which helped me develop many new skillsets. I would also like to express my thanks to the VMRC cooperator, Starker Forests, Inc., for allowing me to conduct research on their Species Trial study.

Thank you to the Center for Intensive Planted-forest Silviculture (CIPS) and the Center for Advanced Forestry Systems (CAFS) for their funding and support of this thesis project, as well as for the opportunities I have had to share this research with others. Thank you to Sukhyun Joo for his great help with statistical analyses as well as to Andrew Merschel and Harold Zald for their help with processing my tree ring samples.

Finally, I would like to thank my family for always being there for me, my dear friends, Sara Lirosi and Iván Raigosa Garcia, for inspiring me and believing in me, and my loving partner, Dario Barone, for everything.

# TABLE OF CONTENTS

Page

TABLE OF CONTENTS (Continued)

Page

TABLE OF CONTENTS (Continued)

Page

TABLE OF CONTENTS (Continued)

Page

# LIST OF FIGURES

Figure Page

# LIST OF FIGURES (Continued)

Page

# LIST OF TABLES

Table Page

# LIST OF TABLES (Continued)

Page

# LIST OF TABLES (Continued)

Page

# LIST OF APPENDIX FIGURES

Figure Page

# 1. Literature Review: Evaluating Tree Growth Response to Climate Variability and Drought Conditions

## 1.1. Introduction

The temperate evergreen forests in the Pacific Northwest (PNW) of the United States contain some of the longest living trees and stands with the greatest productivity and biomass accumulation (Baldocchi et al., 2018). However, the expected increase in growing season water deficit as a result of climate change can be detrimental to the growth and survival of tree species in the PNW given that water deficit is the primary limiting growth factor in this region (Peterson et al., 2014). Further, the extent to which trees will be sensitive to the increase in water deficit will vary between species. Being able to predict how ecosystems will respond to these conditions can allow for more informed management decisions that can enhance the health, resistance, and resilience of forests to climate change. However, accurate predictions can only be made by expanding upon our knowledge of species-specific growth-climate relationships. This chapter will explore the impact of climate change on PNW forests, how growth-climate relationships can be determined at the intra- and inter-annual scale from growing season phenology and wood properties, and the characteristics of different commercially and ecologically valuable species in the PNW.

## 1.2 Literature Review

### 1.2.1 U.S. Pacific Northwest Forestry and Climate Change

The private timberlands of western Oregon and Washington are some of the most productive within the United States, contributing to over 14% of private softwood production despite comprising only 3% of the total private timberland landcover (Adams and Latta, 2007).

In comparison to national averages, timberland in this area produces twice the inventory per acre and has two to two and a half times the growth rate. Federal timber harvesting in this region has also dramatically decreased since the 1990s, resulting in the total U.S. timber harvests coming from private timberland increasing from 60% in the 1970s to almost 85% since the early 2000s (Adams and Latta, 2007). Future changes in this area, from climate to disturbances, can have a major impact on commercial forestry in the PNW. Finding means of enhancing forest resistance and resilience while increasing timber production will be essential.

Unprecedented changes in forested ecosystems have been observed as a result of climate change in recent decades, which are expected to continue with the increase of anthropogenic greenhouse gas emissions (Stocker, 2013). Since 1750, atmospheric $CO_2$ levels have risen from 280 to over 390 ppm, with projected increases reaching 450 to 875 ppm by 2100, depending on fossil fuel emissions scenarios (Peterson et al., 2014). During this century, climate change is expected to cause an increase in average temperatures and changes in precipitation regimes, which can impact water availability by altering the timing and amount of precipitation, snowpack dynamics, and evapotranspiration rates (Peterson et al., 2014). As a result of this trend, the PNW of the United States is predicted to have an average warming of 2.1 °C by the 2040s and 3.8 °C by the 2080s (Raymond et al. 2014). Climate models predict a range for the annual change in precipitation of -4.7% to 13.5%, and would involve seasonal changes characterized by less precipitation during the growing season and more during the winter (Case et al., 2021).

With an increase in temperature and reduced summer rainfall, growing season evapotranspiration is expected to increase, as are the frequencies and severities of summer droughts. There is also an expected reduction in snowpack and an earlier onset of snowmelt, which can further affect water availability. Site productivity within the PNW region is influenced

by growing season moisture availability and the monthly temperature range (Weiskittel et al. 2011). This is because soil moisture deficit and a high vapor pressure deficit (VPD) can limit stomatal function and water transport, therefore limiting $CO_2$ fixation (Mathys et al., 2014). High enough water deficits can also result in hydraulic failure, carbon starvation, or increased vulnerability to other biotic and abiotic threats due to drought-induced stress (McDowell et al., 2008). Therefore, the higher evapotranspiration demands due to higher temperatures and the expected increase in water deficit can be detrimental to the growth and survival of tree species in the PNW. In western North America, climate change has been linked to increasingly widespread mortality rates in recent decades (Mildrexler et al., 2016). The abiotic stresses associated with climate change can also result in forests becoming more vulnerable to disturbances, such as insect outbreaks, diseases, and wildfires, as well as alter landscape structure and composition (Chmura et al. 2011).

A consequence of climate change is the increase in prevalence and severity of forest pathogens. Climate can impact the rate of pathogen development, alter host resistance to disease, and change the physiological relationship between hosts and pathogens (Coakley et al., 1999). Further, pathogens have greater ability to adapt to changing climate due to having a faster reproductive rate compared to their hosts. They also have greater ability to migrate to areas more conducive to their survival and reproduction (Peterson et al., 2014). Inter-annual changes in climate can therefore result in favorable conditions for pathogens. Additionally, stress associated with climate change may result in greater tree vulnerability to other insects and diseases (Mildrexler et al., 2016). In the PNW, where Douglas-fir is considered one of the most valuable timber species on a global scale due to its wood quality and high productivity, Swiss needle cast (SNC) has evolved to become a significant threat to its growth (Mildrexler et al., 2019). SNC is a

foliar disease specific to Douglas-fir caused by an endemic ascomycete fungus (*Nothophaeocryptopus gaeumannii*) that can result in chlorosis, a decrease in needle retention, and the reduction of stomatal conductance due to needle stomates occlusion by fruiting bodies of the fungus (psuedothecia), all of which affect overall gas exchange and tree growth (Manter et al., 2000). Along Oregon's coastal range, the projected increase in winter temperatures and spring precipitation is also associated with more severe SNC outbreaks. Considering SNC is most prevalent in coastal, private timberlands, an increase in its severity would be detrimental for commercial forestry operations in this region.

Since the mid-1980's, the western Unites States has had significantly longer wildfire seasons as well as higher recurrences and longer durations of wildfires. Further, these trends are associated with higher growing season temperatures, longer summer droughts, and earlier spring snowmelt due to climate change. While land-use histories such as past fire suppression can influence the impact of wildfire on certain landscapes, inter-annual and decadal climate variation generally play a larger role in wildfire frequency, duration, and severity on a regional scale (Trouet et al. 2006). Further, the interaction between climate change and vegetation can result in changes in fuel production, composition, and continuity. Therefore, climate change mitigation and management tactics should be implemented to address wildfires. The projected increase in the prevalence and severity of wildfires can result in loss of lives and property, detriment to natural resources, and a greater use of resources to combat it, with over 2.5 billion USD already spent annually between 2016-2020 on firefighting support (Congressional Budget Office, 2022).

Climate change also has the potential to influence ecosystem function, composition, and structure, which can impact habitat availability, species distribution, ecosystem services, productivity, and overall forest health (Anderegg et al., 2013). Further, due to changes in

biophysical conditions that can cause a higher frequency and intensity of disturbances, resulting in widespread mortality, ecosystem respiration may potentially exceed ecosystem photosynthesis in the PNW, which would result in the region transitioning from a carbon sink to a carbon source (Baldocchi et al., 2018). The temperate climate of the PNW, characterized by high annual precipitation rates and dry summer growing seasons, result in annual variation in net carbon exchange being heavily influenced by early growing season temperature and late summer water deficits. Therefore, the exacerbation of climate change may result in rates of respiration surpassing those of photosynthesis, which would result in a positive feedback loop that can further extend climate change and increase its effects. Widespread tree mortality as a result of disturbances, such as fire, insects, and disease, as well as physiological stress can also contribute to local extinction of species along the edges of their range (Peterson et al., 2014). While widespread mortality has not necessarily been observed in the PNW, if the frequency and intensity of droughts continue to increase, then widespread regeneration failure, mortality, and disturbances would be expected.

Given that there are many uncertainties associated with climate change, ranging from regional long-term climate projections, ecosystem responses, and interaction between disturbances, adaptive strategies have become the forefront of forest management in the PNW (Agne et al., 2018). These strategies, including referencing the historical conditions of ecosystems, enhancing ecosystem complexity, developing genetic resistance, and using assisted species migration, attempt to improve stand resistance and resilience to climate change and its associated disturbances. These strategies also involve active monitoring and making management changes when needed.

In order to make informed adaptive management decisions, there should be an understanding of projected species sensitivity, and therefore vulnerability, to climate change. It can also help in maximizing productivity of commercially and ecologically valuable species, understanding changes in carbon sequestration over time, and better predict ecosystem responses (Peterson and Case, 2005). Sensitivity can be defined as "the degree to which a system is affected, either positively or negatively and directly or indirectly, by climate-related stimuli" (Solomon et al. 2007). Plants are vulnerable to changes in climate factors, such as inter-annual and intra-annual changes in temperature and precipitation, when they surpass species-specific physiological stress thresholds (Mildrexler et al., 2016). Therefore, climate and vegetation distribution across the landscape are closely connected.

### 1.2.2 Plant Physiology and Seasonal Climate Dynamics

Climate variability, as well as elevated atmospheric $CO_2$ concentrations, can affect plant physiological processes such as reproduction, transpiration, respiration, and photosynthesis (Peterson et al., 2014). These physiological processes can in turn alter plant growth and survival, as well as biotic and abiotic ecosystem interactions. Because climate and atmospheric $CO_2$ levels can influence photosynthesis and respiration, as well as the uptake of water and nutrients, they can ultimately influence biomass production (Peterson et al., 2014). Considering the immobility of plants and the distinct seasonal changes in climate within the temperate PNW region, plants are able to adapt to biotic and abiotic transitions from daily, seasonal, inter-annual, and more extended timeframes. They also have the ability to adapt to slightly more extreme conditions such as brief periods of drought and colder temperatures. However, climate change and elevated $CO_2$ levels can alter resource availability and environmental conditions over the various timeframes, which can impact plant growth.

Photosynthesis allows plants to convert $CO_2$, water, and sunlight into glucose that can be used for plant growth and other functions. Warming temperatures can elevate photosynthesis rates and lengthen the growing season while allowing plants to maintain carbon-use efficiency (Boisvenue and Running, 2006). However, greater photorespiration, evapotranspiration, and surpassing a photosynthetic optimum threshold can reduce those rates. Additionally, water availability has a significant influence on transpiration and photosynthesis by affecting stomatal conductance and hydraulic conductivity. Considering the PNW tends to have lower soil water availability during the growing season, water deficit is the forefront physiological stress factor in the PNW (Peterson et al., 2014). Further, water deficit, followed by low winter temperatures, are the primary limitations of net primary productivity in the PNW (Grier and Running, 1977). With more severe and frequent droughts being expected under climate change in this region, a reduction of productivity may be observed, particularly at middle to lower elevations. The expected increase in temperature can also exacerbate physiological stress associated with drought and reduce the timing of drought-induced mortality (Adams et al., 2009). Drought-induced tree mortality can be caused by a variety of mechanisms, including reduced stomatal conductance that can limit gas exchange and ultimately stunt growth or starve the tree of carbon. It can also be caused by hydraulic failure due to cavitation or by increasing vulnerability to insects, diseases, and wildfires. However, there is variation in species tolerance to drought and heat stress, which would allow some species to have a higher survival and growth rate compared to others. Determining species sensitivity to these conditions can help to predict their growth and survival rates under climate change projections.

Climate factors can also affect plant growth by influencing growing season length and plant phenology, or the timing of plant development. In the temperate woodlands of the PNW,

winter chilling, spring forcing, and photoperiod have the greatest impact on plant phenology due to its influence on processes such as budbreak as well as root and shoot growth (Polgar and Primack, 2011). Phenological events also include flowering, leaf fall, and radial growth initiation.

For conifers in the PNW, temperature, particularly in the spring, is one of the main drivers that signal phenological events to occur. Greater chilling hours typically allows for earlier radial growth initiation, although the amount of forcing needed typically decreases as chilling increases (Harrington et al., 2016). The expected warming as a result of climate change will often result in an earlier start to the growing season due to warmer early spring temperatures, although it also has the potential to delay phenological events for a given species depending on the relationship between chilling and forcing in a given location and species sensitivity to temperature (Harrington et al., 2015). While a certain amount of chilling is not necessary for radial growth initiation to occur in the species involved with this study, the timing of growth initiation is still influenced by chilling and forcing.

Photoperiod also plays a role in determining the timing of growth initiation in temperate forests, where response to photoperiod attempts to time growth initiation to when frost risk is minimal while maximizing the length of the growing season, although these conditions may vary from year to year. Some species may be more sensitive to photoperiod than temperature to avoid growth initiation too early in the season as a result of unusually warm spells and risk subsequent frost events (Polgar and Primack, 2011). However, due to the expectation of warmer temperatures under climate change, the relative sensitivity of a given species to photoperiod versus temperature, as well as its phenotypic plasticity, can determine whether or not species growth will begin earlier to take advantage of favorable growing conditions; species that rely on

photoperiod may not be as responsive to warming cues. While early growing season moisture in temperate regions can contribute to the timing of growth initiation, it is marginal compared to factors such as temperature, forcing and chilling, and photoperiod (Huang et al., 2020). Meanwhile, growth cessation at the end of the growing season in low elevation, temperate regions is typically a function of temperature and frost events given that warmer temperatures and delay of autumn freezes can extend the growing season.

However, there can be differences in the timing and extent of species phenological responses due to differences in climate sensitivity (Harrington and Clair, 2016). Phenology syncing with climate can allow trees to grow during periods of ideal resource availability. The timing of phenological events matching with favorable climate conditions is important given that initiating growth too early or too late in the growing season can result in the risk of frost damage or the underuse of favorable growing conditions that can contribute to productivity. Due to differences in species sensitivity to climate cues, as well as the projected increase in temperatures in the PNW, shifts in phenology and seasonal growth patterns may be observed in response to climate change.

There is also evidence that elevated atmospheric $CO_2$ concentrations can help alleviate the effects of lower water availability and increased temperatures on photosynthesis and carbon uptake. Considering the opening of stomates to acquire $CO_2$ also results in a loss of water through transpiration, greater availability of $CO_2$ can improve the efficiency of the carbon fixation process while reducing stomatal aperture, thereby increasing water use efficiency (Drake et al., 1997). Further, it has been found that stomatal response to higher $CO_2$ concentrations result in a relatively proportional change in leaf-level transpiration under conditions where temperature and humidity remain unchanged (Hsiao and Jackson et al., 1999; Bhattacharya et al.,

1994). In temperate forests, this phenomenon is especially apparent on sites with high nitrogen availability, which is a limiting soil nutrient in the PNW, and in sites with mild to moderate seasonal drought conditions (McCarthy et al., 2010). Further, higher $CO_2$ availability can result in increased rates of photosynthesis and greater carbon allocation to fine root development for enhancing access to soil water and nutrients (Palmroth, 2006). However, these positive changes in photosynthesis, carbon allocation, and stomatal conductance are heavily site dependent, species-specific, and influenced by climate and resource availability.

The extent to which species growth and survival are impacted by climate change depend on species sensitivity to climate variability. The level of sensitivity can also be influenced by species-specific physiological characteristics that have developed through adaptations to climate, geology, and competing vegetation (Mathys et al., 2017). These include phenotypic plasticity, local adaptation, and migration (Peterson et al., 2014).

Phenotypic plasticity is characterized as the alteration of functional traits in response to environmental triggers. These traits include physiological processes, such as growth phenology and respiration rates, reproduction, and plant morphology. Phenotypic plasticity allows plants to respond to and compensate for resource limitations due to biotic and abiotic changes across varying timescales (Peterson et al., 2014). For example, plants can adjust the rate of stomatal conductance in response to varying rates of evaporative demand in order to regulate gas exchange and maintain internal water balance (Hetherington and Woodward, 2003). Evaluating phenotypic plasticity in plants would allow for an understanding of potential vegetation response to climate change. Phenotypic plasticity can also play a role in local adaptation by minimizing selective pressure on genotypes, which would allow for plants to remain genetically diverse for future adaptation needs. It can also allow plants with one genotype to survive in many different

environments (Matesanz and Sultan, 2013). However, limitations such as stress and delayed responses to environmental triggers can restrict the extent that phenotypic plasticity can allow plants to adapt. When this process fails to be sufficient, genetic adaptation and migration processes may be used.

Local genetic adaptation involves natural selection processes to allow genotypes more suited for current conditions to prevail (Peterson et al., 2014). This method tends to be successful when high levels of genetic diversity exist in a population, or when long-distance pollen or seed dispersal is successful in expanding the genetic variability in an area or into new habitats. Local adaptation would allow plants to genetically adapt to a changing climate and its associated stresses within their current range. It would also allow them to successfully migrate to new areas with more favorable conditions. However, limitations include the extent of genetic variability, levels of new seed production, and the range of seed dispersal. While genetic adaptation is seen more readily in annual plants, this process can be successful in trees, depending on the species, because of their high levels of genetic diversity, large seed production over the course of their lifespans, and effective means of seed dispersal. These traits, as well as their enhanced abilities for phenotypic plasticity due to their long lifespans, suggests that genetic adaptation can play a role in species adaptation to climate change. However, some studies suggest that several generations would be required for a tree population to become genetically adapted via evolution to a new climate (Beaulieu and Rainville, 2005).

Species migration allows for plants to “maintain their current bioclimatic niches by tracking changes in climate across landscapes and regions” (Peterson et al., 2014). Biogeographical model projections indicate that most species would have to migrate in response to climate change within the next century to avoid reduced ranges or even extinction. The

"velocity of change" concept refers to the rate of migration in response to changes in bioclimatic conditions, which is used to evaluate the potential for species to successfully migrate into favorable conditions given different climate change scenarios (Peterson et al., 2014). However, not all species may be able to adapt or migrate in time to areas conducive for growth or survival due to the unprecedented rate of climate change. Fragmentation may also impede on the ability for plants to migrate. Therefore, assisted migration tactics may be implemented to help species migrated through human intervention. Assisted migration is a management tactic that can be used in response to climate change that involves relocating species and populations to allow for their natural range to expand (Vitt et al., 2010). Benefits of this process include reducing risk of species extinction, maintaining ecosystem services and biodiversity, and reducing economic losses (Williams and Dumroese, 2013). For example, commercial tree populations and seed sources can be relocated to areas that are projected to have more favorable habitats under climate change, within their range or outside their current range, to prevent economic losses associated with reduced growth. However, the practicality of this management technique is widely contended due to uncertainties associated with climate projections, risk of introducing or exposing species to pathogens, introducing invasive species, and the potential to compromise ecosystem health in terms of function and genetics genetic pollution (Williams and Dumroese, 2013). Therefore, more information is likely needed to properly implement this management tactic.

These physiological characteristics can allow for plants to adapt to changes in environmental conditions, but an understanding of species sensitivity to seasonal and inter-annual climate variability can help to predict how species will respond to climate change. It can

also help in determining where species would grow best given climate change projections for assisted migration and reforestation purposes.

Determining tree sensitivity to climate change can be done by assessing the extent to which climate variation affects tree growth, reproduction, and survival (Peterson et al., 2014). This can involve measuring responses, such as growth and net primary productivity (NPP), of individual trees that are representative of their population across sites in relation to climate and elevated $CO_2$ levels. Further, making measurements and comparisons across environmental gradients can provide a comprehensive view on the range of responses of tree growth to climate (Suarez et al., 2015).

An understanding of the growth-climate relationship, particularly with climate factors that directly affect tree performance, can allow for predictions to be made about the effects of climate change on vegetation (Knutson, 2006). It can inform predictive vegetation mapping for species distribution, bioclimatic models, species selection for reforestation purposes, assisted migration tactics, and estimate carbon storage. It can therefore improve the long-term viability of restoration efforts and improve stand resistance and resilience to climate change and its associated disturbances. Further, the potential to increase timber production and enhance carbon storage using these predictions are especially valuable in the PNW considering the high levels of productivity in this region.

### 1.2.3 Wood Properties

Species growth sensitivity to seasonal and interannual climate variation can be determined by evaluating growth through the analysis of wood properties in relation to known climate data. Tree ring studies can reveal the climate and environmental factors that limit growth

and NPP in forests, with past studies validating ecosystem model projections regarding limitations (Peterson et al., 2014). However, significant variation in response to these factors can exist within species. Accounting for growth response variation between different sites and between individuals of the same species may be necessary to more accurately predict climate change impacts on population growth. Variation between individuals in a particular species, even on the same site, can result from localized differences in environment, the relationship between surrounding vegetation, phenotypic plasticity, and genetics (Ettl and Peterson, 1995). Further, identifying limiting factors may be difficult due to the interaction between multiple climate and environmental factors, seasonality, and past disturbances (Lee et al., 2017). However, including multiple metrics of wood properties, such as tree ring widths, earlywood and latewood widths, wood basic density, maximum latewood density, and stable carbon isotope ratios, can provide more information on interannual climate variation considering different growth-related processes can occur over the course of a growing season (Dannenberg et al., 2014). Dendrochronology can be used to assign tree rings to a particular year, while dendroecology involves using this assigned timing and either reconstructing climate and environmental variation or correlating it to observed variation during that time from a season scale to across the tree's lifespan (Fritts, 1971).

Tree ring width and wood basic density can provide information on the sensitivity of growth to climate variation over time, including changes in annual and seasonal hydroclimate. Tree rings reflect past climate variation given that cambial processes, including the number of cells formed in the tree ring and cell enlargement, are sensitive to climate and other environmental factors (Dannenberg and Wise 2016). In general, a wider tree ring reflects a higher growth rate due to a higher rate of cell production by the cambium. The factors that encourage or limit growth, ranging from soil water availability, temperature, and growing season

length, may vary across species, regions, and ecosystems. In temperate forests, this process typically occurs during a cooler, moister growing season given that high water availability and low evapotranspirative demand are conducive to growth (Littell et al., 2008). However, growth may be benefited by a warmer growing season given that there is sufficient soil water availability (Ettl and Peterson, 1995). In contrast, a narrower tree ring reflects a lower growth rate due to a lower rate of cell production within the cambium, which typically occurs during warmer and drier growing seasons when water balance deficits are high (Dannenberg and Wise 2016). Climate variation across seasons is reflected in the earlywood to latewood ring widths as well as the measurement of inter-annual diameter increment, which can be sensitive to temperature and water deficits during different times of the growing season. Earlywood, comprised of large lumen diameters and thin cell walls, is formed early in the growing season and typically accounts for 40-80% of the ring width. Latewood, comprised of narrow lumen diameters and thick cell walls, is formed later in the growing season when growth slows and finally ceases (Aernouts et al., 2018). Considering that summer rainfall makes up only 10% of the total annual rainfall in the PNW, low soil moisture availability during the growing season is agreed to be the major limiting growth factor; summer soil water deficit typically occurs while high density latewood is being produced (Waring and Franklin, 1979; Brix, 1972). The timing of the earlywood to latewood transition, which is influenced by growing season climate conditions, is important in determining the percentage of latewood to earlywood within tree rings (Filipescu et al., 2014).

The percentage of earlywood to latewood is influenced by water availability during their formation in the early growing season and later in the growing season. Earlywood and latewood tree rings have different densities, with latewood having thicker tracheid cell walls and smaller lumen diameters. Therefore, greater percentages of latewood results in denser and stronger

wood. Hydroclimate can impact growth by influencing the number and size of tracheids produced as well as drive wood basic density by affecting the lumen diameters and the cell wall thickness of tracheids. When wood basic density is high, lumen volume is low and maximum moisture content is restricted (Simpson, 1993). The smaller lumen diameters and thicker cell walls of latewood reduce hydraulic conductance while preventing embolism when there is reduced water availability or when transpiration exceeds the rate of water uptake, resulting in the xylem water potential dropping. Wood basic density for most North American conifers is highly correlated with the percentage of latewood; when water is not limited during the formation of latewood, there is a higher wood basic density due to the extended growing season that formed the latewood. Alternatively, drought stress during the early growing season can decrease the percentage of earlywood to latewood (Domec and Gartner, 2002). Further, maximum latewood density can be used as a proxy for summer temperature, as they are positively correlated (D'Arrigo et al.,1992). Tree ring width and density is therefore related to temperature, soil water availability, and the growing season length (Dannenberg and Wise, 2016). In conifers, using density as a proxy for climate offers lower frequency in variability compared to ring widths, making it easier to relate density to climate factors (Loader et al., 2003). Measuring seasonal ring widths and densities in relation to known climate can determine the extent to which different climate factors limit growth.

Wood density can also be used as an indicator for wood quality through its strong relationship with valued mechanical properties, including wood strength, stiffness, hardness, workability, and decay resistance (Jozsa and Middleton, 1994; Rathgeber et al., 2006). Mechanical properties can determine the suitability of wood for certain products. For example, strong, high-density wood would be ideal for products such as structural timber, laminated

veneer, and plywood while low density wood might be more suitable for paper products and pulp (Filipescu et al., 2014). Given that latewood percentage has been determined to be a good indicator of wood density for conifers, latewood percentage can also be used to predict wood quality (Lachenbruch et al., 2010; Barnett and Jeronimidis, 2003).

### 1.2.4 Tree Species of the PNW

While there are many uncertainties associated with climate change, understanding the growth-climate relationship of ecologically and commercially valuable species in the PNW can help to inform management decisions for reforestation purposes as well as climate change adaptation and mitigation. Examples of these species include coastal Douglas-fir (*Pseudotsuga menziesii* (Mirb.) Franco), Port-Orford-cedar (*Chamaecyparis lawsoniana* (A. Murr.) Parl.), Willamette Valley ponderosa pine (*Pinus ponderosa* var. *willamettensis* (Douglas ex P. Lawson and C. Lawson)), western white pine (*Pinus monticola* (Douglas ex D. Don) Nutt), western red cedar (*Thuja plicata* (Donn ex D. Don)), giant sequoia (*Sequoiadendron giganteum* (Lindl.) Buchholz), Sitka spruce (*Picea sitchensis* (Bongard) Carriere), western hemlock (*Tsuga heterophylla* (Raf.) Sarg), grand fir (*Abies grandis* (Dougl.) Lindl.), and Leyland cypress (× *Cupressocyparis leylandii* (Hartw.) Bartel and (D. Don) Spach).

Coastal Douglas-fir is a long lived, evergreen conifer species found from western to central British Columbia southward to central California (Uchytil, 1991). In Oregon and Washington, it is continuously distributed from the Pacific Ocean to the Cascade Range. Douglas-fir is considered the most dominant tree species in the Pacific Northwest region due to its adaptive nature. It grows best in mild, moist climates with well-aerated soils. Although Douglas-fir can adapt to a variety of soil textures, it tends to thrive in clay loam to silt loam soils

that are deep, moist, and well drained. While this species tends to be shade intolerant, it can be more shade tolerant on drier sites. Douglas-firs are considered one of the most valuable timber species on a global scale due to its wood quality and high productivity (Hermann and Lavender, 1999). It yields the greatest amount of timber compared to any other tree in North America (Fowells, 1965). It is one of the hardest and heaviest softwoods available while being stiff and strong (Wood Database, n.d.). The lumber is often used for construction purposes or processed into veneer and plywood. With proper treatment, they can be used for poles and piling or grown as Christmas trees. The seeds of Douglas-firs are a valuable food source for smaller mammals such as mice, voles, and shrews.

Port-Orford-cedar is a long lived, evergreen conifer species with a small range from the Pacific Ocean to southwestern Oregon and northwestern California. It thrives best along the coast or where conditions are moist. It is most often classified as both an early seral and climax species that can form pure stands, but is most often found in mixed conifer stands. It is shade tolerant and adaptive to many soil types, but does best in mesic sites. It is also sensitive to low temperatures. Historically, Port-Orford-cedar's strong, lightweight, and decay resistant wood was used for a variety of products, including lumber for houses, ship building, and furniture. Since World War II, Port-Orford-cedar has almost exclusively been harvested for exporting to Japan. Its wood is highly valued due to its similarity to hinoki (*Chamaecyparis obtusa*) wood, which is often used in the construction of traditional houses and temples (Uchytil, 1990). It is also valued as an ornamental tree in Europe. While of little wildlife importance, animals such as deer and elk may occasionally browse on its foliage.

Willamette Valley ponderosa pine is a shade intolerant, evergreen conifer. This species can adapt to a variety of sites, but generally thrives in dry environments. It tends to be the

dominant species on xeric sites, resulting in a savanna-like structure, or co-dominate on wetter sites. This species tends to regenerate most successfully after disturbances, particularly fire. Fire exclusion can result in overly dense stands that favor more shade tolerant species. While ponderosa pine is native throughout most of the PNW and California, the variety *willamettensis* is native throughout the Willamette Valley of western Oregon, particularly on sites with deep, well drained soils (Fletcher, 2007). Willamette Valley ponderosa pine tends to be a hardy and well adapted species within the valley. The seeds of ponderosa pine are consumed by a variety of wildlife species. It is also considered a valuable lumber species that is often used to make construction material or processed into veneer and plywood (Wood Database, n.d.).

Western white pine is a long-lived, evergreen conifer tree native to the PNW, but thrives most in northern Idaho and surrounding areas. It is a seral species living in a variety of habitats across its range, but can be dominate in early seral and riparian habitats. It is a shade tolerant, drought intolerant species that thrives best on deep, porous soils. Western white pine has highly valued wood due to it being lightweight, straight grained, and having high dimensional stability, making it ideal of window and door production (Griffith, 1992). Its foliage is browsed by some wildlife species, including black-tailed deer, and its seeds are consumed by red squirrels and deer mice. Due to its susceptibility to white pine blister rust, resistant varieties have been developed.

Western redcedar is a shade tolerant, evergreen conifer species with a range along the western PNW region and a band from central Oregon to southern British Columbia (Tesky, 1992). It tends to be a dominate or co-dominate species on riparian and moist, low elevation sites. It thrives best on acidic, nutrient rich, well drained soils. It can be present in all stages of forest succession. Western red cedar is considered an important commercial species due to its growth on productive sites, which yields high volumes. The wood tends to be soft and low in

strength, but it is also very decay resistant, making it useful for exterior building material. This species is valuable to wildlife such as black-tailed deer and elk for browsing.

Giant sequoia is a very large, evergreen conifer found within a small range in the western Sierra Nevada of California (Habeck, 1992). It tends to grow in scattered groves with other conifers, particularly California white fir (*Abies concolor* var. *lowiana*). It may reproduce through seed or vegetatively through stump sprouts. Giant sequoia is sensitive to low temperatures and thrives best in humid conditions, middle to high elevation sites, and moist, well drained, sandy loam soils. Younger giant sequoia trees have somewhat favorable wood due to its decay resistance, and was used for lumber, veneer, and plywood. Meanwhile, old growth giant sequoia has low quality, brittle wood with low tensile strength (Piirto, 1986). However, commercial harvesting generally lasted from the1850s to the 1950s. Over 30 bird species use giant sequoia or food or shelter, as well as a few mammals such as chickarees (Habeck, 1992).

Sitka spruce is a shade intolerant, long-lived conifer with a narrow range along the Pacific coast from south-central Alaska to northern California (Griffith, 1992). This species is considered the world's largest spruce tree. It is a pioneer species on sandy, undeveloped soils and a climax species in coastal forests. This species is moderately salt tolerant and can survive along the coast and near brackish water. It thrives best in deep, moist, well drained soils as well as in areas with a cool, moist growing season and high annual precipitation rate. Its shallow root system can make the tree susceptible to windthrow. While of low browsing value, this species offers critical habitat to a variety of wildlife species, particularly mammals. Sitka spruce is also considered the most valuable timber species in Alaska (Alaska DCRA, n.d.). Its wood is strong of its weight, easy to work, and has high resonance quality, making it ideal for construction

lumber, high grade pulp, and musical instruments. Because this species is susceptible to Sitka spruce weevil (*Pissodes strobi*), resistant varieties have been developed.

Western hemlock is a large, shade tolerant conifer species found along the coast ranges of northwestern California to southern Alaska, the western slopes of the Cascade Range, and in the northern Rocky Mountains (Tesky, 1992). It is typically a dominate or co-dominate species in moist, low to mid elevation sites. Western hemlock can establish on moist, nutrient poor sites, but thrives on sites with high nutrient availability, particularly nitrogen. It does best in mild, humid climates with adequate moisture during the growing season. This species is valued by browsers, such as Roosevelt elk and black-tailed deer, while its seeds are consumed by deer mice. Western hemlock dominated forests also provide shelter for grizzly bears, the northern spotted owl, and the northern flying squirrel. The pulpwood of western hemlock is considered one of the best for paper and related products (NRCS, 2019). Its wood is also used for construction and in alpha cellulose fibers to be used in various plastics. Western hemlock stands can produce very high yields along the Pacific coast.

Grand fir is a moderately shade tolerant, evergreen conifer species with a range from southern British Columbia to northwestern California and east to the Cascade Range in Oregon. It also occurs from southeastern British Columbia to eastern Oregon, northern Idaho, and western Montana (Howard and Aleksoff, 2000). In the PNW, this species is typically found on productive, mixed conifer stands with moist to dry soils. While this species can survive on a variety of sites, it tends to dominate moderately moist sites with nutrient rich soils. Grand fir provides valuable shelter for arboreal animals such as owls and the marbled murrelet. It is also a commercially valuable timber species due to its wood having minimal shrinkage and a high

stiffness to weight ratio. Its wood is often used for construction lumber and pulp, and the tree is often grown as Christmas trees or ornamentals.

Leyland cypress is a hybrid between the Nootka cypress (*Callitropsis nootkatensis*) and the Monterey cypress (*Hesperocyparis macrocarpa*). It is a fast-growing conifer that is often planted in temperate regions as an ornamental tree or in landscaping as hedges and screening. Leyland cypress is moderately shade intolerant and prefers well drained sites, although it can grow on a variety of soil types. It is also tolerant of salt, frost, and pollution (Danti et al., 2014). However, this species is susceptible to cypress canker (*Seiridium* spp.). Leyland cypress is considered one of the most commercially important trees in Europe due to its ornamental and horticultural value. It was found that over 20% of the urban trees in England are Leyland cypress (Raddi et al., 2014). This species is not typically grown for timber production, but its wood has been used for utility lumber and furniture.

### 1.2.5 Conclusion

Planting the right species, at the right time, and at the right place is essential for successfully reforesting ecosystems, but it has become increasingly challenging due to climate change (USDA Forest Service, n.d). Water deficit levels in the Pacific Northwest (PNW) are expected to become more severe as a result of increasing temperatures and reduced summer water availability. Considering site productivity in the PNW is primarily influenced by temperature and summer water deficit, the projected increase in frequency and intensity of summer drought conditions can be detrimental to the health of forest ecosystems in the PNW (Weiskittel et al. 2011; Bottero et al., 2017). In the PNW, increased water deficits can negatively affect tree recruitment, reduce tree growth, and increase rates of mortality, which can

fundamentally change ecosystem structure, function, composition, and productivity (Bottero et al., 2017). Therefore, one of the primary management challenges moving forward is determining how to continue the provision of ecosystem services despite the exceptional rates of water deficits (Millar et al., 2007). Developing these management strategies and informing forest adaptation methods require an understanding of how forests will respond to the expected levels of water deficit. While many biotic and abiotic factors exist that may influence forest vulnerability to drought and climate variability, a primary factor is species type considering tree physiology and climate sensitivity can differ significantly between species. Therefore, predicting forest response to the changing climate conditions involve studying species-specific growth-climate relationships given that individual tree response to climate influence their function and effects in forest ecosystems (Jin et al., 2021).

## 1.3 Significance and Research Questions

An understanding of these relationships can be used to predict the impact of climate change on forest health and productivity as well as its ability to provide ecosystem services, such as carbon sequestration (Jin et al., 2021; Millar et al., 2007). It can also be used to inform forest growth models, which have the ability to predict forest characteristics by taking into account many biotic and abiotic variables, including climate conditions and species type. This understanding can also help to determine tree species distribution in the PNW under climate change, which is primarily determined by water availability (Mathys et al., 2014). It can additionally aid in increasing timber production by providing insight on which species to plant on a given site, determining how climate will affect carbon sequestration potential for various species, improving the long-term viability of restoration efforts, and minimizing the effect of disturbances associated with climate change on reforested ecosystems. Knowledge of species-

specific growth-climate relationships and tree development at the intra-annual scale can also be used to inform management decisions related to the timing of activities such as planting, fertilizer application, and herbicide application.

There is a critical need for knowledge of species-specific growth-climate relationships, particularly in relation to species sensitivity to the increasing water deficits that are expected in the PNW and are fundamental to influencing forest health and productivity. This knowledge can be used to make more informed predictions on forest response to climate change and therefore more informed management decisions, particularly regarding species selection for reforestation purposes to improve stand resistance and resilience to projected climate changes. Determining species sensitivity can be done by assessing the extent to which climate variation and water deficit affects their growth, which involve measuring growth responses in relation to contrasting climate conditions. Therefore, this study focuses on evaluating the growing season phenological responses, productivity, and tree ring characteristics of many different commercially and ecologically valuable PNW species in relation to seasonal climate variation across a water deficit gradient in western Oregon. The research questions for this study include: 1) How does species-specific climate sensitivity influence growing season radial growth phenology under contrasting levels of water deficit for 11 native and non-native conifer species in western Oregon? 2) How does the productivity of 11 native and non-native conifer species differ under contrasting levels of water deficit in western Oregon? 3) How does species-specific climate sensitivity influence tree ring properties under contrasting levels of water deficit for 11 native and non-native conifer species in western Oregon? 4) How does overall wood density vary under contrasting levels of water deficit between 11 native and non-native conifer species in western Oregon?

## 1.4 References

Adams, D. M., & Latta, G. S. (2007). Timber trends on private lands in Western Oregon and Washington: a new look. *Western Journal of Applied Forestry*, *22*(1), 8-14.

Adams, H. D., Guardiola-Claramonte, M., Barron-Gafford, G. A., Villegas, J. C., Breshears, D. D., Zou, C. B., ... & Huxman, T. E. (2009). Temperature sensitivity of drought-induced tree mortality portends increased regional die-off under global-change-type drought. *Proceedings of the national academy of sciences*, *106*(17), 7063-7066.

Aernouts, J., Gonzalez-Benecke, C. A., & Schimleck, L. R. (2018). Effects of Vegetation Management on Wood Properties and Plant Water Relations of Four Conifer Species in the Pacific Northwest of the USA. *Forests*, *9*(6), 323.

Agne, M. C., Beedlow, P. A., Shaw, D. C., Woodruff, D. R., Lee, E. H., Cline, S. P., & Comeleo, R. L. (2018). Interactions of predominant insects and diseases with climate change in Douglas-fir forests of western Oregon and Washington, USA. *Forest Ecology and Management*, *409*, 317-332.

Alaska's Division of Community and Regional Affairs (DCRA). (n.d.). *Forest products*. Sitka Spruce, DCRA. Retrieved from https://www.commerce.alaska.gov/web/dcra/ForestProducts/CommercialTimberSpecies/SitkaSpruce.aspx.

Anderegg, W. R., Kane, J. M., & Anderegg, L. D. (2013). Consequences of widespread tree mortality triggered by drought and temperature stress. *Nature climate change*, *3*(1), 30-36.

Andreu-Hayles, L. A. I. A., Planells, O., Gutierrez, E., Muntan, E., Helle, G., Anchukaitis, K. J., & Schleser, G. H. (2011). Long tree-ring chronologies reveal 20th century increases in water-use efficiency but no enhancement of tree growth at five Iberian pine forests. *Global Change Biology*, *17*(6), 2095-2112.

Baldocchi, D., Chu, H., & Reichstein, M. (2018). Inter-annual variability of net and gross ecosystem carbon fluxes: A review. *Agricultural and Forest Meteorology*, *249*, 520-533.

Beaulieu, J., & Rainville, A. (2005). Adaptation to climate change: genetic variation is both a short-and a long-term solution. *The Forestry Chronicle*, *81*(5), 704-709.

Bhattacharya, N. C., Radin, J. W., Kimball, B. A., Mauney, J. R., Hendrey, G. R., Nagy, J., ... & Ponce, D. C. (1994). Leaf water relations of cotton in a free-air $CO_2$-enriched environment. *Agricultural and forest meteorology*, *70*(1-4), 171-182.

Boisvenue, C., & Running, S. W. (2006). Impacts of climate change on natural forest productivity–evidence since the middle of the 20th century. *Global Change Biology*, *12*(5), 862-882.

Case, M. J., & Peterson, D. L. (2005). Fine-scale variability in growth climate relationships of Douglas-fir, North Cascade Range, Washington. *Canadian Journal of Forest Research*, *35*(11), 2743-2755.

Case, M. J., Johnson, B. G., Bartowitz, K. J., & Hudiburg, T. W. (2021). Forests of the future: Climate change impacts and implications for carbon storage in the Pacific Northwest, USA. *Forest Ecology and Management*, *482*, 118886.

Chmura, D. J., Anderson, P. D., Howe, G. T., Harrington, C. A., Halofsky, J. E., Peterson, D. L., ... & Clair, J. B. S. (2011). Forest responses to climate change in the northwestern United States: ecophysiological foundations for adaptive management. *Forest Ecology and Management*, *261*(7), 1121-1142.

Coakley, S. M., Scherm, H., & Chakraborty, S. (1999). Climate change and plant disease management. *Annual review of phytopathology*, *37*(1), 399-426.

Congressional Budget Office. (2022, June). *Wildfires*. Retrieved from https://www.cbo.gov/publication/58212#:~:text=Wildfires%20affect%20the%20federal%20budget%20both%20directly%20and%20indirectly.,dollars)%20between%202016%20and%202020.

Creutzburg, M. K., Scheller, R. M., Lucash, M. S., LeDuc, S. D., & Johnson, M. G. (2017). Forest management scenarios in a changing climate: trade-offs between carbon, timber, and old forest. *Ecological Applications*, *27*(2), 503-518.

Dannenberg, M. P., & Wise, E. K. (2016). Seasonal climate signals from multiple tree ring metrics: A case study of *Pinus ponderosa* in the upper Columbia River Basin. *Journal of Geophysical Research: Biogeosciences*, *121*(4), 1178-1189.

Dannenberg, M., Wise, E. K., & Keung, J. H. (2014, December). Seasonal Climate Signals in Multiple Tree-Ring Parameters: A Pilot Study of Pinus ponderosa in the Columbia River Basin. In *AGU Fall Meeting Abstracts* (Vol. 2014, pp. PP43B-1485).

Danti, R., Barberini, S., Pecchioli, A., Di Lonardo, V., & Della Rocca, G. (2014). The epidemic spread of Seiridium cardinale on Leyland cypress severely limits its use in the Mediterranean. *Plant Disease*, *98*(8), 1081-1087.

D'Arrigo, R. D., Jacoby, G. C., & Free, R. M. (1992). Tree-ring width and maximum latewood density at the North American tree line: parameters of climatic change. *Canadian Journal of Forest Research*, *22*(9), 1290-1296.

Domec, J. C., & Gartner, B. L. (2002). How do water transport and water storage differ in coniferous earlywood and latewood?. *Journal of experimental botany*, *53*(379), 2369-2379.

Drake, B. G., Gonzàlez-Meler, M. A., & Long, S. P. (1997). More efficient plants: a consequence of rising atmospheric $CO_2$? *Annual review of plant biology*, *48*(1), 609-639.

Elliott, G. K. (1970). Wood density in conifers. Tech. Comm. No. 8, Commonw. For. Bur.

Ettl, G. J., & Peterson, D. L. (1995). Extreme climate and variation in tree growth: individualistic response in subalpine fir (*Abies lasiocarpa*). *Global Change Biology*, *1*(3), 231-241.

Fahey, R. T., Alveshere, B. C., Burton, J. I., D'Amato, A. W., Dickinson, Y. L., Keeton, W. S., ... & Hardiman, B. S. (2018). Shifting conceptions of complexity in forest management and silviculture. *Forest Ecology and Management*, *421*, 59-71

Filipescu, C. N., Lowell, E. C., Koppenaal, R., & Mitchell, A. K. (2014). Modeling regional and climatic variation of wood density and ring width in intensively managed Douglas-fir. *Canadian journal of forest research*, *44*(3), 220-229.

Fletcher, R. (2007). *Willamette Valley Ponderosa Pine- A Primer*. Corvallis, Oregon; OSU Extension Service.

Fritts, H. C. (1971). Dendroclimatology and dendroecology. *Quaternary Research*, *1*(4), 419-449.

Gavin, D. G., & Hu, F. S. (2006). Spatial variation of climatic and non-climatic controls on species distribution: the range limit of Tsuga heterophylla. *Journal of Biogeography*, *33*(8), 1384-1396.

Grier, C. G., & Running, S. W. (1977). Leaf area of mature northwestern coniferous forests: relation to site water balance. *Ecology*, *58*(4), 893-899.

Griffith, Randy Scott. 1992. Picea sitchensis. In: Fire Effects Information System, [Online]. U.S. Department of Agriculture, Forest Service, Rocky Mountain Research Station, Fire Sciences Laboratory (Producer). Available: https://www.fs.fed.us/database/feis/plants/tree/picsit/all.html

Habeck, R. J. (1992). *Sequoiadendron giganteum*. In: Fire Effects Information System, [Online]. U.S. Department of Agriculture, Forest Service, Rocky Mountain Research Station, Fire Sciences Laboratory (Producer). Available: https://www.fs.fed.us/database/feis/plants/tree/seqgig/all.html

Hetherington, A. M., & Woodward, F. I. (2003). The role of stomata in sensing and driving environmental change. *Nature*, *424*(6951), 901-908.

Howard, Janet L.; Aleksoff, Keith C. 2000. Abies grandis. In: Fire Effects Information System, [Online]. U.S. Department of Agriculture, Forest Service, Rocky Mountain Research Station, Fire Sciences Laboratory (Producer). Available: https://www.fs.fed.us/database/feis/plants/tree/abigra/all.html

Hsiao, T. C., & Jackson, R. B. (1999). Interactive effects of water stress and elevated $CO_2$ on growth, photosynthesis, and water use efficiency. In *Carbon dioxide and environmental stress* (pp. 3-31). Academic Press.

Jin, Y., Li, J., Bai, X., Zhao, Y., Cui, D., & Chen, Z. (2021). High temperatures constrain latewood formation in *Larix gmelinii* xylem in boreal forests. *Global Ecology and Conservation*, *30*, e01767.

Jozsa, L. A., & Middleton, G. R. (1994). A discussion of wood quality attributes and their practical implications.

Knutson, K. C. (2006). Climate-growth relationships of western juniper and ponderosa pine at the pine-woodland ecotone in southern Oregon.

Lee, E. H., Wickham, C., Beedlow, P. A., Waschmann, R. S., & Tingey, D. T. (2017). A likelihood-based time series modeling approach for application in dendrochronology to examine the growth-climate relations and forest disturbance history. *Dendrochronologia*, *45*, 132-144.

Linares, J. C., & Camarero, J. J. (2012). From pattern to process: linking intrinsic water-use efficiency to drought-induced forest decline. *Global Change Biology*, *18*(3), 1000-1015.

Littell, J. S., Peterson, D. L., & Tjoelker, M. (2008). Douglas-fir growth in mountain ecosystems: water limits tree growth from stand to region. *Ecological Monographs, 78*(3), 349-368.

Loader, N. J., Robertson, I., & McCarroll, D. (2003). Comparison of stable carbon isotope ratios in the whole wood, cellulose and lignin of oak tree-rings. *Palaeogeography, Palaeoclimatology, Palaeoecology, 196*(3-4), 395-407.

Manter, D. K., Bond, B. J., Kavanagh, K. L., Rosso, P. H., & Filip, G. M. (2000). Pseudothecia of Swiss needle cast fungus, *Phaeocryptopus gaeumannii*, physically block stomata of Douglas fir, reducing $CO_2$ assimilation. *New Phytologist, 148*(3), 481-491.

Matesanz, S., & Sultan, S. E. (2013). High-performance genotypes in an introduced plant: insights to future invasiveness. *Ecology, 94*(11), 2464-2474.

Mathys, A. S., Coops, N. C., & Waring, R. H. (2017). An ecoregion assessment of projected tree species vulnerabilities in western North America through the 21st century. *Global change biology, 23*(2), 920-932.

Mathys, A., Coops, N. C., & Waring, R. H. (2014). Soil water availability effects on the distribution of 20 tree species in western North America. *Forest Ecology and Management, 313*, 144-152.

McCarroll, D., & Loader, N. J. (2004). Stable isotopes in tree rings. *Quaternary Science Reviews, 23*(7-8), 771-801.

McCarthy, H. R., Oren, R., Johnsen, K. H., Gallet-Budynek, A., Pritchard, S. G., Cook, C. W., & Finzi, A. C. (2010). Re-assessment of plant carbon dynamics at the Duke free-air $CO_2$ enrichment site: interactions of atmospheric [$CO_2$] with nitrogen and water availability over stand development. *New Phytologist, 185*(2), 514-528.

McCarthy, H. R., Oren, R., Johnsen, K. H., Gallet-Budynek, A., Pritchard, S. G., Cook, C. W., ... & Finzi, A. C. (2010). Re-assessment of plant carbon dynamics at the Duke free-air $CO_2$ enrichment site: interactions of atmospheric [$CO_2$] with nitrogen and water availability over stand development. *New Phytologist, 185*(2), 514-528.

McDowell, N., Pockman, W. T., Allen, C. D., Breshears, D. D., Cobb, N., Kolb, T., ... & Yepez, E. A. (2008). Mechanisms of plant survival and mortality during drought: why do some plants survive while others succumb to drought?. *New phytologist, 178*(4), 719-739.

Mildrexler, D. J., Shaw, D. C., & Cohen, W. B. (2019). Short-term climate trends and the Swiss needle cast epidemic in Oregon's public and private coastal forestlands. *Forest Ecology and Management, 432*, 501-513.

Mildrexler, D., Yang, Z., Cohen, W. B., & Bell, D. M. (2016). A forest vulnerability index based on drought and high temperatures. *Remote Sensing of Environment, 173*, 314-325.

Palmroth, S., Oren, R., McCarthy, H. R., Johnsen, K. H., Finzi, A. C., Butnor, J. R., ... & Schlesinger, W. H. (2006). Aboveground sink strength in forests controls the allocation of carbon below ground and its [$CO_2$]-induced enhancement. *Proceedings of the National Academy of Sciences, 103*(51), 19362-19367.

Peterson, D. W., Kerns, B. K., & Dodson, E. K. (2014). Climate change effects on vegetation in the Pacific Northwest: A review and synthesis of the scientific literature and simulation model

projections. *Gen. Tech. Rep. PNWGTR-900. Portland, OR: US Department of Agriculture, Forest Service, Pacific Northwest Research Station. 183 p., 900.*

Polgar, C. A., & Primack, R. B. (2011). Leaf-out phenology of temperate woody plants: from trees to ecosystems. *New phytologist*, *191*(4), 926-941.

Raddi, P., Danti, R., & Della Rocca, G. (2014). x Cupressocyparis leylandii. *Enzyklopädie der Holzgewächse: Handbuch und Atlas der Dendrologie*, 1-17.

Raymond, C. L., Peterson, D. L., & Rochefort, R. M. (2014). Climate change vulnerability and adaptation in the North Cascades region, Washington. *Gen. Tech. Rep. PNW-GTR-892. Portland, OR: US Department of Agriculture, Forest Service, Pacific Northwest Research Station. 279 p., 892*.

Simpson, W. T. (1993). Specific gravity, moisture content, and density relationship for wood. *(General technical report FPL, GTR-76): 13 p.: ill.; 28 cm., 76*.

Solomon, S., Manning, M., Marquis, M., & Qin, D. (2007). Climate change 2007-the physical science basis: Working group I contribution to the fourth assessment report of the IPCC.

Stocker, T. F., Qin, D., Plattner, G. K., Alexander, L. V., Allen, S. K., Bindoff, N. L., ... & Xie, S. P. (2013). Technical summary. In *Climate change 2013: the physical science basis. Contribution of Working Group I to the Fifth Assessment Report of the Intergovernmental Panel on Climate Change* (pp. 33-115). Cambridge University Press.

Suarez, M. L., Villalba, R., Mundo, I. A., & Schroeder, N. (2015). Sensitivity of *Nothofagus dombeyi* tree growth to climate changes along a precipitation gradient in northern Patagonia, Argentina. *Trees*, *29*(4), 1053-1067.

Tesky, Julie L. (1992). Thuja plicata. In: Fire Effects Information System, [Online]. U.S. Department of Agriculture, Forest Service, Rocky Mountain Research Station, Fire Sciences Laboratory (Producer). Available: https://www.fs.fed.us/database/feis/plants/tree/thupli/all.html

Tesky, Julie L. 1992. Tsuga heterophylla. In: Fire Effects Information System, [Online]. U.S. Department of Agriculture, Forest Service, Rocky Mountain Research Station, Fire Sciences Laboratory (Producer). Available: https://www.fs.fed.us/database/feis/plants/tree/tsuhet/all.html

Trouet, V., Taylor, A. H., Carleton, A. M., & Skinner, C. N. (2006). Fire-climate interactions in forests of the American Pacific coast. *Geophysical Research Letters*, *33*(18).

Uchytil, Ronald J. (1990). *Chamaecyparis lawsoniana*. In: Fire Effects Information System, [Online]. U.S. Department of Agriculture, Forest Service, Rocky Mountain Research Station, Fire Sciences Laboratory (Producer). Available: https://www.fs.fed.us/database/feis/plants/tree/chalaw/all.html

USDA Forest Service, Rocky Mountain Research Station. (n.d.). *Return of the king: Western white pine conservation and restoration in a changing climate: Rocky Mountain Research Station*. Retrieved from https://www.fs.usda.gov/rmrs/return-king-western-white-pine-conservation-and-restoration-changing-climate

Vitt, P., Havens, K., Kramer, A. T., Sollenberger, D., & Yates, E. (2010). Assisted migration of plants: changes in latitudes, changes in attitudes. *Biological conservation*, *143*(1), 18-27.

Warren, W. G. (1979). The contribution of earlywood and latewood specific gravities to overall wood specific gravity. *Wood and Fiber Science*, *11*(2), 127-135.

Weiskittel, A. R., Crookston, N. L., & Radtke, P. J. (2011). Linking climate, gross primary productivity, and site index across forests of the western United States. *Canadian Journal of Forest Research*, *41*(8), 1710-1721.

Westerling, A. L., Hidalgo, H. G., Cayan, D. R., & Swetnam, T. W. (2006). Warming and earlier spring increase western US forest wildfire activity. *science*, *313*(5789), 940-943.

Williams, M. I., & Dumroese, R. K. (2013). Preparing for climate change: forestry and assisted migration. *Journal of Forestry*, *111*(4), 287-297.

Xinxiao, Y. U., Weiwei, L. U., Guodong, J. I. A., Hanzhi, L. I., & Ziqiang, L. I. U. (2018). Responses of intrinsic water-use efficiency and tree growth to climate change in semi-arid areas of North China. *Scientific reports*, *8*(1), 1-10.

Zobel, D. B. (1985). *Ecology, pathology, and management of Port-Orford-cedar (Chamaecyparis lawsoniana)* (Vol. 184). US Department of Agriculture, Forest Service, Pacific Northwest Forest and Range Experiment Station.

# 2 Variation in Productivity and Sensitivity of Growing Season Phenology to Climate Variation for 11 Conifer Species Across a Water Deficit Gradient

## 2.1 Introduction

The temperate evergreen forests in the Pacific Northwest (PNW) region of the United States contain highly productive and long living stands (Baldocchi et al., 2018). Given that site productivity within this region is most influenced by growing season moisture availability and the monthly temperature range, the expected increase in water deficit under climate change as a result of increasing temperatures and summer drought is likely to be detrimental to the growth and survival of tree species in the PNW (Weiskittel et al. 2011). Given that the suitability of a given species to their range will likely be altered as a result of climate change, their ability to compete and their susceptibility to forest disturbances and stressors will likely be impacted (Chapin et al., 2010). However, the extent to which species growth and survival are impacted by climate change depends on individual species' sensitivity to climate variability.

Conservationists and forest managers have expressed a need to predict where species are likely to remain in or expand from their current range, and where they will likely be vulnerable to increased climate variability in order to better inform management decisions that can enhance the health, resistance, and resilience of forests to climate change (Coops and Waring, 2011). However, these predictions of how species and forests will respond to climate change across their range require an understanding of species-specific growth-climate relationships (Innes, 1994). However, the current knowledge of these relationships are limited by the lack of empirical studies involving different species and the relationship between growth dynamics and climate variability across different timescales and contrasting abiotic conditions, such as environmental

and climate gradients (Suarez and Kitzberger, 2010). Therefore, studying the growth dynamics of many ecologically and commercially valuable species across a gradient in water deficit and their relationship with climate variability on different timescales, from their cumulative growth and survival over the course of 25 years to their intra-annual radial growth phenology, can contribute to filling this knowledge gap.

## 2.2 Literature Review

### 2.2.1 Growth Dynamics and Water Deficit

As previously mentioned, the most limiting growth factors in the temperate forests of the PNW is growing season moisture availability and the monthly temperature range; an increase in the frequency and intensity of drought can result in a reduction of gross primary productivity and in an increase in total ecosystem respiration (Law et al., 2002; Bréda et al., 2006). Annual wood production, which can be determined through measurements of radial growth, is determined by the rate of cell division and cell enlargement, which are respectively influenced by temperature and water availability (Beedlow et al., 2013; Hsiao and Acevedo, 1974). Water availability can determine nearly 80% of the variability in height and radial growth increments inter-annually in temperate forests, with higher water deficits resulting in a reduction of these growth metrics (Bréda et al., 2006). Therefore, given that climate change is expected to increase temperatures and shift precipitation regimes in the PNW, resulting in higher growing season water deficit, it is likely that tree growth and survival will be negatively impacted. However, the extent to which water deficit affects growth can vary depending on species sensitivity to drought conditions.

Potential evapotranspiration, which is primarily determined by vapor pressure deficit and irradiance, is responsible for the water potential gradient in a plant that allows water to travel

from the soil throughout the plant. High water deficit, as a result of an increase in evaporative demand and a decrease in soil water availability, can cause a decrease in water potential throughout the plant and result in stomatal closure to reduce water loss while leading to a reduction in $CO_2$ assimilation (Bréda et al., 2006). A further increase in water deficit can also cause embolism, resulting in tree mortality. However, drought tolerant species have lower vulnerability to embolism and can continue to have their stomata open at a lower soil water potential compared to less drought tolerant species, resulting in a comparatively smaller reduction in photosynthesis (Niinemets, 2010; Bréda et al., 2006), suggesting that the extent to which water deficit affects growth and survival can differ between species.

While it is well documented that water deficit can significantly impact the growth and survival of tree species in temperate forests, often to varying degrees, the relationship between water deficit and growing season phenology, including the initiation and cessation of radial growth that ultimately determines the length of the growing season, is not as defined in temperate forests. Typically, it has been reported that variables related to temperature were the main determinants of the timing of radial growth (Harrington et al., 2015). However, the longer growing seasons predicted under climate change, involving warmer early spring temperatures and later frosts in the autumn, would only result in increased growth given adequate conditions, including sufficient water availability (Walthall et al., 2013). Further, it has been suggested that a longer growing season, along with higher growing season temperatures, may not increase productivity due to increased water deficit (Barber et al., 2000; Bernal et al., 2011). Therefore, while changes in temperature may provide conditions that can allow for a longer growing season, water deficit instead has the greatest impact on total radial growth, which can vary depending on species sensitivity to drought conditions.

### 2.2.2 Growing Season Phenology

Climate factors can affect tree growth by influencing tree phenology, or the timing of reoccurring biological events. Tree phenology is derived from natural selection and is therefore a result of species' adaptation to their local environment (Chuine, 2010). Tree phenology enhances growth and development activities in relation to the environmental conditions of their range. In the temperate forests and woodlands of the PNW, winter chilling, spring forcing, and photoperiod have the greatest impact on tree phenology due to its influence on processes such as budbreak as well as root and shoot growth (Polgar and Primack, 2011). Phenological events also include flowering, leaf fall, and growing season metrics such as radial growth initiation and cessation. While an increased number of chilling hours typically results in earlier growth initiation in the PNW, there can be differences in the timing and extent of species' phenological responses due to differences in climate sensitivity (Harrington and St. Clair, 2016). For example, different species can require different levels of chilling and forcing during the dormant season to ensure a prompt growth response in the spring.

Phenology syncing with climate patterns can allow trees to grow during periods of ideal resource availability. The ability for tree species to match their phenology to seasonal changes in climate can influence species distribution, species fitness, and ecosystem function (Chuine, 2010; Ford et al., 2016). The timing of phenological events matching with favorable climate conditions is important given that initiating growth too early or too late in the growing season can result in the risk of frost damage or the underuse of favorable growing conditions that can contribute to productivity.

In the PNW, warmer temperatures, reduced frost risk, and the depletion of available soil water are predicted to start occurring earlier in the year (Ford et al., 2016). Due to differences in species sensitivity to climate cues, as well as the projected climate changes in the PNW, shifts in phenology and seasonal growth patterns may be observed in response to climate change. Tree species resilience to projected climate changes will therefore be dependent on species promptly and adequately adjusting their phenology in response to earlier environmental cues. While most research conducted on tree species phenology is focused on tree budburst and flowering, more information on other aspects of tree phenology, such as growing season metrics and their relationship with species and climate conditions, is needed to make more informed predictions of growth under different environmental circumstances, such as climate change (Harrington and St. Clair, 2016).

In the PNW, the phenology of diameter initiation and cessation in response environmental conditions, as well as its implication for tree resiliency under climate change, have been studied for some species. Radial growth initiation and growth rates for a few PNW species, including coastal Douglas-fir (*Pseudotsuga menziesii* (Mirb.) Franco), western redcedar (*Thuja plicata* (Donn ex D. Don), and Sitka spruce (*Picea sitchensis* (Bongard) Carriere), have been found to vary in response to intra-annual differences in temperature and precipitation (Harrington and Clair, 2016). While growth trends were similar between all species, with radial growth initiation occurring in the beginning of spring, rapid growth occurring during the summer, and the slowing of growth occurring in the fall, western redcedar followed an indeterminate growth trend that was more linear than sigmoidal, indicating that western red cedar has a comparatively longer growing season (Harrington and Clair, 2016). Coastal Douglas-fir has also been shown to match favorable climate conditions, including warmer spring temperatures,

and initiate radial growth earlier in the spring at high latitudes and elevations, but failed to take advantage of favorable conditions during the early spring at lower latitudes and elevations due to reduced winter chilling hours (Ford et al., 2016). Another study determined that warmer temperatures at higher latitudes and elevations would delay the cessation of Douglas-fir radial growth and therefore extend the growing season, while warmer temperatures at lower latitudes and elevations would only marginally extend the growing season because growth cessation in these areas is more sensitive to shortened photoperiod rather than temperature (Ford et al., 2017). Therefore, coastal Douglas-fir may not be as resilient to changing climate conditions in the warmer areas of its distribution.

## 2.3 Study Background and Significance

Given the importance of studying the relationship between growth and climate in order to make predictions under climate change, and given that differences exist in species sensitivity to shifting climate cues, this study focuses on evaluating the overall productivity as well as phenological responses of many different commercially and ecologically valuable PNW species to climate variation across a water deficit gradient. There has been increased demand in determining tree growth and development processes under contrasting environmental conditions, such as climate gradients (Suarez and Kitzberger, 2010). Making measurements and comparisons across these gradients can provide a comprehensive view on the range of tree growth responses to climate and therefore contributes to a better understand tree sensitivity to changes in future climate variability (Suarez et al., 2015). Considering site productivity within the PNW region is most influenced by growing season moisture availability and the monthly temperature range, conducting this study across a water deficit gradient can provide valuable information on species growth response to these relevant climate factors (Weiskittel et al., 2011).

This study utilized the Starker Forests, Inc. Species Trial study, which included 11 native and non-native conifer species that were planted in 1996 in three sites spanning a gradient in water deficits across the Oregon Coast Range to the Willamette Valley. The planted species included coastal Douglas-fir, Port-Orford-cedar (*Chamaecyparis lawsoniana* (A. Murr.) Parl.), Willamette Valley ponderosa pine (*Pinus ponderosa* var. *willamettensis* (Douglas ex P. Lawson and C. Lawson)), western white pine (*Pinus monticola* (Douglas ex D. Don) Nutt), western redcedar, giant sequoia (*Sequoiadendron giganteum* (Lindl.) Buchholz), Sitka spruce, a weevil resistant variety of Sitka spruce, western hemlock (*Tsuga heterophylla* (Raf.) Sarg), grand fir (*Abies grandis* (Dougl.) Lindl.), and Leyland cypress (× *Cupressocyparis leylandii* (Hartw.) Bartel and (D. Don) Spach). In 2021, daily climate measurements were recorded for each site and monthly diameter growth measurements were recorded for each species at each site in order to better understand species phenological response to seasonal climate variation. In 2021 and 2022, full inventories were conducted to determine differences in tree size and survival between species and across sites. Therefore, this study considers the relationship between growth and climate conditions for many different species at different timescales, including intra-annual (2021), annual (2021-2022), and cumulative (1996-2021).

Determining the relationship for different species between climate and the timing of important phenological processes, including the initiation and cessation of growth as well as the length of the growing season, can inform predictions on how climate change will affect forest health and productivity. It can also be used to inform management decisions, including the timing of activities such as planting, fertilizer application, and herbicide application in relation to tree development productivity. It can provide information on species-specific range limitations and interactions in mixed species stands (Harrington and Clair, 2016). Further, the growing

season phenology of many of the species included in this study have not been evaluated in the existing literature, so the results will provide novel insights into growth-climate relationships for several species.

Determining the differences in measurements of tree size and survival at 25 years old between species and across sites can also provide insight on long-term species response to contrasting climate conditions, which can further inform our understanding of each species' growth-climate relationships and sensitivity to water deficit. Knowing which species have higher relative growth rates under different levels of water deficit can help to inform management decisions on species selection for reforestation purposes to improve stand resistance and resilience to projected climate changes. This knowledge can also aid in increasing timber production by providing insight on which species to plant on a given site, improving the long-term viability of restoration efforts, and minimizing the effect of disturbances associated with climate change on a reforested ecosystem.

## 2.4 Research Questions, Objectives, and Hypotheses

The broad goals of this study are to contribute to knowledge for predicting tree species resiliency to projected climate changes and to inform species selection for reforestation efforts in the PNW. Therefore, research questions for this study include: 1) How does species-specific climate sensitivity influence growing season phenology under contrasting water deficit conditions for 11 native and non-native conifer species in western Oregon? 2) How does the productivity of 11 native and non-native conifer species differ across a water deficit gradient in western Oregon? Objectives for this study include: 1) measure and compare indicators of productivity, including tree size and survival, for the 11 species and across the water deficit

gradient; 2) determine how timing of radial growth initiation and cessation, as well as the growing season length, differs between species and across sites; 3) identify which climate variables most influence the cumulative basal area increment and radial growth initiation and cessation for each species; and 4) determine the extent to which species sensitivity to different climate variables differ in relation to growing season phenology. Specifically, it is hypothesized that:

Hypothesis 1: The extent to which water deficit limits growth is partially species-dependent, and productivity tends to become more limited as water availability decreases eastward along the water deficit gradient from the Willamette Valley to the Coast Range for conifers that are adapted to areas with high water availability as indicated by their native range, including grand fir, giant sequoia, western hemlock, Port-Orford-cedar, Sitka spruce, and to a less extent, western redcedar and western white pine. Conifers such as Douglas-fir and Leyland cypress that are adapted to a wider range of conditions, as indicated by their native and introduced ranges, tend to be less sensitive to differences in climate conditions and would therefore have decreased productivity eastward across the sites at a lower magnitude compared to the more drought sensitive species as well as higher relative growth in drier sites compared to more drought sensitive species. Conifers such as Willamette Valley ponderosa pine that are more adapted to drier conditions as indicated by their range would have increased productivity moving eastward along the water deficit gradient and would have lower relative growth on sites with higher water availability compared to species adapted to moist conditions.

Hypothesis 2: The length of the growing season, as determined by the initiation and cessation of radial growth, would be relatively consistent across the water deficit gradient for less sensitive conifers, such as Douglas-fir and Leyland cypress, that are adapted to a wide range

of conditions as indicated by their native and introduced ranges. The length of the growing season would progressively decrease eastward along the water deficit gradient for more sensitive conifers that are adapted to areas with high water availability as indicated by their range, such as grand fir, giant sequoia, western hemlock, Port-Orford-cedar, Sitka spruce, and to a lesser extent, western redcedar and western white pine. In contrast, the length of the growing season would decrease westward along the water deficit gradient for conifers that are adapted to drier conditions as indicated by their range, such as ponderosa pine.

## 2.5 Methods

### 2.5.1 Study Design and Starker Forests, Inc Species Trial

#### *2.5.1.1 Water Deficit Gradient*

The study sites were located along a gradient in climate conditions and water deficit ranging from the central Oregon Coast Range to the foothills of the Willamette Valley in western Oregon, USA. The Oregon Coast Range is characterized as having a mild maritime climate with cool, dry summers and mild, wet winters with total annual precipitation ranging from 1,500 mm to 3,000 mm (McGarigal and McComb, 1995). The Oregon Coast Range creates a rain shadow effect that results in warmer conditions with less precipitation, typically ranging from 900 mm to 1600 mm, in the Willamette Valley of Oregon, which is located on the lee side of the Oregon Coast Range. While western Oregon is considered to be a highly productive area, the distinct climate gradient across the Coast Range and Willamette Valley ecoregions can be used to inform the growth-climate relationships for commercially and ecologically valuable species.

#### 2.5.1.2 *Starker Forests, Inc Species Trial and Site History*

In 1996, the Starker Forests, Inc. Species Trial (SFIST) was established to determine how well 12 different native and non-native conifer species would grow across the range of Starker Forests, Inc.'s ownership from the Oregon Coast Range to the Willamette Valley of western Oregon. The purpose of the SFIST was to identify potential alternative timber species considering the expected changes in climate and its associated disturbances may negatively impact the primary crop species, namely Douglas-fir, grown in this region. Douglas-fir plantations across the Coast Range have become increasingly susceptible to Swiss needle cast and summer drought conditions, which can stunt growth and reduce yield (Mildrexler et al., 2019). Therefore, the SFIST was initially established to determine how well other species grow across the range of climate conditions found in this region in order to reduce yield losses associated with species-specific and climate related disturbances. Three sites, named Huffman, Underhill, and Campbell, were chosen to represent the gradient of water deficit across the company's property from the central Coast Range to the borders of the Willamette Valley of western Oregon.

The Huffman site has the highest average annual rainfall of 2,000 mm and lowest average annual potential evapotranspiration of 800 mm between the three sites based on historical PRISM data (PRISM Climate Group, n.d.). It is located close to Eddyville, Oregon, within the central Oregon Coastal Range, specifically at the coordinates 44°37'58.0"N 123°45'17.3"W. The Huffman site is the furthest west of the three sites chosen for this study and is located in the Mid-Coastal Sedimentary ecoregion of the Oregon Coast Range (Thorson et al., 2003). The site has an elevation of 138 m and consists of soils from the Bohannon-Preacher Complex (NRCS, n.d.). The Bohannon and Preacher soil series are characterized as having moderately deep to very deep, well-drained, fine-loamy soils. Areas with this complex contain mesic udic forests that

may receive an average annual rainfall of 2,400 mm and have an average temperature of 9.4°C. The udic moisture regime is characterized as having either a well-distributed rainfall pattern or enough seasonal rainfall to where available water equals or exceeds the amount of evapotranspiration. Considering the observed climate and soil characteristics, the Huffman site represented the wettest site for this study and will hereafter be referred to as the Huffman (wet) site.

The Underhill site has the intermediate average annual precipitation of 1,700 mm and the intermediate average annual potential evapotranspiration of 850 mm based on historical PRISM data. It is located close to Blodgett, Oregon, found in the eastern side of the Oregon Coast Range between the Huffman and Campbell sites, specifically at the coordinates 44°37'00.2"N 123°34'48.6"W. It is located 14.5 kilometers east of the Huffman site and found in the Mid-Coastal Sedimentary ecoregion of the Oregon Coast Range (Thorson et al., 2003). The site has an elevation of 328 m and consists of soils from the Preacher-Bohannon-Slickrock complex and the Apt-McDuff complex (NRCS, n.d.). The former consists of moderately deep to very deep, well-drained, fine-loamy soils while the latter consists of moderately deep to very deep, well-drained, silty-clay-loam soils. Areas with these complexes contain mesic udic forests that may receive an average annual rainfall between 1,900 and 2,400 mm and have an average temperature of 10.5°C. Considering the observed climate and soil characteristics, the Underhill site represented the intermediate site for this study and will be hereafter referred to as the Underhill (intermediate) site.

The Campbell site has the lowest average annual precipitation of 1,300 mm and highest average annual potential evapotranspiration of 940 mm among the three sites based on historical PRISM data. It is located in Corvallis, Oregon in the western Willamette Valley, at 44°35'42.6"N

123°21'07.3"W. It is located 11 miles east of the Underhill site and found in the Valley Foothills ecoregion of the Willamette Valley (Thorson et al., 2003). The site has an elevation of 196 m and consists of soils from the Dixonville-Gellatly complex and the Philomath series (NRCS, n.d.). The Dixonville-Gellatly complex is characterized as having moderately to very deep, well-drained, silty-clay-loam soils. The Philomath series is characterized as having shallow, well-drained, silty-clay soils. Areas with these soils contain mesic habitats that receive an average annual rainfall between 1,140 and 1,270 mm and have an average temperature of 11°C. Considering the observed climate and soil characteristics, the Campbell site will represent the dry site for this study and will be hereafter referred to as the Campbell (dry) site. The locations of these sites are indicated in Figure 2.1.


Figure 2.1: Locations of Huffman (wet), Underhill (intermediate), and Campbell (dry) sites in western Oregon, USA (Google Earth Pro 6.2.1.6014 (beta)).

The species that were initially planted for the SFIST included coastal Douglas-fir (DF), Port-Orford-cedar (POC), Willamette Valley ponderosa pine (WVPP), western white pine (WWP), western redcedar (WRC), giant sequoia (GS), Sitka spruce (SSP), a weevil resistant

variety of Sitka spruce (WRSP), western hemlock (WH), grand fir (GF), Leyland cypress (LC), and Japanese larch (*Larix kaempferi* (Lamb.) Carr.)) (Figure 2.2). However, Japanese larch was excluded from this study due to the nearly 100% mortality observed at all three sites.

Before these sites were established for SFIST, the land was forested and managed for commercial timber production. Prior to the start of the study, each site was cleared of brush and subsoiled using a winged subsoiler to loosen and break up hardpacked soils. At each site, 12 plots that were approximately 52 m x 55 m were established, with each plot containing a single species. Each of the 12 species were randomly assigned to a plot. These plots were either immediately adjacent to each other or were within relatively close range of one other to ensure that overall site characteristics were shared between the stands (Figure 2.2).

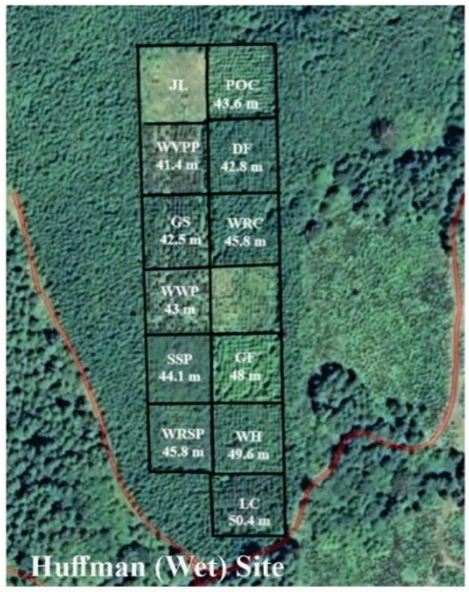


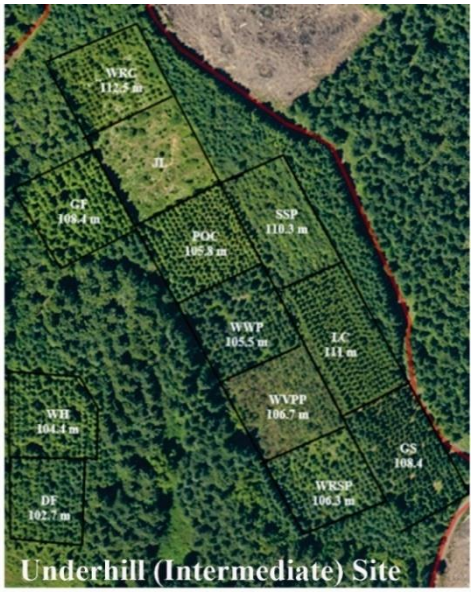


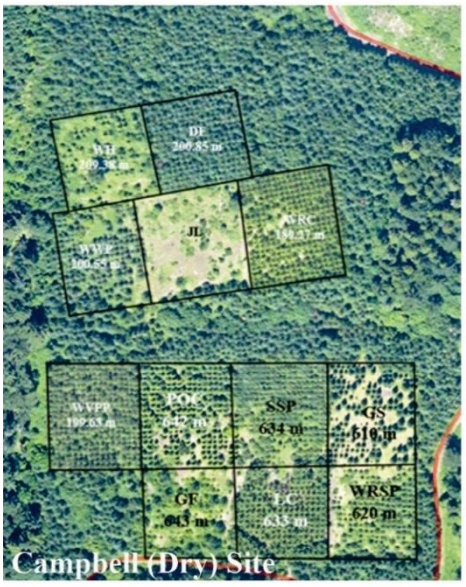


| Species | Abbreviation |
|---|---|
| Douglas-fir | DF |
| Grand Fir | GF |
| Giant Sequoia | GS |
| Japanese larch | JL |
| Leyland cypress | LC |
| Port Orford Cedar | POC |
| Sitka Spruce | SSP |
| Sitka Spruce (Weevil Resistant) | WRSP |
| Western Hemlock | WH |
| Western redcedar | WRC |
| Willamette Valley Ponderosa Pine | WVPP |
| Western White Pine (Blister rust resistant) | WWP |

Figure 2.2: Plot structure of Huffman (wet), Underhill (intermediate), and Campbell (dry) sites with plot center elevation (m) and key showing the list of species and associated abbreviations.

The trees at each site were planted between 1996 and 1998. The planting year depended on seedling availability from local nurseries. The majority of trees were planted between 1996 and 1997, with the exception of WRSP being planted in 1998. Each seedling was grown in a Styro-5 or Styro-6 container and planted with a biodegradable Vexar mesh tube supported by

bamboo stakes surrounding each seedling to protect them from ungulate browsing. Seedlings were planted at a 3 m x 3 m spacing (1,111 trees per ha). Herbicide was regularly applied during the first two years of growth to reduce the presence of competing vegetation. No previous measurements have been recorded for the SFIST since its establishment.

#### 2.5.1.3 *Plot Layout*

After discarding Japanese larch plots, each site contained 11 plots that were included within this study, with each plot containing only one of the 11 species. Most plots were approximately 52 m x 55 m with a tree spacing of 3 m x 3 m and contained about 306 planted trees. In January of 2021, measurement plots within each site were designed and installed. Within the center of each plot, a 30.5 m x 30.5 m measurement plot was established that contained approximately 100 trees consisting of 10 rows of 10 trees. These measurement plots were used to sample trees in this study. Each measurement plot had a surrounding buffer of about 3 to 4 rows to minimize the impact of edge effects in this study. A few stands, specifically SSP, LC, and GS at the Underhill (intermediate) site, had an 18 m x 52 m measurement plot that was established with 6 rows of 17 trees to account for the rectangular size of the plot. These measurement plots had a surrounding buffer of about 3 to 5 rows. To mark the plot boundaries, a 0.7 m PVC pipe was installed at each of the four corners of the plot, with an orange PVC pipe marking the corner adjacent to tree #1. The first and last tree within each row were marked with flagging tape that had the associated row number written on it. Figure 2.3 demonstrates the structure of the plots.

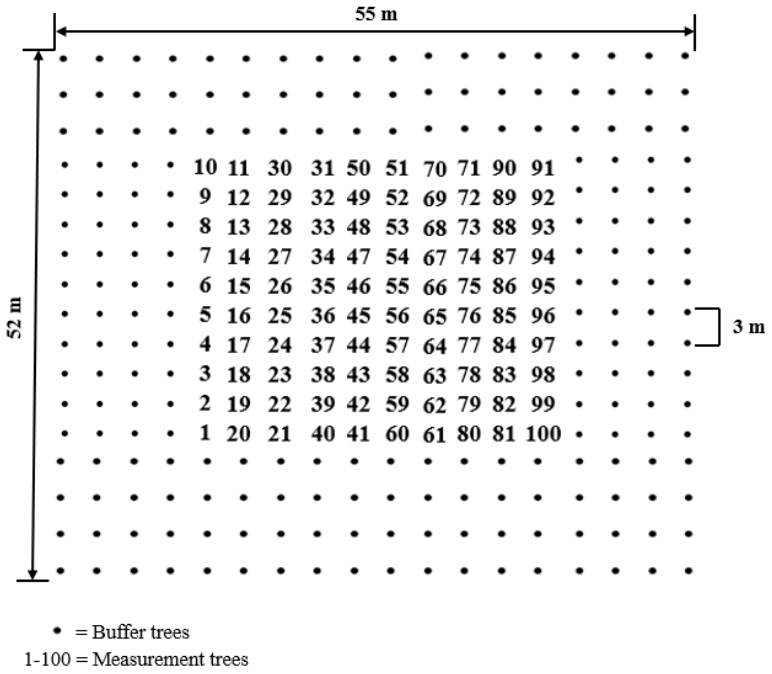


Figure 2.3: Plot layout showing 3-4 rows of buffer trees and 1-100 measurement trees.

### 2.5.2 Climate Measurements

An automatic weather station was installed in a cleared area within 0.3 miles of each site to measure global solar radiation (CS301, Apogee Instruments), air temperature, relative humidity (RH), (HMP60, Vaisala) and rainfall (TE525MM, Texas Electronics). Weather measurements were taken every 30 seconds and averaged every 30 minutes by a datalogger (CR300, Campbell Scientific).

Daily and monthly climate data since 1996 was collected through PRISM, a model based in the PNW that collects climate information from many different sources and uses modeling techniques to determine short and long term climate patterns (PRISM Climate Group, n.d.). PRISM is a useful tool for estimating past daily and monthly averages of climate variables in a

given area, including rainfall, mean, minimum, and maximum temperature, minimum and maximum vapor pressure deficit (VPD), and solar radiation. However, averages provided by PRISM are only an approximation for our study sites and may be overestimating or underestimating actual climate values. Therefore, installing weather stations at each site and collecting site-specific climate information over the course of one year allowed for the calibration of past PRISM data and improved its accuracy for use in analyses. Calibration was conducted through a linear regression using the recorded weather station data and respective PRISM data for the same time period to determine the correlation coefficient and regression equation for each climate variable at each site. At a monthly scale, the $R^2$ was 0.9 or higher for all variables, indicating very high correlation between the weather station and PRISM data. The regression equation for each site-specific climate variable was then applied to all PRISM data for calibration.

The cumulative Growing Degree Days (GDD) were then calculated for every month since 1996 at each site and every day during the 2021 growing season at each site. GDD are a heat unit that can be utilized to predict tree development stages considering the timing of growth is partly a function of the temperature being at a specific threshold conducive to initiating growth (McMaster and Wilhelm, 1997; Miller et al., 2001). GDD takes into account the optimal temperature for photosynthesis. It is calculated by referring to the mean daily temperature and adding the number of degrees above 5°C and below 25°C. If the mean temperature is at or below the 5°C threshold, the GDD for that day would be zero. The GDD for each day in a given month is then summed to determine the monthly GDD.

Monthly potential evapotranspiration (PET) values were calculated for each site using the temperature-based equation derived from Hamon (1963), which was then used to calculate

monthly water deficit and water surplus. This equation accounts for saturated water vapor concentration, mean temperature, and day length to determine PET. The equation is as follows:

$$PET\ (mm) = 1.2 * D * 0.1651 * \left(2 * \frac{L}{86{,}400}\right) * 216.7 * V \quad (1)$$

$$V = \frac{\left(6.108 * e^{\frac{17.26939 * T}{T+237.3}}\right)}{T+237.3}$$

Where:

*D* is the number of days in a given month; *L* is the mean day length (seconds) for a given month; *T* is the mean monthly air temperature (°C); and *V* is the saturated vapor density at the daily mean air temperature *T* (g $m^3$).

PET refers to the maximal atmospheric capacity to remove water, while assuming an unlimited supply of water is available, from plant transpiration processes and water evaporation under specific climate conditions (Rey, 1999). A water surplus occurs when precipitation (P) values are greater than potential evapotranspiration values. A water deficit occurs when precipitation values are less than potential evapotranspiration values.

$$Water\ surplus\ (mm) = P\ (\text{mm}) - PET\ (mm) \quad (2)$$

When P>PET

A water deficit occurs when precipitation values are greater than potential evapotranspiration values. (3)

$$Water\ deficit\ (mm) = PET\ (mm) - P\ (\text{mm})$$

When P<PET

Monthly values of the Palmer Drought Severity Index (PDSI) were calculated for each site using the scPDSI package in R (R Core Team, 2020. v4.0.5; Zhong et al., 2017. v0.1.3). PDSI accounts for water balance supply and demand by using measurements of temperature, precipitation, and available water content in the soil to estimate relative dryness represented by standardized values that can be used to compare moisture conditions across space and time (Dai et al., 2019). PDSI values range from -10 (dry) to 10 (wet).

Relevant 2021 seasonal climate variables for each site were also calculated, including GDD, chilling, forcing, photoperiod, and number of frost days. Chilling days were calculated considering a certain number of chilling days during dormancy is often required for many species to promptly respond to spring warming in the form of initiating budbreak (Schwartz and Hanes, 2010). Chilling days were determined by adding the number of days that had temperatures above 0°C and below 7.2°C from November 1$^{st}$ of 2020 until the beginning of the growing season (Fu et al.; 2015; Huang et al., 2020). Forcing, which is also required for the initiation of spring growth, was determined by adding the number of days above 5°C from January 1$^{st}$, 2021 until the beginning of the growing season (Hänninen et al., 2019). Daily photoperiod can influence the rate of growth as well as the length of the growing season, with longer photoperiods typically encouraging the rate and duration growth (Jackson, 2009), and was calculated as the time between sunrise and sunset. The number of frost days, in which temperatures were below 0°C, since the start of the growing season in May of 2021 until the end of the growing season were also determined given that frost events can influence the length of the growing season (Kramer et al., 2000).

Using recorded and derived climate variables allowed for measurements to be determined at the annual, seasonal, and monthly scale from 1996 to 2021 and at the daily scale in 2021 for rainfall (mm), mean, minimum, and maximum temperature (°C), mean and maximum VPD (kPa), RH (%), PET (mm), PDSI, radiation (MJ $m^2$), GDD, chilling, forcing, photoperiod (minutes), and frost days.

### 2.5.3 2021-2022 Stand Inventory Measurements

#### 2.5.3.1 *2021 Stand Inventory Measurements*

Once the 11 measurement plots were established at each of the three sites, diameter at breast height (1.4 m from the ground; DBH) and height measurements of trees as well as the survival within each measurement plot were recorded. This information was collected in February of 2021 when most trees were 25 years old.

DBH was measured in centimeters to the nearest 0.1 cm using a diameter tape. This measurement was recorded for all trees within each measurement plot. If a tree had multiple stems, the DBH of the two largest and single smallest stems was recorded. The height of every third tree was measured within each measurement plot (approximately 33 trees). A Vertex IV was used to measure tree heights in meters to the nearest 0.1 m. To interpolate the heights of the remaining trees that were not measured, a linear regression model using the reciprocal of DBH measurements and natural log of known height measurements for a given plot was used to predict unknown tree heights. Standing dead trees and noticeable gaps in the 3 m x 3 m tree spacing within the plot that indicated a missing tree were recorded as dead trees, which was used to determine the survival (trees $ha^{-1}$) for each plot.

Recording DBH and height measurements can allow for calculations to be made of more informative response variables related to growth, including stem volume and basal area (BA). Stand tree volume ($m^3$ $ha^{-1}$) is considered an important measure for timber yield considering it takes into account both DBH and height measurements of trees in a stand as well as species-specific tree taper. Region-specific volume equations with species-specific coefficients were used to calculate stem volume over bark (VOB, $m^3$ $ha^{-1}$) for each species at each site. Volume equations and species-specific coefficients from Gonzalez-Benecke et al. (2018), Wensel and Krumland (1983), Zhou and Hemstrom (2010), Zianis et al. (2005), Pillsbury et al. (1998), and Poudel et al. (2019) were used. If several applicable equations were found for a given species, the average of the outputs was calculated. All equations are listed in Appendix (S.2).

#### 2.5.3.1 *2022 Stand Inventory Measurements*

The DBH of all trees within each plot, the heights of every third tree within each plot, and the survival of each plot were measured again in January of 2022 to determine the Current Annual Increment (CAI), or the growth increment in volume ($m^3$ $ha^{-1}$ $year^{-1}$) over a period of one year, in this case from when most trees aged 25-26 years. CAI for each species at each site was measured by subtracting the 2022 average volume by their 2021 average volume. The measurements were also used to calculate the Basal Area Increment (BAI), or the annual growth increment in BA ($m^2$ $ha^{-1}$ $year^{-1}$). BAI for each species at each site was calculated by subtracting the 2022 average BA by their 2021 average BA. The measurements collected in 2022 were also utilized to measure the BA ($m^2$ $ha^{-1}$), VOB ($m^3$ $ha^{-1}$), and survival (trees $ha^{-1}$) of each species plot at each site since 1996-1998 to their current age.

### 2.5.4 Intra-Annual Growth Measurements

Dendrometer bands were installed at breast height on ten trees per plot in March of 2021. The dendrometer bands were made of a durable plastic that was secured around the circumference of the tree with a spring. The spring permitted the band to expand as the tree grew, which allowed for measurements of monthly diameter increment (mm $month^{-1}$) and BAI ($cm^2$ $month^{-1}$) to be recorded over the course of one year. The ten trees were chosen to represent the range of diameter classes within each plot. The diameters of all trees in a given plot were organized from the largest to the smallest measurement and divided into 20th percentile classes ($100^{th}$-$80^{th}$, $80^{th}$-$60^{th}$, $60^{th}$-$40^{th}$, $40^{th}$-$20^{th}$, $20^{th}$-0). Two trees were randomly selected in each class using a random number generator. Monthly diameter increments were marked and measured to the 0.01mm using a digital caliper.

During the first month of measurements in April 2021 after the dendrometer bands were installed, shrinkage was observed across the majority of the banded trees. It is often recommended to allow dendrometer bands one month of settling before measurements should be taken (Just and Frank, 2019). Therefore, we did not include the April 2021 observations in this study and instead considered May 2021 to be the first month of usable measurements and March 2022 to be the last month of measurements.

Measurement dates were transformed to the Julian day of the year structure, which allows for the date to be considered a continuous variable for function fitting. When plotting day of the year (DOY) versus monthly cumulative basal area increment (CBAI) for each banded tree over the course of the 2021 growing season, the growth pattern tended to follow a sigmoidal curve, which contains one inflection point. This shape is a result of slow initial growth during the beginning of the growing season, rapid exponential growth during the peak of the growing season, and subsequently slows and ceases in growth at the end of the growing season.

Therefore, sigmoidal functions can be used to create parametrizations for intra-annual growth measurements that can allow for growth and phenology metrics to be obtained. There are many different modifications of the sigmoid equation that can be used to describe growth trends, including the Logistic, Gompertz, and Chapman-Richards functions that are often used in forestry research (Pödör et al., 2014). In addition to these functions, the use of the Weibull and Hill functions with three parameters were considered for this study.

Shrinkage was observed from some measurements during the summer months of 2021, which is the result of bark shrinkage in response to summer drought. These growth measurements typically recovered on the onset of the rainy season in October. For the purposes of ensuring a proper fit when applying the different functions, data points indicating extreme shrinkage during the summer were removed. Utilizing the SAS Studio 3.8 software (SAS Institute, Cary NC) and SigmaPlot version 14.5 (Systat Software, San Jose, CA), the six sigmoid functions were applied to the monthly cumulative BAI measurements and associated DOY for each banded tree using the NLIN procedure in the SAS Software with inputted parameter estimates derived from the Curve Fit function in SigmaPlot. The NLIN procedure uses the Gauss-Newton, or non-linear least squares method, for curve fitting. The most appropriate function for this dataset was determined by comparing the significance ($P < 0.05$), standard errors, and AIC to determine goodness-of-fit of all coefficients generated from each function. The modified sigmoid function was selected due to it generating the greatest number of significant coefficients with low standard errors and low AIC. The selected three-parameter simple logistic sigmoid function is described below:

$$y = \frac{A}{1 + e^{\left(-\frac{x-x0}{b}\right)}} \tag{4}$$

Where:

*y* is the CBAI; *A* is the maximum growth indicated by the upper asymptote; *x0* is the inflection point of the curve; and *b* represents the distance on the x axis between the inflection point and the point where the response equals: $0.73A = \frac{A}{1+ e^{-1}}$.

These three-parameter functions allow for the calculation of basic and derived curve parameters, which can be used as metrics for radial growth phenology (Pödör et al., 2014). Basic parameters are obtained from the sigmoidal equation directly, which include the upper asymptote, which represents total cumulative growth over the course of the growing season (*A*), and the deviation of the curve from the lower asymptote y = 0 as derived by the inflection point *x0*, representing the start of the growing season (Fig. 2.4). Considering manually marking the dendrometer bands and measuring monthly differences with a digital caliper may not result in as highly precise data as compared to using an automatic dendrometer band, and considering the measurements were collected on a monthly rather than weekly or daily scale because monthly changes could be detected visually, the initiation and cessation of the growing season was approximated and given room for error by determining the DOY in which 10% of the total annual growth had been reached ($G_{10}$) and the DOY in which 90% of the total annual growth had been reached ($G_{90}$). A similar process had been used in other studies that also collected measurements at less frequent intervals and may have moderate to high measurement error (Pödör et al., 2014). Further, the length of the growing season (GSL) can be derived from these calculated parameters, which is the distance, in days, between the initiation and cessation of growth ($GSL = G_{90} - G_{10}$).

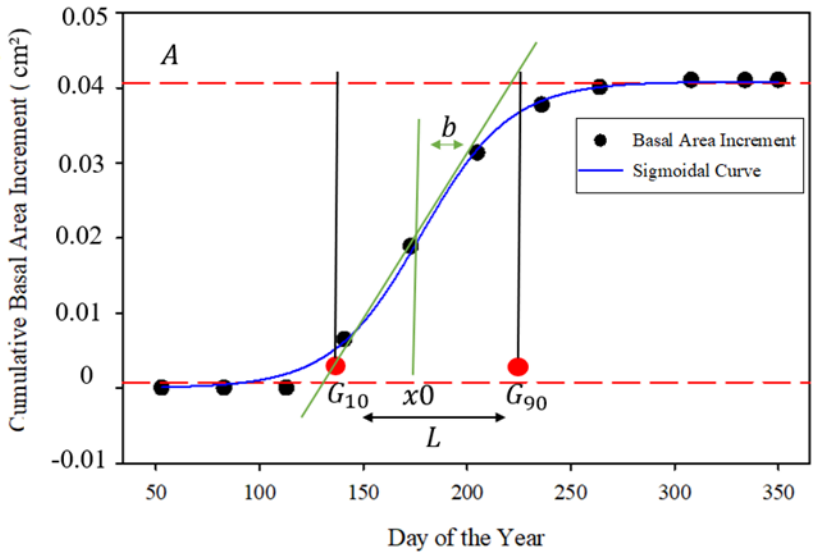


Figure 2.4: Basic and calculated parameters from simple logistic sigmoid function.

### 2.5.5 Statistical Analyses

Given that there was no replication in site and species combinations for the 2021 and 2022 inventory measurements, a formal statistical analysis could not be conducted and causal inferences about the relationship between site and tree growth cannot be made. However, general trends and observations were reported.

A one-way ANOVA and Tukey's multiple comparisons test were utilized to determine if there was a significant difference between relevant climate variables, including monthly rainfall, PET, and VPD between the three sites, and the extent to which they differ. A two-way ANOVA and Tukey's multiple comparisons test were also utilized to determine if there was a significant difference in the mean $G_{10}$, $G_{90}$, GSL, and CBAI for species, sites, and species by site interactions. Tukey's multiple comparisons test was used considering all possible comparisons

between many groups were being compared, the groups had equal sample sizes, and it avoids the risk of an inflated type 1 error while making multiple comparisons.

A general linear regression model was used to determine the relationship between the onset date of radial growth for each species, or $G_{10}$, and variables such as the cumulative number of chilling days, forcing days, and the amount of rainfall until $G_{10}$, the photoperiod of $G_{10}$, the mean annual temperature, sum of annual rainfall, and mean temperature and sum of rainfall for each month in 2021 in the manner outlined in Huang et al. (2020). The model assumptions were checked to ensure that they were met. The assumptions of a linear regression model include: 1) observations are independent at each configuration of explanatory variables; 2) the response variable follows a gaussian distribution; and 3) subpopulations share equal variance.

The independence assumption was met for all models given that species were randomly assigned to plots and the trees from which growing season phenology metrics were acquired from were randomly selected using a stratified random sampling approach. To check the normality assumption, a Normal Q-Q plot of residuals was used. If the data is normally distributed, the sample quantiles compared to the theorical quantiles would be organized in a linear fashion. To check the assumption of constant variance, a standardized residuals vs fitted plot was used. If the plot reveals data points in a dispersed and random pattern, this assumption would be met. Given that all model assumptions were met, linearly dependent variables were removed from the model and the best model was determined based on parameter significance, $R^2$ values, and model AIC values while checking for multicollinearity from the model variance inflation factor (VIF).

As outlined in Jiménez et al. (2019), a Pearson correlation analysis was conducted to determine the relationship between CBAI and 10 climate variables that would reflect water

supply, evaporative demand, and energy, including the sum of rainfall, the mean of daily average, minimum, and maximum temperature, mean VPD, maximum VPD, RH, radiation, and GDD for each interval of CBAI measurements. Linearly dependent climate variables were checked using the VIF removed. All analyses were conducted using R Core Team (2020. v4.0.5.).

## 2.6 Results

### 2.6.1 2021 Weather

The Huffman (wet), Underhill (intermediate), and Campbell (dry) sites are located along a gradient in climate conditions ranging from the central Oregon Coast Range to the foothills of the Willamette Valley in western Oregon. The primary climate variables of interest that differentiate the three sites include variables that impact levels of water deficit, including rainfall, PET, and maximum VPD. In general, water deficit during the year 2021 was more extreme than average conditions since 1996. Averages of selected climate variables of year 2021 across sites are listed in Table 2.1.

| **Average Climate Conditions Across Sites (2021)** | | | |
|---|---|---|---|
| **Climate** | **Huffman (Wet)** | **Underhill (Intermediate)** | **Campbell (Dry)** |
| Rainfall (mm) | 1905 | 1602 | 1293 |
| PET (mm) | 880 | 904 | 967 |
| Maximum VPD (kPa) | 0.83 | 0.95 | 1.16 |
| Maximum Temperature (°C) | 16 | 16 | 17 |
| Average Temperature (°C) | 10 | 11 | 11 |
| Minimum Temperature (°C) | 6 | 6 | 7 |
| Relative Humidity (%) | 86.08 | 82.70 | 77.03 |
| Radiation (MJ $m^2$ $month^{-1}$) | 444 | 446 | 458 |
| GDD (°C) | 2082 | 2175 | 2507.43 |

Table 2.1: Average climate variables from 2021 for the Huffman (wet), Underhill (intermediate), and Campbell (dry) sites, including total yearly rainfall (mm), average annual PET (mm), and PDSI, the maximum VPD (kPa) as an average of daily maximum values, the maximum, average, and minimum temperature (°C) as an average of daily maximum, mean, and minimum values, mean monthly radiation (MJ $m^2$ $month^{-1}$), mean daily relatively humidity (%), and GDD (°C) from the total accumulation of daily mean temperature between 5-25°C for all days of the year.

#### 2.6.1.1 *2021 Water Balance*

2021 rainfall was significantly different across sites (one-way ANOVA, $P < 0.0001$). 2021 rainfall was significantly higher at the Huffman (wet) site and Underhill (intermediate) site than at the Campbell (dry) site. 2021 PET was also significantly different across sites (one-way ANOVA, $P = 0.0279$). 2021 PET was significantly higher at the Huffman (wet) site than at the Campbell (dry) site.

The 2021 water balance at each site was determined from the difference between monthly rainfall and monthly PET (Figure 2.5). At the Campbell (dry) site, the period of water deficit began in early March and lasted until mid-September, which was the longest among the three sites. This site also had the highest water deficit peak in July of 157.2 mm and lowest peak water surplus in December of 301.6 mm among all sites. At both the Underhill (intermediate) and Huffman (wet) sites, the period of water deficit lasted from mid-March until early September. While the period of water deficit was similar in length between the two sites, the peak water deficit in July was similar across the Underhill (intermediate) and Huffman (wet) sites, averaging 136 mm. Further, the Huffman (wet) site had the highest peak water surplus of 411 mm in December while the Underhill (intermediate) site had a peak water surplus in December of 349.8 mm. Compared to annual averages since 1996, the period of water deficit in 2021 began nearly a month earlier for all sites and had a higher peak water deficit in July of 2021 for all sites.

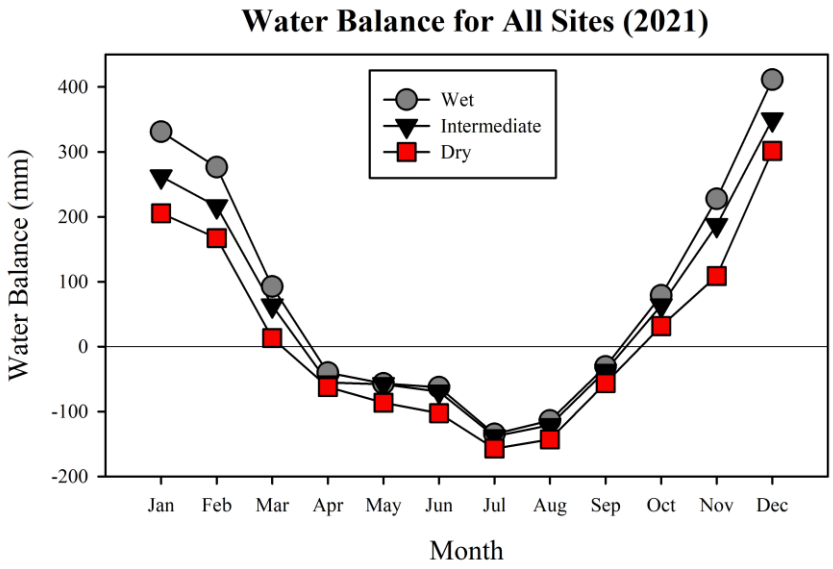


Figure 2.5: Average water balance in 2021 for the Huffman (wet), Underhill (intermediate), and Campbell (dry) sites. Periods of water surplus are indicated by measurements above the line at zero while periods of water deficit are indicated by measurements below the line at zero.

#### 2.6.1.2 *2021 Maximum Vapor Pressure Deficit*

2021 maximum VPD was significantly different across sites (one-way ANOVA, $P$ = 0.0323). 2021 maximum VPD was significantly higher at the Campbell (dry) site than at the Huffman (wet) site. The maximum VPD for the Campbell (dry) site was typically higher throughout the year compared to the other sites and had the highest peak in August of 2.5 kPa. The maximum VPD for the Huffman (wet) site was typically lower throughout the year compared to the other sites, but shared a similar peak with the Underhill (intermediate) site of 1.9 kPa (Figure 2.6).

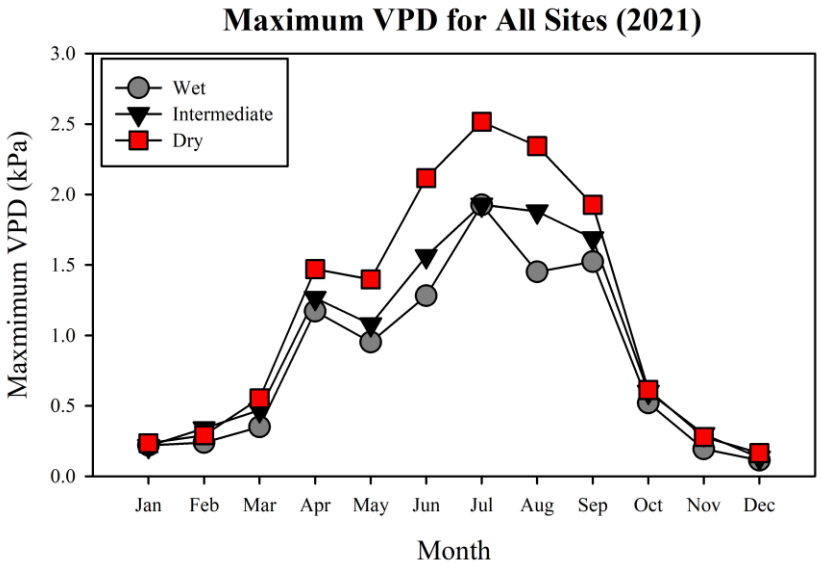


Figure 2.6: Monthly average of maximum VPD (kPa) in 2021 for the Huffman (wet), Underhill (intermediate), and Campbell (dry) sites.

### 2.6.2 2021-2022 Inventory

The 2021 and 2022 inventory across all species and sites allowed for the calculation of metrics associated with growth and survival, including the average DBH (cm), average height (m), BA ($m^2$ $ha^{-1}$), VOB ($m^3$ $ha^{-1}$), and the number of living trees per hectare (TPH, trees $ha^{-1}$) that had accumulated since 1996 (Tables 2.2 and 2.3). When considering all species at each site, the Huffman (wet) site tended to have the range with the largest measurements for average DBH, average height, BA, VOB, and survival, followed by the Underhill (intermediate) site and the Campbell (dry) site. For many species, these metrics dropped dramatically at the Campbell (dry) site. However, not all species had decreased growth and survival progressively from the Huffman (wet) site to the Campbell (dry) site, and the extent to which species growth and survival differ across sites vary.

| 2021 Inventory Across Species and Sites (Age 25 years) | | | | | | |
|---|---|---|---|---|---|---|
| **Site** | **Species** | **DBH (cm) 2021** | **Height (m) 2021** | **BA ($m^2$ $ha^{-1}$) 2021** | **VOB ($m^3$ $ha^{-1}$) 2021** | **TPH (trees $ha^{-1}$) 2021** |
| Dry | DF | 22.7 | 17.0 | 40.1 | 275.0 | 949 |
| Dry | GF | 10.8 | 6.4 | 5.1 | 16.4 | 527 |
| Dry | GS | 20.5 | 8.6 | 23.4 | 71.8 | 613 |
| Dry | LC | 18.6 | 12.7 | 30.1 | 181.8 | 1033 |
| Dry | POC | 17.7 | 8.6 | 7.0 | 32.6 | 266 |
| Dry | SSP | 14.2 | 6.5 | 12.3 | 29.9 | 725 |
| Dry | WH | 16.3 | 8.6 | 7.8 | 27.6 | 355 |
| Dry | WRC | 19.7 | 11.0 | 32.3 | 157.1 | 946 |
| Dry | WRSP | 12.1 | 6.6 | 10.7 | 25.3 | 842 |
| Dry | WVPP | 19.4 | 12.7 | 30.7 | 154.9 | 980 |
| Dry | WWP | 19.4 | 11.5 | 19.3 | 91.7 | 624 |
| Intermediate | DF | 23.8 | 19.8 | 41.6 | 333.6 | 893 |
| Intermediate | GF | 24.2 | 18.0 | 42.2 | 336.5 | 823 |
| Intermediate | GS | 30.2 | 14.9 | 78.1 | 346.2 | 924 |
| Intermediate | LC | 20.5 | 17.4 | 38.2 | 280.2 | 1077 |
| Intermediate | POC | 23.3 | 15.0 | 46.6 | 323.6 | 1044 |
| Intermediate | SSP | 21.1 | 9.8 | 29.4 | 102.1 | 859 |
| Intermediate | WH | 23.8 | 17.1 | 40.8 | 283.7 | 850 |
| Intermediate | WRC | 17.0 | 9.5 | 20.9 | 96.0 | 829 |
| Intermediate | WRSP | 18.7 | 9.8 | 23.6 | 78.9 | 832 |
| Intermediate | WVPP | 20.7 | 13.3 | 35.1 | 183.6 | 990 |
| Intermediate | WWP | 23.0 | 15.4 | 32.9 | 213.9 | 753 |
| Wet | DF | 23.3 | 20.2 | 42.0 | 345.9 | 947 |
| Wet | GF | 26.6 | 21.9 | 57.8 | 490.4 | 980 |
| Wet | GS | 38.2 | 19.5 | 95.1 | 553.3 | 873 |
| Wet | LC | 23.8 | 19.4 | 35.8 | 292.3 | 775 |
| Wet | POC | 23.9 | 13.9 | 49.6 | 321.7 | 1066 |
| Wet | SSP | 23.2 | 12.2 | 48.0 | 211.3 | 1045 |
| Wet | WH | 24.8 | 19.8 | 52.3 | 407.0 | 1012 |
| Wet | WRC | 18.4 | 9.7 | 27.8 | 129.1 | 874 |
| Wet | WRSP | 22.3 | 13.5 | 44.0 | 213.2 | 1024 |
| Wet | WVPP | 21.2 | 13.3 | 20.4 | 109.4 | 584 |
| Wet | WWP | 22.4 | 14.5 | 27.9 | 170.0 | 667 |

Table 2.2: Inventory data recorded during the winter of 2021, when most trees were 25 years old, for each species across the Huffman (wet), Underhill (intermediate), and Campbell (dry) sites, including average DBH (cm) per plot, average height (m) per plot, basal area ($m^2$ $ha^{-1}$), VOB ($m^3$ $ha^{-1}$), and survival (trees $ha^{-1}$) accumulated between 1996 and 2021.

| 2022 Inventory Across Species and Sites (Age 26 years) | | | | | | |
|---|---|---|---|---|---|---|
| **Site** | **Species** | **DBH (cm) 2022** | **Height (m) 2022** | **BA ($m^2$ $ha^{-1}$) 2022** | **VOB ($m^3$ $ha^{-1}$) 2022** | **TPH (trees $ha^{-1}$) 2022** |
| Dry | DF | 23.32 | 17.49 | 42.39 | 298.18 | 949 |
| Dry | GF | 11.33 | 6.67 | 5.62 | 18.62 | 527 |
| Dry | GS | 21.52 | 9.07 | 25.54 | 81.82 | 613 |
| Dry | LC | 19.00 | 13.27 | 31.37 | 195.70 | 1033 |
| Dry | POC | 18.59 | 8.79 | 7.64 | 34.75 | 266 |
| Dry | SSP | 14.68 | 6.90 | 13.25 | 30.72 | 725 |
| Dry | WH | 16.83 | 8.77 | 8.34 | 30.11 | 355 |
| Dry | WRC | 20.53 | 11.51 | 35.03 | 175.28 | 946 |
| Dry | WRSP | 12.79 | 6.81 | 12.07 | 29.16 | 842 |
| Dry | WVPP | 19.87 | 13.25 | 32.13 | 168.33 | 980 |
| Dry | WWP | 20.21 | 11.79 | 21.01 | 100.41 | 624 |
| Intermediate | DF | 24.44 | 20.63 | 43.73 | 363.53 | 893 |
| Intermediate | GF | 24.69 | 18.54 | 44.10 | 358.22 | 823 |
| Intermediate | GS | 30.95 | 15.72 | 81.84 | 384.36 | 924 |
| Intermediate | LC | 20.85 | 17.76 | 39.40 | 293.79 | 1077 |
| Intermediate | POC | 23.88 | 15.56 | 48.98 | 349.28 | 1044 |
| Intermediate | SSP | 21.87 | 10.23 | 31.53 | 105.92 | 859 |
| Intermediate | WH | 24.49 | 17.59 | 43.18 | 308.62 | 850 |
| Intermediate | WRC | 17.95 | 9.92 | 23.53 | 111.44 | 829 |
| Intermediate | WRSP | 19.61 | 10.25 | 25.91 | 90.53 | 832 |
| Intermediate | WVPP | 21.09 | 13.66 | 36.48 | 195.84 | 990 |
| Intermediate | WWP | 23.65 | 15.92 | 34.76 | 231.35 | 753 |
| Wet | DF | 23.57 | 21.39 | 43.15 | 375.79 | 947 |
| Wet | GF | 27.00 | 22.38 | 59.71 | 517.81 | 980 |
| Wet | GS | 38.66 | 21.33 | 97.50 | 617.76 | 873 |
| Wet | LC | 24.30 | 19.99 | 37.00 | 308.56 | 775 |
| Wet | POC | 24.20 | 14.62 | 51.06 | 344.11 | 1066 |
| Wet | SSP | 23.63 | 12.83 | 49.71 | 215.58 | 1045 |
| Wet | WH | 25.36 | 20.19 | 54.72 | 451.42 | 1012 |
| Wet | WRC | 19.06 | 10.35 | 29.92 | 145.71 | 874 |
| Wet | WRSP | 22.82 | 14.38 | 46.17 | 240.59 | 1024 |
| Wet | WVPP | 21.54 | 13.59 | 21.19 | 116.22 | 584 |
| Wet | WWP | 22.90 | 15.39 | 29.26 | 189.29 | 667 |

Table 2.3: Inventory data recorded during the winter of 2022, when most trees were 26 years old, for each species across the Huffman (wet), Underhill (intermediate), and Campbell (dry) sites, including average DBH (cm) per plot, average height (m) per plot, basal area ($m^2$ $ha^{-1}$), VOB ($m^3$ $ha^{-1}$), and survival (trees $ha^{-1}$) accumulated between 1996 and 2022.

#### 2.6.2.1 *Stem Volume per Hectare*

At age 25 years, the Campbell (dry) site had the lowest overall VOB of 96.7 $m^3$ $ha^{-1}$ when averaged across all species. The Underhill (intermediate) site had the second highest overall VOB, which was 59% higher than at the Campbell (dry) site, while the Huffman (wet)

site had the highest overall VOB, which was 21% higher than at the Underhill (intermediate) site. When averaging VOB for each species across the sites, the highest average VOB was associated with GS while the lowest average VOB was associated with WRSP. In general, species such as GF, GS, WH, POC, and SSP had a dramatic decrease in VOB progressively from the Huffman (wet) site to the Campbell (dry) site (Figure 2.7). Species such as DF and LC had a VOB that was relatively consistent across sites, but still showed a slight decrease in VOB progressively from the Huffman (wet) site to the Campbell (dry) site. WRC and WWP were also relatively consistent across sites, but WRC had a decrease in VOB at the Underhill (intermediate) site while WWP had its highest VOB at the Underhill (intermediate) site and the lowest at the Campbell (dry) site. In contrast, WVPP had its lowest VOB at the Huffman (wet) site.

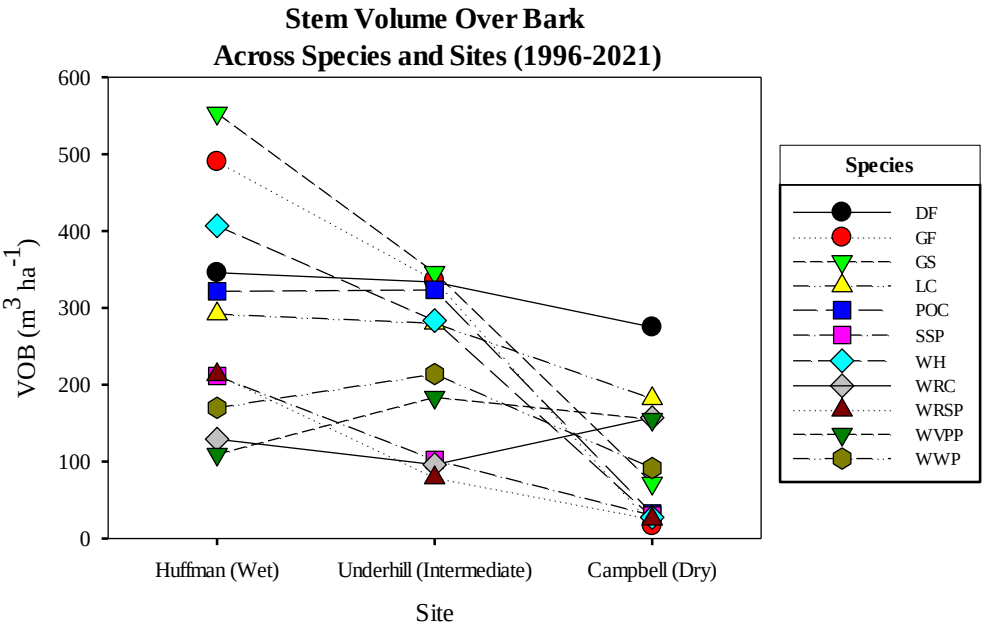


Figure 2.7: VOB ($m^3$ $ha^{-1}$) of each species across the Huffman (wet), Underhill (intermediate), and Campbell (dry) sites, which represents the total accumulation of VOB between 1996 and 2021.

### 2.6.2.2 *Basal Area*

At age 25 years, the Campbell (dry) site had the lowest overall BA of 19.9 $m^2$ $ha^{-1}$ when averaged across all species. The Underhill (intermediate) site had the second highest average BA, which was 39% higher than at the Campbell (dry) site, while The Huffman (wet) site had the highest average BA, which was 14.3% higher than at the Underhill (intermediate) site. Similar to VOB, when averaging BA for each species across the sites, the highest average BA was associated with GS while the lowest average BA was associated with WRSP. BA across species and sites generally followed a similar trend as VOB. However, the extent to which BA differed across species and sites were generally less extreme compared to VOB given that BA does not account for tree height and tapering.

#### 2.6.2.3 *DBH*

At age 25 years, the Campbell (dry) site had the lowest overall DBH of 17.4 cm when averaged across all species. The Underhill (intermediate) site had the second highest overall DBH, which was 22.4% higher than at the Campbell (dry) site, while the Huffman (wet) site had the highest overall DBH, which was 8.1% higher than at the Underhill (intermediate) site. Similar to VOB and BA, when averaging DBH for each species across the sites, the highest average DBH was associated with GS while the lowest average DBH was associated with WRSP. In general, DBH across species and sites followed a similar trend as VOB and BA, but typically had fewer extreme differences, particularly between the Huffman (wet) and Underhill (intermediate) sites.

#### 2.6.2.4 *Height*

At age 25 years, the Campbell (dry) site had the lowest overall height of 10 m when averaged across all species. The Underhill (intermediate) site had the second highest overall

height, which was 31% higher than at the Campbell (dry) site, while the Huffman (wet) site had the highest overall height, which was 10% higher than at the Underhill (intermediate) site. Unlike VOB, BA, and DBH, when averaging heights for each species across the sites, the highest average height was associated with DF while the lowest average height was associated with SSP. In general, average height across species and sites followed a similar trend as VOB, BA, and DBH; heights across most species and sites tended to decrease progressively from the Huffman (wet) site to the Campbell (dry) site or were otherwise consistent in the Huffman (wet) and Underhill (intermediate) site and decreased at the Campbell (dry) site. However, WVPP remained relatively consistent in height across the sites while WRC increased in height progressively from the Huffman (wet) site to the Campbell (dry) site.

#### 2.6.2.5 *Survival*

At age 25 years, the Campbell (dry) site had the lowest overall trees per hectare (TPH) of 715 trees $ha^{-1}$ when averaged across all species. The Underhill (intermediate) and Huffman (wet) site had a very similar TPH of 896 and 898 trees $ha^{-1}$, respectively. When averaging TPH for each species across the sites, the highest average tree survival was associated with LC while the lowest was associated with WWP. In general, species such as DF, WRC, and WWP had relatively consistent TPH across sites. Other species such as GF, GS, POC, SSP, WH, and WRSP generally had lower survival progressively from the Huffman (wet) to the Campbell (dry) site or otherwise had similar TPH between the Huffman (wet) and Underhill (intermediate) site while having much lower TPH on the Campbell (dry) site (Figure 2.8). WVPP and LC, in contrast, had lower TPH on the Huffman (wet) site compared to the other two sites. However, LC at this site had been severely affected by a wind storm prior to the start of this study, which had affected survival.

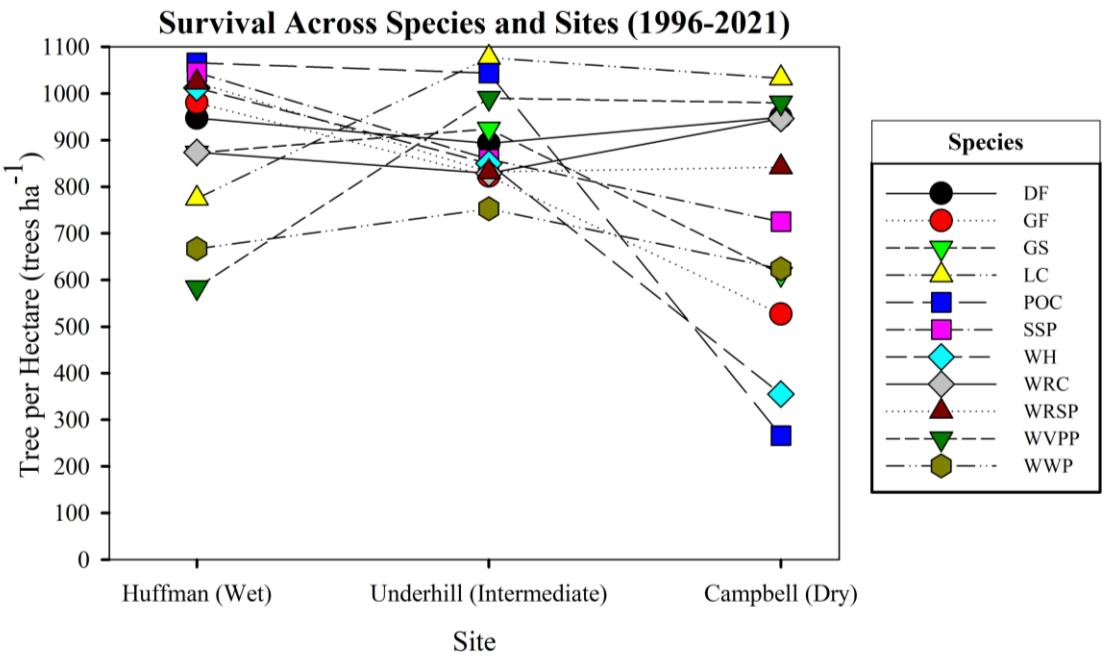


Figure 2.8: Survival (trees $ha^{-1}$) of each species across the Huffman (wet), Underhill (intermediate), and Campbell (dry) sites, which represents the total tree survival between 1996 and 2021.

### 2.6.2.5 *Stem Volume Growth (2021-2022)*

The Campbell (dry) site had the lowest overall CAI of 9 $m^3$ $ha^{-1}$ $year^{-1}$ when averaged across all species. The Underhill (intermediate) site had the second highest overall CAI, which was 117% higher than at the Campbell (dry) site, while the Huffman (wet) site had the highest overall CAI, which was 30% higher than at the Underhill (intermediate) site. When averaging CAI for each species across the sites, the highest average CAI of 37.5 $m^3$ $ha^{-1}$ $year^{-1}$ was associated with GS while the lowest CAI of 3 $m^3$ $ha^{-1}$ $year^{-1}$ was associated with SSP. Further, GS at the Huffman (wet) site and SSP at the Campbell (dry) site had the highest and lowest CAI, respectively, across all species and sites (Table 2.4). In general, species such as GF, GS, SSP, WH, WRSP, and WWP had a dramatic decrease in CAI progressively from the Huffman (wet) site to the Campbell (dry) site. The CAI of species such as DF and POC tended to be consistent

across the two wetter sites, but dropped at the Campbell (dry) site while the CAI of LC tended to be consistent across the two drier sites, but higher at the Huffman (wet) site. In contrast, WRC and WVPP had its highest CAI at the Campbell (dry) site. These trends were fairly consistent with those observed in the 2021 inventory metrics.

| | CAI (2021-2022) | | |
|---|---|---|---|
| **Species** | **Campbell (Dry) Site** | **Underhill (Intermediate) Site** | **Huffman (Wet) Site** |
| DF | 23.2 | 29.9 | 29.9 |
| GF | 2.2 | 21.7 | 27.4 |
| GS | 10 | 38.2 | 64.4 |
| LC | 13.9 | 13.6 | 16.3 |
| POC | 2.2 | 25.7 | 22.4 |
| SSP | 0.8 | 3.8 | 4.3 |
| WH | 2.6 | 24.9 | 44.5 |
| WRC | 18.1 | 15.4 | 16.6 |
| WRSP | 3.9 | 11.7 | 27.4 |
| WVPP | 13.5 | 12.2 | 6.8 |
| WWP | 8.7 | 17.4 | 19.3 |

Table 2.4: CAI ($m^3$ $ha^{-1}$ $year^{-1}$) of each species across the Huffman (wet), Underhill (intermediate), and Campbell (dry) sites, which represents the amount of volume that had accumulated between 2021 and 2022.

### 2.6.3 Intra-Annual Radial Growth Dynamics

#### 2.6.3.1 *Model Fitting*

Growing season metrics for each species across the three sites are reflected in the sigmoidal curves for cummulative individual basal area increment shown in Figure 2.9. Associated parameters for the simple logistic sigmoid equation that were used to develop each curve are shown in Table 2.5. Some species, such as DF, GS, SSP, and WWP, appear to have an equidistant difference in CBAI across the three sites, although the range of difference was higher for GS and lower for WWP. The CBAI for the remaining species appeared to be particularly responsive to one site through a distinctly higher or lower CBAI; GF had a distinctly lower

CBAI at the Campbell (dry) site, LC and POC had a distinctly higher CBAI at the Huffman (wet) site, WH, WRC, and WRSP had a dinstictly higher CBAI at the Underhill (intermediate) site, and WVPP had a distinctly lower CBAI at the Huffman (wet) site.

The CBAI and the growing season length can inform the rate of growth. For most of these species, CBAI at the Campbell (dry) site tended to be lower than the other two sites while having a longer growing season. In contrast, CBAI at the Huffman (wet) site or at the Underhill (intermediate) site tended to be higher while having a shorter growing season; the CBAI at the Campbell (dry) site was attained at a lower rate over a longer period of time compared to the other two sites, where CBAI was attained at a higher rate over a shorter period of time. Major exceptions include DF, WVPP, WRC, and GS. DF had the highest CBAI at the Huffman (wet) site while also having the longest growing season among the three sites. While WVPP appeared to have the longest growing season at the Campbell (dry) site, it also resulted in the highest CBAI compared to the other two sites. While WRC and GS also had a longer growing season at the Campbell (dry) site, its CBAI was was the second highest among the sites.

Further, WVPP and LC had a growing season that was distinctly later in the year, which lasted from July until late November and early December, respectively, compared to the remaining species, which typically had a growing season that lasted from April or May until August, September, or October.

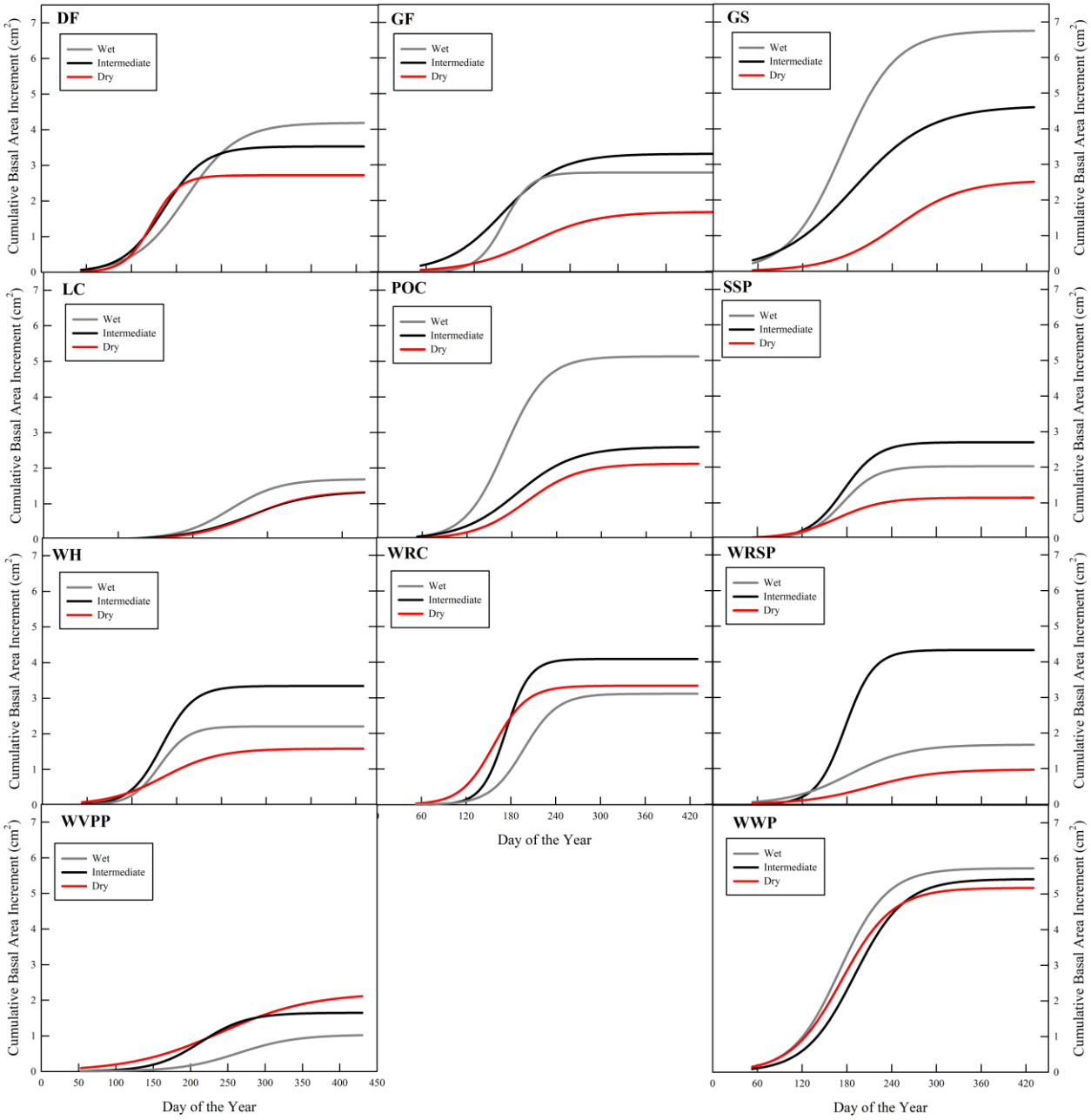


Figure 2.9: 2021 Growing season sigmoidal curve for each species across the Huffman (wet), Underhill (intermediate), and Campbell (dry) sites, which was constructing by applying the simple logistic sigmoid equation to the monthly recorded cumulative basal area increment ($cm^2$).

| Species-Specific Sigmoid Parameters | | Campbell (Dry) Site | | Underhill (Intermediate) Site | | Huffman (Wet) Site | |
|---|---|---|---|---|---|---|---|
| **Species** | **Parameter** | **Parameter estimate** | **SE** | **Parameter estimate** | **SE** | **Parameter estimate** | **SE** |
| DF | a | 2.723 | 0.000106 | 3.532 | 0.000127 | 4.195 | 0.000119 |
| | b | 18.305 | 4.885 | 27.155 | 5.725 | 34.436 | 4.581 |
| | c | 147.258 | 5.502 | 162.852 | 6.776 | 192.933 | 5.447 |
| GF | a | 1.679 | 0.0000453 | 3.310 | 0.000239 | 2.784 | 5.99E-05 |
| | b | 16.97 | 2.135 | 35.40 | 13.016 | 40.05 | 6.036 |
| | c | 157.52 | 2.605 | 156.28 | 15.105 | 192.56 | 7.18 |
| GS | a | 4.646 | 0.000368 | 2.550 | 0.0000667 | 6.754 | 0.000292 |
| | b | 51.01 | 14.569 | 43.95 | 3.729 | 35.73 | 7.414 |
| | c | 188.01 | 17.234 | 246.56 | 4.69 | 173.36 | 8.789 |
| LC | a | 1.348 | 0.0000498 | 1.343 | 0.0000741 | 1.692 | 4.19E-05 |
| | b | 38.12 | 3.605 | 44.04 | 6.584 | 38.95 | 3.634 |
| | c | 258.31 | 4.505 | 275.91 | 9.031 | 278.74 | 4.859 |
| POC | a | 2.124 | 0.0000976 | 2.593 | 0.0000819 | 5.139 | 0.000122 |
| | b | 38.17 | 6.365 | 35.25 | 6.183 | 27.29 | 3.731 |
| | c | 187.25 | 7.571 | 199.68 | 7.325 | 171.06 | 4.437 |
| SSP | a | 1.145 | 0.0000533 | 2.702 | 0.0000373 | 2.028 | 6.37E-05 |
| | b | 31.23 | 7.723 | 23.15 | 2.03 | 22.67 | 4.587 |
| | c | 167.58 | 9.157 | 175.38 | 2.4 | 174.87 | 5.416 |
| WH | a | 1.583 | 0.0000467 | 3.342 | 0.0000822 | 2.209 | 0.0001 |
| | b | 19.19 | 2.961 | 21.32 | 3.599 | 36.86 | 11.345 |
| | c | 157.16 | 3.541 | 160.38 | 4.269 | 162.58 | 13.26 |
| WRC | a | 3.339 | 0.000111 | 4.089 | 0.0000805 | 3.112 | 7.08E-05 |
| | b | 22.28 | 5.002 | 16.01 | 2.661 | 22.66 | 3.155 |
| | c | 156.99 | 5.915 | 173.07 | 2.926 | 197.21 | 3.713 |
| WRSP | a | 0.976 | 0.0000407 | 4.330 | 0.0000271 | 1.674 | 0.000111 |
| | b | 43.56 | 6.855 | 19.21 | 0.866 | 40.12 | 11.536 |
| | c | 210.49 | 8.218 | 177.30 | 1.006 | 183.14 | 13.684 |
| WVPP | a | 2.207 | 0.000196 | 1.649 | 0.000086 | 1.033 | 0.000103 |
| | b | 60.87 | 12.757 | 31.27 | 7.863 | 38.94 | 12.818 |
| | c | 241.00 | 20.621 | 213.50 | 9.147 | 263.83 | 16.388 |
| WWP | a | 5.175 | 0.000196 | 5.421 | 0.000086 | 5.723 | 0.000188 |
| | b | 60.87 | 12.757 | 31.271 | 7.863 | 34.222 | 6.155 |
| | c | 240.997 | 20.621 | 213.503 | 9.147 | 173.09 | 7.308 |

Table 2.5: 2021 Growing season sigmoidal curve parameter estimates and standard errors (SE) for each species across the Huffman (wet), Underhill (intermediate), and Campbell (dry) sites, which are applicable to the simple logistic sigmoidal equation. All parameters were significant ($P < 0.05$).

### 2.6.5 Seasonal Radial Growth Metrics and Climate

P-values associated with differences in GSL, $G_{10}$, and $G_{90}$ for species and sites, as well as whether there was a species by site interaction, are presented in Table 2.6.

| Source | GSL | G10 | G90 | CBAI |
|---|---|---|---|---|
| **Species** | <0.0001 | <0.0001 | <0.0001 | 0.00728 |
| **Site** | 0.4236 | 0.3489 | 0.149964 | <0.0001 |
| **Species by site** | 0.0917 | 0.0387 | 0.000102 | 0.00103 |

Table 2.6: P-values associated with the growing season length (GSL), the growing season starting date ($G_{10}$), the growing season cessation date ($G_{90}$), and the cumulative basal area increment (CBAI) for species, sites, and species by site interaction (two-way ANOVA). Significant P-values, where $P < 0.05$, are indicated with an asterisk (*).

#### 2.6.5.1 *Growing Season Length*

GSL, in days, was not different between the three sites (two-way ANOVA, $P = 0.4236$). The longest growing season was generally associated with the Campbell (dry) site while the shortest was generally associated with the Huffman (wet) site. The species and site interaction was also non-significant ($P = 0.0917$).

However, GSL was significantly different between species (two-way ANOVA, $P < 0.0001$). There was a significant difference in GSL for between GS (GSL = 152 days) and four other species, with GSL for GS averaging 58 to 64 days longer than SSP, WH, WRC, and WRSP. All other comparisons in GSL between species were non-significant (Table 2.7; Figure 2.10).

| Growing Season Length (GSL, days) Across Species and Sites | | | | Growing Season Length Across Species | | |
|---|---|---|---|---|---|---|
| **Species** | **Site** | **GSL (days)** | **SE** | **GSL (days)** | **SE** | |
| DF | Wet | 158 | 15.1 | 120 | 12.9 | ab |
| | Intermediate | 131 | 16.1 | | | |
| | Dry | 79 | 14.2 | | | |
| GF | Wet | 68 | 23.3 | 96 | 13.8 | ab |
| | Intermediate | 151 | 32.9 | | | |
| | Dry | 151 | 32.9 | | | |
| GS | Wet | 141 | 23.5 | 152 | 11.5 | a |
| | Intermediate | 143 | 23.5 | | | |
| | Dry | 172 | 23.5 | | | |
| LC | Wet | 162 | 18.6 | 131 | 13.8 | ab |
| | Intermediate | 124 | 19.9 | | | |
| | Dry | 97 | 21.5 | | | |
| POC | Wet | 149 | 21.2 | 145 | 13.5 | ab |
| | Intermediate | 148 | 18.4 | | | |
| | Dry | 138 | 18.4 | | | |
| SSP | Wet | 82 | 35.1 | 91 | 14.1 | b |
| | Intermediate | 105 | 24.8 | | | |
| | Dry | 81 | 24.8 | | | |
| WH | Wet | 75 | 23.3 | 89 | 13.2 | b |
| | Intermediate | 87 | 26 | | | |
| | Dry | 117 | 32.9 | | | |
| WRC | Wet | 97 | 15.4 | 93 | 12.4 | b |
| | Intermediate | 81 | 15.4 | | | |
| | Dry | 99 | 13.8 | | | |
| WRSP | Wet | 69 | 22.7 | 94 | 12.4 | b |
| | Intermediate | 84 | 17.6 | | | |
| | Dry | 119 | 17.6 | | | |
| WVPP | Wet | 94 | 33.7 | 139 | 14.5 | ab |
| | Intermediate | 130 | 36.4 | | | |
| | Dry | 184 | 33.7 | | | |
| WWP | Wet | 134 | 13.2 | 138 | 13.5 | ab |
| | Intermediate | 136 | 16.1 | | | |
| | Dry | 145 | 14.9 | | | |

Table 2.7: The estimated marginal mean and standard error (SE) of 2021 growing season length (GSL) in days for each individual species and for species across the Huffman (wet), Underhill (intermediate), and Campbell (dry) sites. Significance letters were included to represent significance differences in GSL for individual species.

### 2.6.5.2 *Growing Season Starting Date*

The species by site interaction was significant for $G_{10}$ ($P = 0.0387$). WVPP and LC had a significantly later $G_{10}$ in the Underhill (intermediate) site than many other species and site combinations. WVPP also had a significantly later $G_{10}$ in the Huffman (wet) site while this was

the case for LC at the Campbell (dry) site. In contrast, WVPP at the Campbell (dry) site and LC at the Huffman (wet) site tended to have a similar $G_{10}$ compared to the majority of species and site combinations.

WVPP and, to a lesser extent, LC, had a $G_{10}$ that was significantly later in the year compared to many other species and site combinations, particularly combinations involving the Huffman (wet) and Campbell (dry) sites. Further, many of these combinations overlapped between the two species, which typically involved species such as WRC, GS, WWP, and GF. WVPP at the Underhill (intermediate) site ($G_{10}$ = 227) had a significantly later $G_{10}$ compared to nine other species and site combinations by 97 to 118 days, with combinations evenly distributed across the three sites, while WVPP at the Huffman (wet) site ($G_{10}$ = 203) had a significantly later $G_{10}$ than two species and site combinations by 94 to 100 days, which were exclusive to the Campbell (dry) site. LC at the Underhill (intermediate) site ( $G_{10}$ = 203) had a significantly later $G_{10}$ compared to four species and site combinations by 94 to 99 days, particularly at the Campbell (dry) site, while LC at the Campbell (dry) site ($G_{10}$ = 191) had a significantly later $G_{10}$ compared to four other species and site combinations by 92 to 111 days, which were evenly distributed between the Huffman (wet) and Campbell (dry) sites. All other significant differences in $G_{10}$ between species by site interactions are demonstrated in Table 2.8.

| $G_{10}$ Across Species and Sites | | | | | $G_{10}$ Across Species | |
|---|---|---|---|---|---|---|
| **Species** | **Site** | **$G_{10}$ (DOY)** | **SE** | **Significance** | **$G_{10}$ (DOY)** | **SE** |
| DF | Wet | 136 | 13.5 | abcdef | 129 | 9.78 |
| | Intermediate | 132 | 14.4 | abcdef | | |
| | Dry | 122 | 12.7 | bcdef | | |
| GF | Wet | 155 | 20.6 | bcdef | 130 | 10.46 |
| | Intermediate | 120 | 20.6 | bcdef | | |
| | Dry | 122 | 16 | abcdef | | |
| GS | Wet | 116 | 10.6 | cdef | 136 | 8.75 |
| | Intermediate | 182 | 10.6 | abcdef | | |
| | Dry | 109 | 10.6 | ef | | |
| LC | Wet | 215 | 20.3 | abcde | 201 | 10.46 |
| | Intermediate | 203 | 18.8 | abc | | |
| | Dry | 191 | 17.6 | ab | | |
| POC | Wet | 129 | 24.4 | abcdef | 141 | 10.22 |
| | Intermediate | 158 | 21.1 | abcdef | | |
| | Dry | 134 | 21.1 | abcdef | | |
| SSP | Wet | 146 | 29.4 | abcdef | 147 | 10.72 |
| | Intermediate | 127 | 20.8 | bcdef | | |
| | Dry | 168 | 20.8 | abcdef | | |
| WH | Wet | 137 | 16.4 | bcdef | 137 | 9.99 |
| | Intermediate | 147 | 13 | abcdef | | |
| | Dry | 129 | 11.6 | abcdef | | |
| WRC | Wet | 153 | 6.27 | abcdef | 133 | 9.4 |
| | Intermediate | 143 | 6.27 | abcdef | | |
| | Dry | 108 | 5.6 | ef | | |
| WRSP | Wet | 144 | 14.6 | abcdef | 150 | 9.4 |
| | Intermediate | 137 | 11.3 | abcdef | | |
| | Dry | 168 | 11.3 | abcdef | | |
| WVPP | Wet | 203 | 37.5 | abcd | 200 | 10.99 |
| | Intermediate | 227 | 37.5 | a | | |
| | Dry | 173 | 34.7 | abcdef | | |
| WWP | Wet | 107 | 5.45 | f | 110 | 10.22 |
| | Intermediate | 123 | 5.88 | bcdef | | |
| | Dry | 103 | 4.8 | def | | |

Table 2.8: The estimated marginal mean and standard error (SE) of the 2021 growing season start date in which 10% of growth was attained ($G_{10}$) for each individual species and for species across the Huffman (wet), Underhill (intermediate), and Campbell (dry) sites. Significance letters were included to represent significance differences in $G_{10}$ for species by site interactions.

### 2.6.5.3 *Growing Season Starting Date and Climate*

Forcing was significant in determining $G_{10}$ for all species, while other elements of temperature, such as chilling and early growing season mean temperature, were significant for the majority of species. In contrast, only a few species had a $G_{10}$ that was significantly influenced

by variables associated with rainfall and photoperiod. Further, $G_{10}$ for DF, GF, and GS was exclusively driven by forcing (Table 2.9).

| Growing Season Starting Date | | | | | | |
|---|---|---|---|---|---|---|
| **Species** | **Parameter** | **Parameter Estimate** | **SE** | **Adj. R2** | **RMSE** | **CV** |
| DF | Forcing | 1.008519 | 0.01618 | 0.8922 | 1.786215 | 0.014679 |
| GF | Forcing | 1.00435 | 0.005296 | 0.9704 | 1.052218 | 0.008121 |
| GS | Forcing | 0.98475 | 0.05903 | 0.9173 | 7.652872 | 0.063408 |
| LC | Forcing | 1.075989 | 0.025683 | 0.9453 | 1.761653 | 0.009165 |
| | April Rainfall | -1.33366 | 0.18599 | | | |
| POC | Cumulative Rainfall | -3.98E-03 | 6.87E-04 | 0.9624 | 0.377902 | 0.002833 |
| | Forcing | 9.78E-01 | 4.55E-02 | | | |
| SSP | Forcing | 1.004493 | 0.001584 | 0.9747 | 0.288205 | 0.001958 |
| | April Rainfall | -1.0177 | 0.012542 | | | |
| WH | Chilling | 0.76624 | 0.17784 | 0.9556 | 6.198275 | 0.046588 |
| | Forcing | 1.05015 | 0.04935 | | | |
| WRC | Forcing | 0.991643 | 0.002419 | 0.9308 | 0.285161 | 0.002152 |
| WRSP | Forcing | 0.98157 | 0.02452 | 0.9869 | 4.005326 | 0.026641 |
| | April Rainfall | -1.19187 | 0.12823 | | | |
| WVPP | Chilling | 1.018601 | 0.01954 | 0.9948 | 0.349807 | 0.001954 |
| | Forcing | 1.004482 | 0.001504 | | | |
| | Photoperiod | 0.272407 | 0.10818 | | | |
| WWP | Cumulative Rainfall | -0.004083 | 0.001028 | 0.9984 | 0.580804 | 0.005298 |
| | Chilling | 0.975477 | 0.026191 | | | |
| | Forcing | 1.008519 | 0.01024 | | | |

Table 2.9: Climate variable parameters associated with the growing season starting date across species and sites, including parameter estimates, standard error (SE), adjusted $R^2$ (Adj. $R^2$), residual mean square error (RMSE), and the coefficient of variation (CV; %). All parameters listed were significant ($P < 0.05$). Variables include forcing, or the accumulation of days since January in which temperatures were above 5°C, chilling, or the accumulation of days since the previous November in which temperatures were between 0-5°C, photoperiod (hours), April rainfall (mm), April mean temperature (Tmean; °C), annual rainfall (mm), and cumulative rainfall from January to $G_{10}$.

### 2.6.5.4 *Growing Season Cessation Date*

The species by site interaction was significant for $G_{90}$ ( $P = 0.000102$). WVPP, LC, and GS had a significantly later $G_{90}$ in the Underhill (intermediate) site than many other species and site combinations. LC also had a significantly later $G_{90}$ in the Huffman (wet) site while this was the case for WVPP at the Campbell (dry) site. In contrast, WVPP at the Huffman (wet) site, LC

at the Campbell (dry) site, and GS at the Huffman (wet) and Campbell (dry) site tended to have a similar $G_{90}$ compared to the majority of species and site combinations.

WVPP and, to a lesser extent, LC and GS, had a $G_{90}$ that was significantly later in the year compared to many other species and site combinations, particularly combinations involving the Huffman (wet) and Underhill (intermediate) sites. Further, the majority of these combinations overlapped between these three species and typically involved WWP, WRSP, WH, GF, WRC, and DF. WVPP at the Campbell (dry) site ($G_{90}$ = 358) had a significantly later $G_{90}$ than 12 other species and site combinations by 124 to 167 days while WVPP at the Underhill (intermediate) site ($G_{90}$ = 357) had a significantly later $G_{10}$ compared to 11 other species and site combinations by 129 to 155 days. LC at the Underhill (intermediate) site ($G_{90}$ = 327) had a significantly later $G_{90}$ compared to eight species and site combinations by 106 to 125 days while LC at the Huffman (wet) site ($G_{90}$ = 352) had a significantly later $G_{90}$ compared to seven other species and site combinations by 115 to 151 days. GS at the Underhill (intermediate) site ($G_{90}$ = 325) had a significantly later $G_{90}$ compared to eight other species and site combinations by 105 to 124 days. All other significant differences in $G_{90}$ for site by species interactions are demonstrated in Table 2.10.

| $G_{90}$ Across Species and Sites | | | | | $G_{90}$ Across Species | |
|---|---|---|---|---|---|---|
| **Species** | **Site** | **$G_{90}$ (DOY)** | **SE** | **Significance** | **$G_{90}$ (DOY)** | **SE** |
| DF | Huffman | 294 | 21.1 | abcdeg | 250 | 12 |
| | Underhill | 263 | 22.5 | abcdefg | | |
| | Campbell | 201 | 19.9 | fg | | |
| GF | Huffman | 190 | 14.8 | abcdeg | 225 | 12.8 |
| | Underhill | 216 | 19.1 | defg | | |
| | Campbell | 306 | 20.9 | f | | |
| GS | Huffman | 257 | 21 | abcdefg | 288 | 10.7 |
| | Underhill | 325 | 21 | abc | | |
| | Campbell | 281 | 21 | abcdefg | | |
| LC | Huffman | 352 | 17.2 | abcde | 332 | 12.8 |
| | Underhill | 327 | 18.4 | abcd | | |
| | Campbell | 313 | 19.9 | ab | | |
| POC | Huffman | 278 | 18.9 | abcdefg | 286 | 12.5 |
| | Underhill | 282 | 16.4 | abcdeg | | |
| | Campbell | 296 | 16.4 | abcdefg | | |
| SSP | Huffman | 228 | 28.6 | abcdefg | 238 | 13.1 |
| | Underhill | 232 | 20.3 | cdefg | | |
| | Campbell | 248 | 20.3 | bcdefg | | |
| WH | Huffman | 204 | 22.1 | abcdefg | 225 | 12.2 |
| | Underhill | 234 | 24.7 | cdefg | | |
| | Campbell | 255 | 31.2 | fg | | |
| WRC | Huffman | 249 | 12.1 | abcdefg | 225 | 11.5 |
| | Underhill | 224 | 12.1 | defg | | |
| | Campbell | 207 | 10.8 | efg | | |
| WRSP | Huffman | 213 | 27.5 | defg | 244 | 11.5 |
| | Underhill | 220 | 21.3 | efg | | |
| | Campbell | 287 | 21.3 | abcdeg | | |
| WVPP | Huffman | 298 | 16.9 | abcdefg | 339 | 13.5 |
| | Underhill | 357 | 16.9 | ab | | |
| | Campbell | 358 | 15.6 | a | | |
| WWP | Huffman | 237 | 13.1 | abcdefg | 247 | 12.5 |
| | Underhill | 258 | 16 | abcdefg | | |
| | Campbell | 252 | 13.1 | cdefg | | |

Table 2.10: Estimated marginal mean and standard error (SE) of the 2021 day of the year when 90% of growth had accumulated ($G_{90}$), for each individual species and for each species across the Huffman (wet), Underhill (intermediate), and Campbell (dry) sites. Significance letters were included to represent significance differences in $G_{10}$ for the species by site interactions.

### 2.6.5.5 *Growing Season Cessation Date and Climate*

GDD was significant in determining $G_{90}$ for all species. Other factors associated with temperature, including frost days and annual minimum temperature, were also significant for the

majority of species. Unlike $G_{10}$, climate variables associated with rainfall was significant for the majority of species (Table 2.11).

| Growing Season Cessation Date | | | | | | |
|---|---|---|---|---|---|---|
| **Species** | **Parameter** | **Parameter Estimate** | **SE** | **Adj. R2** | **RMSE** | **CV** |
| DF | GDD | 0.06902 | 0.005136 | 0.9857 | 6.553871 | 0.026995 |
| | Cumulative Rainfall | 0.096354 | 0.013978 | | | |
| | Frost Days | 7.609305 | 1.406175 | | | |
| | Annual Tmin | -18.654543 | 3.261952 | | | |
| GF | GDD | 0.093208 | 0.004807 | 0.9794 | 7.895828 | 0.035279 |
| | Frost Days | 4.779835 | 0.889729 | | | |
| | Annual Rainfall | 0.042249 | 0.01193 | | | |
| GS | GDD | 0.05986 | 0.00981 | 0.9431 | 14.65368 | 0.051459 |
| | Cumulative Rainfall | 0.10132 | 0.0141 | | | |
| | Annual Tmin | -14.22424 | 3.6969 | | | |
| LC | GDD | 0.085 | 0.01581 | 0.8838 | 11.12764 | 0.034124 |
| | Cumulative Rainfall | 0.12046 | 0.01352 | | | |
| | Annual Tmin | -17.92213 | 3.64889 | | | |
| POC | GDD | 0.080495 | 0.003409 | 0.9879 | 4.377034 | 0.015319 |
| | Cumulative Rainfall | 0.109935 | 0.005215 | | | |
| | Annual Tmin | -23.685701 | 1.498918 | | | |
| SSP | GDD | 0.079927 | 0.005298 | 0.9634 | 9.205543 | 0.03876 |
| | Cumulative Rainfall | 0.07567 | 0.016795 | | | |
| | Annual Tmin | -12.205524 | 3.456841 | | | |
| WH | GDD | 0.10 | 3.01E-03 | 0.987 | 6.609713 | 0.029669 |
| | Frost Days | 2.25 | 7.64E-01 | | | |
| WRC | GDD | 0.069679 | 0.005017 | 0.9495 | 7.748866 | 0.034416 |
| | Cumulative Rainfall | 0.055457 | 0.011451 | | | |
| | Annual Tmin | -6.230517 | 2.684351 | | | |
| WRSP | GDD | 0.07196 | 0.003429 | 0.9813 | 6.146867 | 0.026318 |
| | Cumulative Rainfall | 0.039133 | 0.010109 | | | |
| | Frost Days | 5.994666 | 1.343465 | | | |
| | Annual Tmin | -3.655545 | 1.718448 | | | |
| WVPP | GDD | 0.06461 | 0.01125 | 0.8996 | 11.46285 | 0.034527 |
| | Cumulative Rainfall | 0.08506 | 0.0148 | | | |
| | Annual Tmin | -18.02051 | 3.41506 | | | |
| WWP | GDD | 0.092698 | 0.006158 | 0.9489 | 7.856445 | 0.031749 |
| | Frost Days | 9.430737 | 2.054642 | | | |
| | Annual Tmin | -22.222748 | 3.969893 | | | |

Table 2.11: Climate variable parameters associated with the growing season cessation date across species and sites, including parameter estimates, standard error (SE), adjusted $R^2$ (Adj. $R^2$), residual mean square error (RMSE), and the coefficient of variation (CV; %). All parameters listed were significant ($P < 0.05$). Variables include frost days, or the accumulation of days since May in which temperatures were below 0°C, GDD, or the total accumulation of degrees between 5-25°C since May, cumulative rainfall (mm) since May until $G_{90}$, and annual minimum temperature (Tmin; °C), photoperiod (hours), April rainfall (mm), April mean temperature (Tmean; °C), annual rainfall (mm), and cumulative rainfall from January to $G_{10}$.

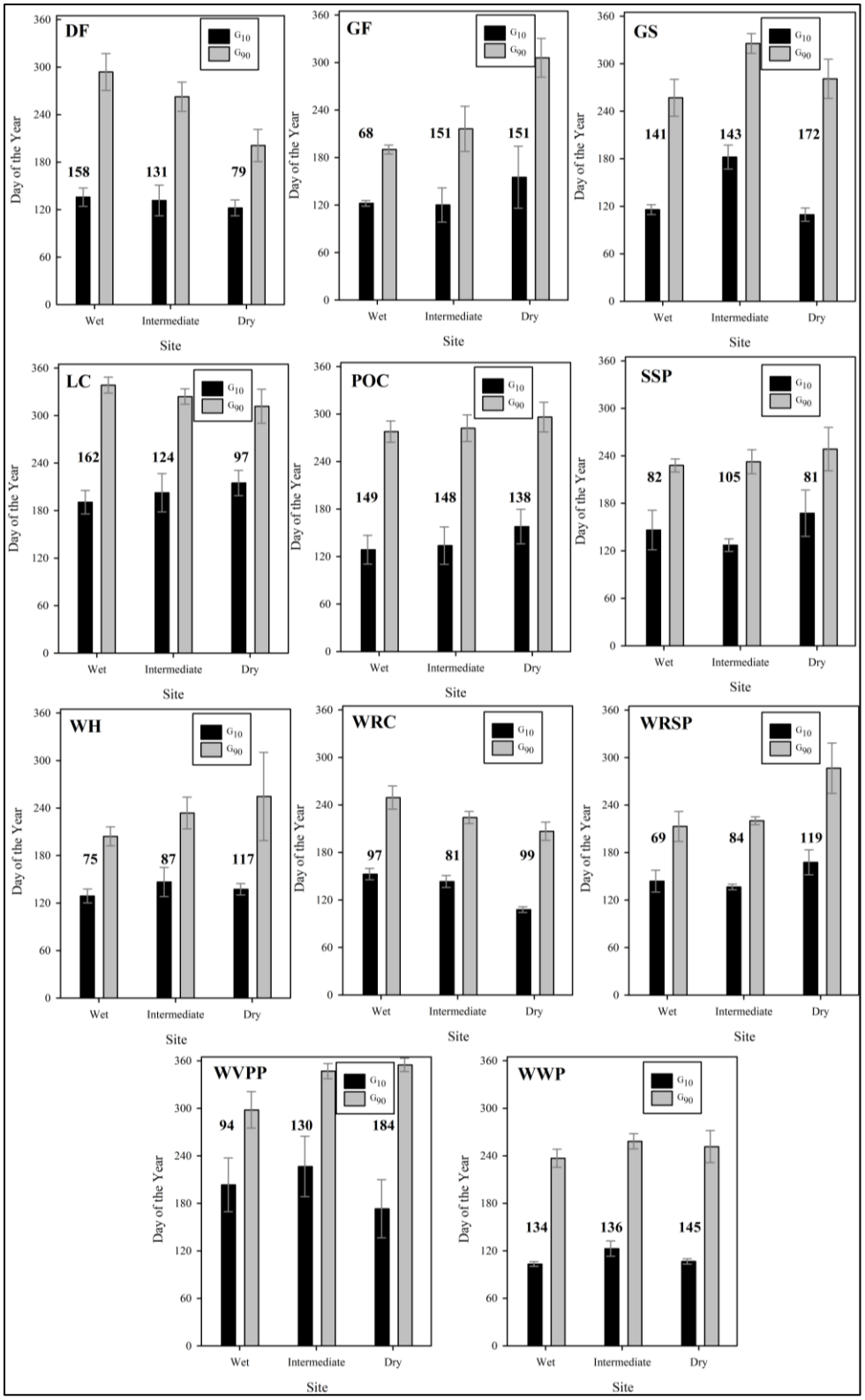


Figure 2.10: 2021 Growing season metrics for each species across the Huffman (wet), Underhill (intermediate), and Campbell (dry) sites, including $G_{10}$, $G_{90}$, and GSL shown in bolded numbers.

### 2.6.5.6 *Cummulative Individual Basal Area Growth*

The species by site interaction was significant for CBAI ( $P = 0.00103$). GS at the Huffman (wet) site tended to have a significantly higher CBAI compared to the majority of species and site combinations while WWP at the Huffman (wet) site tended to have a significantly higher CBAI compared to a few species and site combinations.

GS and, to a lesser extent, WWP, had a CBAI that was significantly higher compared to many other species and site combinations, particularly combinations involving the Campbell (dry) site. Further, only a few of these combinations overlapped between the two species, which typically involved species such as LC, WVPP, and WRSP. GS at the Huffman (wet) site (CBAI = 6.94 $cm^2$) had a significantly higher CBAI than 18 other species and site combinations by 4.06 to 5.95 $cm^2$. WWP at the Huffman (wet) site (CBAI = 5.87 $cm^2$) had a significantly higher CBAI than six other species and site combinations by 4.57 to 4.88 $cm^2$. All other significant differences in CBAI for species by site interactions are demonstrated in Table 2.12.

| Cumulative 2021 BAI Across Species and Sites | | | | | Cumulative 2021 BAI Across Species | |
|---|---|---|---|---|---|---|
| **Species** | **Site** | **CBAI (cm²)** | **SE** | **Significance** | **CBAI (cm²)** | **SE** |
| DF | Huffman | 4.18 | 0.791 | abcd | 3.55 | 0.489 |
| | Underhill | 3.72 | 0.791 | abcd | | |
| | Campbell | 2.84 | 0.746 | bcd | | |
| GF | Huffman | 2.88 | 0.707 | bcd | 2.76 | 0.523 |
| | Underhill | 3.42 | 0.913 | abcd | | |
| | Campbell | 1.73 | 1 | bcd | | |
| GS | Huffman | 6.94 | 0.707 | a | 4.58 | 0.438 |
| | Underhill | 4.39 | 0.707 | abcd | | |
| | Campbell | 2.42 | 0.707 | bcd | | |
| LC | Huffman | 1.51 | 0.845 | cd | 1.33 | 0.532 |
| | Underhill | 1.17 | 0.845 | cd | | |
| | Campbell | 1.29 | 0.913 | cd | | |
| POC | Huffman | 5.21 | 0.913 | abcd | 3.12 | 0.507 |
| | Underhill | 2.47 | 0.791 | bcd | | |
| | Campbell | 2.20 | 0.791 | bcd | | |
| SSP | Huffman | 2.48 | 1.118 | abcd | 2.09 | 0.532 |
| | Underhill | 2.8 | 0.791 | bcd | | |
| | Campbell | 1.22 | 0.791 | cd | | |
| WH | Huffman | 2.31 | 0.707 | bcd | 2.79 | 0.496 |
| | Underhill | 4.08 | 0.791 | abcd | | |
| | Campbell | 1.7 | 1 | bcd | | |
| WRC | Huffman | 3.23 | 0.791 | abcd | 3.61 | 0.467 |
| | Underhill | 4.15 | 0.791 | abcd | | |
| | Campbell | 3.48 | 0.707 | abcd | | |
| WRSP | Huffman | 2.13 | 0.913 | bcd | 2.86 | 0.467 |
| | Underhill | 5.17 | 0.707 | abc | | |
| | Campbell | 0.99 | 0.707 | d | | |
| WVPP | Huffman | 1.03 | 0.913 | cd | 1.69 | 0.561 |
| | Underhill | 1.69 | 1 | bcd | | |
| | Campbell | 2.26 | 0.845 | bcd | | |
| WWP | Huffman | 5.87 | 0.746 | b | 5.6 | 0.507 |
| | Underhill | 5.51 | 0.746 | abc | | |
| | Campbell | 5.34 | 0.845 | abc | | |

Table 2.12: Estimated marginal mean and standard error (SE) of the cumulative basal area increment (CBAI) for each individual species and for each species across the Huffman (wet), Underhill (intermediate), and Campbell (dry) sites. Significance letters were included to represent significance differences in CBAI for the species by site interactions.

### 2.6.5.7 *Growing Season Basal Area Increment and Climate*

Seven climate variables that would reflect water supply, evaporative demand, and energy were tested when determining the relationship between monthly BAI and climate. Rainfall, RH, and solar radiation were determined to be the climate variables that were significantly correlated

to 2021 monthly BAI across all species, with all but solar radiation having a positive relationship with 2021 monthly BAI (Table 2.13). When comparing among these species, rainfall and RH had the strongest correlation with LC and weakest correlation with GF while solar radiation had the strongest correlation with LC and weakest correlation with WH. PET, Mean VPD, maximum VPD, and maximum temperature had a significant negative correlation with the majority of species while GDD had a significant negative correlation with fewer species.

The 2021 BAI of both LC and WVPP were significantly correlated with all 10 climate variables. Otherwise, the majority of climate variables that were significantly correlated with 2021 BAI for DF, GF, GS, SSP, POC, WH, WRC, WRSP, and WVPP were related to water supply and variables that impact evaporative demand, although GF and SSP had fewer climate variables associated with evaportative demand. However, of these species temperature was not significantly correlated with GF, SSP, WH, WRC, and WRSP.

| 2021 Monthly Basal Area Increment and Climate | | | | | | | |
|---|---|---|---|---|---|---|---|
| **SPP** | **Rain** | **PET** | **Tmax** | **VPDmax** | **RH** | **RAD** | **GDD** |
| **DF** | 0.373 | -0.201 | -0.171 | -0.270 | 0.490 | -0.362 | |
| **GF** | 0.224 | | | | 0.306 | -0.233 | |
| **GS** | 0.324 | -0.192 | -0.175 | -0.247 | 0.342 | -0.327 | -0.139 |
| **LC** | 0.623 | -0.561 | -0.526 | -0.526 | 0.597 | -0.709 | -0.452 |
| **POC** | 0.318 | -0.185 | -0.147 | -0.235 | 0.365 | -0.318 | |
| **SSP** | 0.270 | | | -0.183 | 0.388 | -0.240 | |
| **WH** | 0.207 | | | | 0.329 | -0.192 | |
| **WRC** | 0.279 | -0.145 | | -0.143 | 0.348 | -0.294 | |
| **WRSP** | 0.241 | -0.162 | | -0.188 | 0.394 | -0.220 | |
| **WVPP** | 0.394 | -0.388 | -0.367 | -0.388 | 0.459 | -0.478 | -0.308 |
| **WWP** | 0.353 | -0.199 | -0.168 | -0.219 | 0.420 | -0.383 | |

Table 2.13: Significant Pearson correlation coefficients associated with 2021 monthly BAI and monthly climate variables, including rainfall (P; mm), potential evapotranspiration (PET; mm), maximum temperature (Tmax; °C), maximum VPD (VPDmax; kPa), relative humidity (RH; %), radiation (RAD; MJ $m^2$ $month^{-1}$), and growing degree days (GDD°C). All blank cells indicate a non-significant correlation.

## 2.7 Discussion

### 2.7.1 Cumulative Growth and Survival

In general, the tree size and VOB data that was collected from the 2021 inventory when most trees were 25 years old support the hypothesis that species such as DF and LC, which tend to be more drought tolerant but also most productive under conditions of higher water availability, would show a slight decline in tree size and survival eastward across the water deficit gradient. Meanwhile, all other species with the exception of WVPP, which are more drought intolerant, would show a more dramatic decline in tree size and survival eastward across the gradient while WVPP, which is adapted to drier environments, would instead show a decline in tree size and survival westward across the gradient.

The observed trends for WWP and WVPP were slightly different than expected, but still resulted in the lowest productivity at the Campbell (dry) site for WWP and at the Huffman (wet) site for WVPP. The observed trends for WRC were the opposite of what was expected given that the highest productivity was observed at the Campbell (dry) site.

As expected, DF had its largest tree size at the Huffman (wet) site, followed by the Underhill (intermediate) site and then the Campbell (dry) site, but showed a less dramatic decline in VOB from the wet and intermediate sites to the dry site when compared with most other species. Further, survival was relatively consistent across all sites. LC had very similar growth patterns to DF across the three sites. Although survival was lowest at the Huffman (wet) site, it is important to note that windstorms before and during the study had resulted in many down trees, which considerably contributed to the measurements of survival for LC at this site. These trends generally reflect the known ecology of DF and LC. DF tends to be highly productive and is capable of surviving in a wide range of environments compared to most western U.S. conifer species. It is also known to be fairly resistant to drought due to its large root system, strong stomatal control, and high resistance to cavitation (Vejpustková and Čihák, 2019). However, the

growth of DF can still be limited by drought conditions (Weiskittel et al., 2012). Although the drought tolerance of DF tends to vary depending on its population (Rehfeldt, 1979; Chauvin et al., 2019), the growth of DF across its range is primarily limited by summer dryness and tends to be sensitive to higher VPD (Chen et al., 2010; Restaino et al., 2016; Littell et al., 2008), suggesting that the higher water deficit conditions at the Campbell (dry) site are limiting the tree size of DF. Similarly, LC can grow in a very wide range of environments across the United States and is relatively drought tolerant, but can still be sensitive to extreme drought events (Raddi et al., 2014; Niemiera, 2012). Although not much information on the direct relationship between climate and LC is known, both LC and DF appear to be able to thrive in a wide range of environments and climate ranges while being primarily influenced by water balance. Therefore, these two species tended to have large tree sizes that were similar between the two wetter sites given their ability to adapt to many environments and due to the reduced water deficit observed at these two sites, but showed slightly reduced tree sizes at the Campbell (dry) site, likely as a result of its higher water deficit, which both species are still sensitive to. These trends suggest that, while these species are relatively drought tolerant and capable of adapting to a wide variety of sites, they would not be completely immune to the expected increase in growing season water deficit under climate change. Further, their wide distribution could suggest that they become more vulnerable in more places compared to other species with a limited range in areas that are not expected to have extreme changes in water deficit (Coops and Waring, 2011). Given the high commercial value of LC and its vulnerability to disease that is exacerbated by drought (Martinez and Williams-Woodward, n.d.), as well as the high commercial and ecological value of DF, reduced tree size under the expected increase in water deficit, albeit not as severe as many other species, has the potential to affect industry, forest health, and carbon sequestration.

POC and WWP tended to have very similar tree size and survival at the Huffman (wet) and Underhill (intermediate) site, but had a dramatic decline in these metrics at the Campbell (dry) site. Although POC has a limited geographic range along the southern PNW coast, it can thrive in a variety of environments, including the Oregon coastal fog belt and the Willamette Valley (Hayes, 1958; Zobel, 1985). However, greater growth tends to be acquired in areas with moderate to high water availability (Zobel et al., 2001). Although WWP tends to thrive in mild, moist climates, it can also grow across a range of precipitation (Harris, 1990). Similar to POC, WWP has water balance as its primary limiting factor despite its ability to survive under many conditions (Graham, 1990). Given that POC and WWP can thrive in a wide range of moisture levels, but performs best in areas with higher water availability, POC and WWP are likely well adapted to the climate conditions at the Huffman (wet) and Underhill (intermediate) sites but were too sensitive to the higher water deficit conditions at the Campbell (dry) site, suggesting it had surpassed a threshold in drought tolerance. Further, it had been found that POC tends to be more drought tolerant than WH and SSP, but less so compared to most other associated species (Mallams, 2011). While POC did appear to be more tolerant than WH and SPP given that it maintained its productivity across the coastal sites and had larger trees than these two species at the Campbell (dry) site, it may also be more tolerant than other species such as GF. Similar to DF and LC, these trends suggest that, despite the moderate drought tolerance of POC and WWP and their ability to adapt to different conditions, they would not be completely immune to the expected increase in growing season water deficit under climate change. However, their more limited range suggests that the impact of climate change would not be as widespread (Coops and Waring, 2011).

GS had developed a remarkable tree size at the Huffman (wet) site since 1996, with tree size being dramatically higher than all other species at any of the sites. Tree size for GS was also higher at the Underhill (intermediate) site compared to all other species, but was noticeably lower than at the Huffman (wet) site. The tree size and survival of GS at the Campbell (dry) site was dramatically lower than what was observed at the other two sites. Tree size and survival was also lower than a few other species at the Campbell (dry) site, including DF, LC, WRC, and WVPP. These results suggest that under favorable conditions, including mild temperatures and high annual rainfall observed at the two wetter sites, GS has the potential to outgrow all other species included in this study. However, GS appears to be more sensitive to drought than DF, LC, WRC, and WVPP. These trends accurately reflect the ecology of GS, in which its distribution in low elevation sites in the PNW is primarily limited by growing season water deficit and secondarily by higher summer temperatures (Rundel, 1972). Although GS in this study was planted outside of its native range, GS was highly productive in the wetter and milder climates of the western Oregon Coast Range, while the lower water availability and higher evaporative demand at the Campbell (dry) site in the Willamette Valley foothills resulted in comparatively higher mortality and greatly reduced growth. Further, the exceptional growth at the two wetter sites reflects other GS observations in the literature, in which GS, which has the largest volume of any other known tree species, tends to show rapid growth after its initial establishment and can quickly outgrow all associated species (Weatherspoon, 1990).

Similar to GS, WH tended to have very high growth and survival at the Huffman (wet) site compared to the other species at this site, followed by the Underhill (intermediate) and the Campbell (dry) site, in which there was a dramatic decline in growth and survival. The trends in tree size and survival for SSP and WRSP were also similar to those of GS and WH, although

their growth across all sites was comparatively lower than most other species. These findings are generally consistent with our existing understanding of WH and SSP ecology, in which these species thrive in cool and moist maritime climates and are highly sensitive to extended summer drought conditions (Harris, 1990; Ruth and Harris, 1973). The trends in tree size and survival for GF were also similar to those of WH, GS, and SSP. GF is considered to be moderately drought tolerant and grows best under cool, moist conditions, which is consistent with its very high productivity at the Huffman (wet) site and relatively high productivity at the Underhill (intermediate) site (Foiles, 1959; Mátyás et al., 2021). However, it can have dramatically reduced growth after several years of successive drought conditions (Berner and Law, 2015), which may explain its sharp decline in tree size and survival at the Campbell (dry) site relative to the two wetter sites. The decline in tree size and survival eastward across the water deficit gradient and the sharp decline at the driest site for GS, WH, SSP, and GF suggests that these species have the lowest drought tolerance of all species involved with this study, and are particularly sensitive to the low water deficit conditions at the driest site, suggesting a threshold in these conditions in which tree size and survival collapses. Further, this sensitivity has major implications for the impact of climate change on these species in areas that are predicted to have a large increase in summer water deficit; this impact would likely be more severe than most other species in this study that demonstrated greater degree of drought tolerance. While it is possible for most of the suitable habitat range for these species to remain or expand northward given the expected increase in the frost-free period and warm growing season temperatures in the northern areas of the PNW (Spittlehouse, 2008), the areas within their range are expected to have the highest increase in growing season water deficit, such as in their southern limits and at lower elevations, will result in increased vulnerability to disturbances as well as reduced growth and survival.

These predictions have specifically been reported for WH and SSP, with both species being predicted to remain within most of their current range as well as undergo a northward expansion due to climate change while their vulnerability across the southern edge of their range is predicted to increase due to higher temperatures (Coops and Waring, 2011).

While we did not expect WRC to have as extreme differences across sites as GF, GS, WH, POC, or SSP, it was surprising to see that WRC had the highest growth and mortality at the Campbell (dry) site, followed by the Huffman (wet) and Underhill (intermediate) site. WRC can survive in a wide range of environments, including in areas that are warmer and drier than other associated species, but its productivity is highest along its coastal distribution with higher water availability (Grossnickle and Russell, 2006). It has also been reported that WRC is a stress-tolerant generalist with a high survival rate due to its high degree of phenotypic plasticity (Antos et al., 2016; El-Kassaby, 1999). This adaptivity supports why WRC remained productive across all sites, but the drier site having higher productivity than the coastal sites, where WRC tends to have its highest rates of productivity, may be due to other environmental conditions, such as by benefiting from higher minimum temperatures at the Campbell (dry) site (Minore, 1990). Given that it is widely thought that WRC thrives in mild, wet areas, the observed trend for WRC suggests that the climate and environmental conditions that influence WRC may be more variable than previously thought, but does corroborate the adaptability of WRC. Therefore, this suggests that WRC may be less vulnerable to increases in summer water deficit than expected.

Unlike all other species, WVPP had its lowest VOB and survival at the Huffman (wet) site. WVPP tree size and survival were similar between the Campbell (dry) and Underhill (wet) sites. The *willamettensis* variety of ponderosa pine is specific to the Willamette Valley and is more adapted to the wetter conditions of western Oregon than the drier areas typical of

ponderosa pine's range across the rest of the western U.S. While summer rainfall tends to be its limiting growth factor, it requires much less water availability than all other species in this study; the range of ponderosa pine typically has an annual rainfall lower than what has been observed at the Campbell (dry) site (Oliver and Ryker, 1990). While it is likely that the conditions at the Huffman (wet) site were too wet to sustain WVPP, the length of the growing season may have been responsible for the reduced tree size and survival observed at the Huffman (wet) site; WVPP at this site has a significantly later start to the growing season as observed from 2021 measurements, suggesting that it was not able to promptly take advantage of the conditions that allowed most other species at this site to initiate radial growth earlier in the spring. However, the similar tree size and survival at the Underhill (intermediate) and Campbell (dry) site was surprising given that a decline progressively westward across the sites was expected. Although knowledge of the *willamettensis* variety of ponderosa pine is limited, this trend suggests that its adaption to the wetter conditions of the Willamette Valley may extend to the conditions present at the Underhill (intermediate) site along the eastern slopes of the Oregon Coast Range.

In general, although tree size and survival for many of these species declined progressively eastward across the sites, the differences between the Huffman (wet) and Underhill (dry) sites tended to be less extreme compared to the Campbell (dry) site, where growth and survival tended to decline dramatically. This suggests that while these species, including GS, WH, SSP, WRSP, GF, POC, and WWP, can moderately tolerate reduced water availability, there is a threshold of water deficit as a result of reduced rainfall, higher evaporative demand, and more extreme drought conditions as observed at the Campbell (dry) site that results in low survival and severely stunted tree size. Therefore, in areas in which an increase in summer water deficit is expected under climate change, these species would have lower rates of growth and

survival and become more vulnerable to disturbances as a result of drought-induced stress compared to DF, LC, WRC, and WVPP.

### 2.7.2 Growing Season Phenology

The timing of growth initiation and cessation is heavily influenced by temperature, including chilling, forcing, and frost events, as well as photoperiod (Huang et al., 2020; Harrington et al., 2015). Considering water deficit across sites is the primary climate variable of interest, temperature may be a confounding factor; average monthly temperatures at the Campbell (dry) site tend to be higher than average monthly temperatures at the other two sites, which were similar to one another. However, photoperiod was consistent across sites. With this consideration, it was hypothesized that the length of the growing season would be relatively consistent across the water deficit gradient for less sensitive species, such as DF and LC, that are adapted to a wide range of conditions as indicated by their native range. The length of the growing season would progressively decrease eastward along the water deficit gradient for more sensitive species that are adapted to areas with high water availability as indicated by their native range, such as GF, GS, WH, POC, SSP, WRSP, and to a less extent, WWP and WRC. In contrast, the length of the growing season would decrease westward along the water deficit gradient for species that are adapted to drier conditions as indicated by their native range, such as ponderosa pine.

The expected trends as outlined in the hypothesis were not fully supported by the results of this study. The results indicate that species by site interactions were significant for the growing season starting and cessation date, which suggests that these dates were a function of both species and their relationship with site conditions. However, many of the same species and

site combinations had both a significantly later starting and cessation date while growing season length was only significant for species. This suggests that growing season length may be more influenced by species than by water deficit conditions, with some species having a similar growing season length compared to most other species and site combinations, but one that occurs later in the year. Therefore, given that other variables affecting growing season length, such as temperature and photoperiod, are somewhat similar between sites, rainfall may not play a large role in the timing or length of the growing season for most species involved with this study. Instead, species sensitivity to climate cues may be the main driver of the timing of phenological events in this study, which has been increasingly reported in the literature (Chuine et al., 2006; Hänninen 1990; Hunter and Lechowicz 1992; Kramer 1994; Chuine 2000).

The growing season starting date, $G_{10}$, had a significant species by site interaction. WVPP had a significantly later $G_{10}$ in the Huffman (wet) and Underhill (intermediate) sites than many other species and site combinations. $G_{10}$ for WVPP was primarily influenced by chilling, forcing, and photoperiod in this study, which corroborates findings from Wenny et al. (2002) in which WVPP growth initiation was primarily determined by warm spring temperatures, chilling, and photoperiod. Considering photoperiod is consistent across sites, the significantly delayed starting date at the two wetter sites for this species, which is better adapted to warmer and drier conditions, may be a result of WVPP requiring warmer early spring temperatures than the conditions at these two sites allow. $G_{10}$ for LC was also significantly later than many species and site combinations at the Campbell (dry) and Underhill (intermediate) site and was influenced by chilling, forcing, photoperiod, and rainfall accumulation. Little is known about LC's growing season phenology or its relationship with seasonal climate variation. However, the delayed starting date occurring at the two drier sites suggest that accumulated rainfall may be a strong

driver of radial growth initiation for this species despite its drought tolerance, which is further supported by the results of climate drivers that impact $G_{10}$ for LC, which includes early growing season rainfall.

Further, temperature played the largest role in determining $G_{10}$ as determined by the change in model $R^2$. Forcing was also significant for all species. This is consistent with existing literature, where temperature, particularly in the spring, is one of the main drivers that signal phenological events to occur for conifers in the PNW (Harrington et al., 2016). Further, the expected warming as a result of climate change is expected to result in an earlier start to the growing season due to warmer early spring temperatures (Harrington et al., 2015). While early growing season moisture in temperate regions can contribute to the timing of growth initiation, it is typically marginal compared to factors such as temperature, forcing and chilling, and photoperiod (Huang et al., 2020). However, for LC, POC, SSP, WRSP, and WWP, $G_{10}$ was also determined by the accumulation of rainfall or by early spring rainfall, indicating that the timing of growth initiation can, to some degree, be influenced by rainfall depending on the species. However, $G_{10}$ not significantly differing for these species despite the differences in rainfall at each site, with the exception of LC, supports the notion that rainfall is typically not a major driver of growth initiation.

The growing season cessation date, $G_{90}$, also had a significant species by site interaction. WVPP had a significantly later $G_{90}$ at the Underhill (intermediate) and Campbell (dry) sites than many other species and site combinations. $G_{90}$ for WVPP was primarily influenced by annual minimum temperature, GDD, and the accumulation of rainfall, which was nearly consistent with findings by Wenny et al. (2002) in which growth cessation for WVPP was driven by frost and low temperatures, but did not include rainfall. Similar to what was suggested previously, WVPP

may have more specific rainfall and temperature requirements than most other species that result in a delayed growth initiation and a delayed cessation at the Underhill (intermediate) site, resulting in a growing season that occurs later in the year than most other species and site combinations observed in this study. However, given that WVPP had reduced productivity due to moisture at the Huffman (wet) site, it is likely that the cooler temperatures and rainfall at this site resulted in an earlier $G_{90}$ for WVPP that was not significantly different from most species and site combinations.

LC at the Huffman (wet) and Underhill (intermediate) sites and GS at the Underhill (intermediate) site also had a significantly later $G_{90}$ than many other species and site combinations. Given that this delayed cessation for LC occurred in the two wetter sites and was primarily determined by forcing and early growing season moisture, rainfall accumulation may play a large role in extending the growing season for LC, while the delay in GS growth cessation at the Underhill (intermediate) site may suggest that GS requires a specific range of conditions to extend the growing season.

While most species tended to have similar growing season lengths, GS had a significantly longer growing season than SSP, WH, WRC, and WRSP, which may help explain its superior growth. GS had a growing season that lasted from early May to mid-October, which indicates a later growth cessation than most other species. The growing season for GS within their native range is typically between late April to late September, which also suggests that GS in this study had a later growth cessation that what is usually observed for this species. (O'Hara et al., 2008). However, this may be due to the dramatically lower elevations at these study sites compared to its native range, which typically results in warmer temperatures that can extend the growing season (Liu et al., 2016).

In general, the findings of this study support the notion that the effect of rainfall on the timing of phenological events are marginal for the majority of species involved, but that temperature, specifically spring forcing, tended to drive the timing of growth initiation (Huang et al., 2020). However, WVPP tended to have a longer growing season progressively from the Huffman (wet) to the Campbell (dry) as indicated by the timing of its growth initiation and cessation, while LC tended to have a shorter growing season progressively from the Huffman (wet) site and Campbell (dry) site, which follows trends in observed productivity for these species and sites, although there was no significant species by site interaction for growing season length to conclude that the length significantly differed across sites for this species. However, the longer growing season for GS was associated with larger tree sizes, survival, and CBAI. Given that the growing season phenology for the majority of these species did not significantly differ, yet tree size, survival, and CBAI showed distinct trends across sites for each species, water deficit is likely a greater driver of growth rather than growing season length. Therefore, these findings support the existing literature suggesting that although the expected warming of spring temperatures and delay of autumn frosts as a result of climate change may lengthen the growing season, it does not automatically allow for greater growth accumulation, which may still be primarily limited by water deficit (Barber et al., 2000; Bernal et al., 2011).

### 2.7.3 Intra-Annual Cumulative Basal Area Increment

Dendrometers showed sigmoidal curves with low BAI rates in the spring and early summer, high BAI rates in the summer during the middle of the growing season, and decreasing BAI rates nearing the end of the growing season, which was consistent with many other studies (Mäkinen et al., 2003). In general, the trends observed from the cumulative tree size from the 2021 inventory were similar with CBAI for DF, LC, GS, POC, WVPP, and WWP, which makes

sense given that growing season radial growth would contribute to cumulative tree size. Unlike what was observed with tree size, GF, WH, SSP, and WRSP had its highest CBAI at the Underhill (intermediate) site rather than at the Huffman (wet) site, although the lowest CBAI was still observed at the Campbell (dry) site. This may be due to the nearing of canopy closure at the Huffman (wet) site, or an increased sensitivity of trees at the Huffman (wet) site to the drought conditions of 2021 due to phenotypic plasticity and adaption to the wetter conditions at this site. Further, there was a significant species by site interaction for CBAI. WWP and GS, which are both characterized as having a fast growth rate and having water deficit as its limiting growth factor (Rundel, 1972; Weatherspoon, 1990; Graham, 1990), had a significantly higher CBAI at the Huffman (wet) site than many other species and site combinations. While this trend in GS at the Huffman (wet) site was very consistent with observations made in tree size and what is known about GS in the literature, it was surprising to observe this trend with WWP given that it typically exhibited having a low to moderate tree size compared to all other species at this site despite it being known as a fast growing species capable of growing to a large size (Graham, 1990; Kim et al., 2011). It is possible that many of the other, more drought-sensitive species that WWP had a significantly higher CBAI than, such as SSP and WRSP, may have exhibited reduced CBAI in 2021 due to the 2021 drought conditions and heatwave while WWP remained more tolerant.

Harrington et al., (2016) observed that WRC was an indeterministic species with a more linear growth progression than other species such as DF and SSP. However, WRC in this study tended to have a short and defined growing season compared to most other trends across species and site combinations. Further, while the tree size of WRC tended to be highest at the Campbell (dry) site, the CBAI was instead highest at the Underhill (intermediate) site, which may be a

reflection of the 2021 drought conditions and heatwave reducing the radial growth of WRC at the Campbell (dry) site.

In general, the CBAIs for most species were primarily driven by water balance, while GS, LC, and WVPP were driven equally by water balance and energy, such as temperature and GDD. There did not appear to be a strong relationship between growing season length and CBAI, perhaps with the exception of GS, which had both the longest growing season and highest CBAI. A few studies have also made this claim, in which the warmer conditions under climate change may lengthen the growing season but not necessarily result in greater annual growth, which may have been restricted by other factors such as drought (Dow et al., 2022; Bernal et al., 2011).

### 2.7.4 Caveats

There are a few caveats that should be taken into consideration. The 2021 intra-annual growth measurements in this study were recorded during a drought year. Therefore, these seasonal measurements were taken under conditions that had a higher summer water deficit than the average, which also included a heatwave during late June to early July. Further, a few measurements from various trees were not able to be recorded at various times throughout the year as a result of animals interfering with the dendrometer bands, which was promptly addressed by providing a cover for the bands in areas with frequent animal activity. Further, the timing of dendrometer band installation may not have allocated sufficient time for the bands to settle, possibly resulting in very early growing season radial growth to not be recorded. As mentioned in the text, a windstorm prior to the start of the study, as well as in the winter of 2021, had resulted in many down trees at the LC species-plot at the Huffman (wet) site, while many

standing dead trees at the POC species-plot at the Campbell (dry) site are likely attributed to disease. These disturbances had impacted the measurements of survival and are less accurately reflect survival as a function of climate conditions.

## 2.8 Conclusion

This study focused on examining the variation in productivity and growing season phenology for 25 year old stands involving 11 different species under contrasting levels of water deficit in western Oregon in order to determine differences in species growth-climate sensitivity.

It was found that tree size and survival at 25 years old for GS, WH, SSP, WRSP, GF, POC, and WWP declined progressively under higher levels of water deficit, and had declined dramatically at the driest site, indicating low drought tolerance. DF and LC followed a similar trends with less extreme differences across sites, while WVPP and WRC tended to have their largest tree sizes and highest survival at the driest site. It was also found that temperature was a major driver of seasonal growth initiation and cessation and species type was significant in determining the length of the growing season rather than water deficit while seasonal CBAI was typically driven by differences in water deficit. This finding suggests that the warmer conditions under climate change may lengthen the growing season but not necessarily result in greater annual growth, which may be restricted by water deficit depending on species tolerance.

The sensitivity of species to climate cues that allow for growth initiation and cessation, the tolerance of species to high water deficit conditions, and the expected conditions under climate change across the range of these species must all be considered when determining where species will become vulnerable and which species will grow best in a given location under climate change. Being able to make predictions on forest response to climate change requires an

understanding of species-specific growth-climate relationships, although the current knowledge of these relationships are limited by a lack of empirical studies with this focus. Therefore, this study can contribute to filling this knowledge gap. Given that it involves many different commerically and ecologically species, including some such as POC and LC with very little known about their growth-climate relationships, and explores differences in cumulative growth and survival, intra-annual growth, and growing season phenology under different levels of water deficit, which is especially relevant given the expected increase in water deficit in the PNW under climate change.

The results of this study suggests that reforestation efforts for senstive species such as GS, WH, SSP, WRSP, GF, POC, and WWP should be particularly mindful of the areas that are expected to have lower growing season moisture, higher evaporative demand, and more frequent and intense droughts as a result of climate change. This consideration should also, to a lesser extent, be made for more tolerant species such as DF and LC while reforestation efforts for WRC and WVPP should instead be mindful of areas where extreme droughts are expected given their observed tolerance to water deficit. Further, this study can help to inform where proactive management is required across species ranges and prioritize the management of forests that are expected to become the most vulnerable as a result of climate change.

Further research can be done on the intra-annual growth and growing season phenology across different years to determine the impact of inter-annual climate variability. Differences in forest structure and understory composition across species and sites could also be investigated to better understand the full impact of water deficit on forests comprises of these species. The measurements of cumulative tree size and survival will also be conducted regularly to determine the impact of water deficit throughout the rotation age of these species.

## 2.9 References


Antos, J. A., Filipescu, C. N., & Negrave, R. W. (2016). Ecology of western redcedar (*Thuja plicata*): Implications for management of a high-value multiple-use resource. *Forest Ecology and Management, 375*, 211-222.

Baldocchi, D., Chu, H., & Reichstein, M. (2018). Inter-annual variability of net and gross ecosystem carbon fluxes: A review. *Agricultural and Forest Meteorology, 249*, 520-533.

Barber, V. A., Juday, G. P., & Finney, B. P. (2000). Reduced growth of Alaskan white spruce in the twentieth century from temperature-induced drought stress. *Nature*, *405*(6787), 668-673.

Beedlow, P. A., Lee, E. H., Tingey, D. T., Waschmann, R. S., & Burdick, C. A. (2013). The importance of seasonal temperature and moisture patterns on growth of Douglas-fir in western Oregon, USA. *Agricultural and Forest Meteorology, 169*, 174-185.

Bernal, M., Estiarte, M., & Peñuelas, J. (2011). Drought advances spring growth phenology of the Mediterranean shrub *Erica multiflora*. *Plant Biology*, *13*(2), 252-257.

Berner, L. T., & Law, B. E. (2015). Water limitations on forest carbon cycling and conifer traits along a steep climatic gradient in the Cascade Mountains, Oregon. *Biogeosciences, 12*(22), 6617-6635.

Bréda, N., Huc, R., Granier, A., & Dreyer, E. (2006). Temperate forest trees and stands under severe drought: a review of ecophysiological responses, adaptation processes and long-term consequences. *Annals of Forest Science, 63*(6), 625-644.

Chapin, F. S., McGuire, A. D., Ruess, R. W., Hollingsworth, T. N., Mack, M. C., Johnstone, J. F., ... & Taylor, D. L. (2010). Resilience of Alaska's boreal forest to climatic change. *Canadian Journal of Forest Research, 40*(7), 1360-1370.

Chauvin, T., Cochard, H., Segura, V., & Rozenberg, P. (2019). Native-source climate determines the Douglas-fir potential of adaptation to drought. *Forest Ecology and Management, 444*, 9-20.

CHEN, P. Y., Welsh, C., & Hamann, A. (2010). Geographic variation in growth response of Douglas-fir to interannual climate variability and projected climate change. *Global Change Biology*, *16*(12), 3374-3385.

Chuine I (2010) Why does phenology drive species distribution? *Philosophical Transactions of the Royal Society B-Biological Sciences*,365, 3149–3160.

Chuine, I., Belmonte, J., & Mignot, A. (2000). A modelling analysis of the genetic variation of phenology between tree populations. *Journal of Ecology*, 561-570.

Chuine, I., Rehfeldt, G. E., & Aitken, S. N. (2006). Height growth determinants and adaptation to temperature in pines: a case study of *Pinus contorta* and *Pinus monticola*. *Canadian Journal of Forest Research, 36*(5), 1059-1066.

Coops, N. C., & Waring, R. H. (2011). Estimating the vulnerability of fifteen tree species under changing climate in Northwest North America. *Ecological Modelling*, *222*(13), 2119-2129.

Dai, Aiguo & National Center for Atmospheric Research Staff (Eds). Last modified 12 Dec 2019. "The Climate Data Guide: Palmer Drought Severity Index (PDSI)." Retrieved from climatedataguide.ucar.edu/climate-data/palmer-drought-severity-index-pdsi.

Dow, C., Kim, A. Y., D'Orangeville, L., Gonzalez-Akre, E. B., Helcoski, R., Herrmann, V., ... & Anderson-Teixeira, K. J. (2022). Warm springs alter timing but not total growth of temperate deciduous trees. *Nature*, 1-6.

El-Kassaby, Y. A. (1999). Phenotypic plasticity in western redcedar. *For. Genet*, *6*(4), 235-240.

Foiles, M. W. (1959). Silvics of grand fir. *Misc. Pub. No. 21. Ogden, UT: US Department of Agriculture, Forest Service, Intermountain Forest and Range Experiment Station.*

Ford, K. R., Harrington, C. A., Bansal, S., Gould, P. J., & St. Clair, J. B. (2016). Will changes in phenology track climate change? A study of growth initiation timing in coast Douglas-fir. *Global Change Biology*, *22*(11), 3712-3723.

Ford, K. R., Harrington, C. A., & St. Clair, J. B. (2017). Photoperiod cues and patterns of genetic variation limit phenological responses to climate change in warm parts of species' range: Modeling diameter-growth cessation in coast Douglas-fir. *Global change biology*, *23*(8), 3348-3362.

Graham, R. T. (1990). *Pinus monticola* Dougl. ex D. Don western white pine. *Silvics of North America, 1*, 385-394.

Goheen, D. J., Mallams, K., Betlejewski, F., & Hansen, E. (2012). Effectiveness of vehicle washing and roadside sanitation in decreasing spread potential of port-orford-cedar root disease. *Western Journal of Applied Forestry*, *27*(4), 170-175.

Gonzalez-Benecke, C. A., Flamenco, H. N., & Wightman, M. G. (2018). Effect of vegetation management and site conditions on volume, biomass and leaf area allometry of four coniferous species in the Pacific Northwest United States. *Forests*, *9*(9), 581.

Grossnickle, S. C., & Russell, J. H. (2006). Yellow-cedar and western redcedar ecophysiological response to fall, winter and early spring temperature conditions. *Annals of Forest Science*, *63*(1), 1-8.

Hamon, W. R. (1963). Computation of direct runoff amounts from storm rainfall. *Int. Assoc. Sci. Hydrol. Publ.*, *63*, 52-62.

Hänninen, H., Kramer, K., Tanino, K., Zhang, R., Wu, J., & Fu, Y. H. (2019). Experiments are necessary in process-based tree phenology modelling. *Trends in Plant Science*, *24*(3), 199-209.

Harrington, C.A., Ford, K., & Clair, B. S. (2016). Phenology of pacific northwest tree species. *Tree Planters' Notes. 59 (2): 76-85.*, 76-85.

Harrington, C. A., & Gould, P. J. (2015). Tradeoffs between chilling and forcing in satisfying dormancy requirements for Pacific Northwest tree species. *Frontiers in Plant Science*, *6*, 120.

Harris, A. S. (1990). Picea sitchensis (Bong.) Carr. Sitka spruce. *Silvics of North America; Burns, RM, Honkala, BH, Eds*, 260-267.

Hayes, G. L. (1958). Silvical characteristics of Port-Orford-Cedar.

Hsiao, T. C., & Acevedo, E. (1975). Plant responses to water deficits, water-use efficiency, and drought resistance. *Developments in Agricultural and Managed Forest Ecology*, *1*, 59-84.

Huang, J. G., Ma, Q., Rossi, S., Biondi, F., Deslauriers, A., Fonti, P., ... & Ziaco, E. (2020). Photoperiod and temperature as dominant environmental drivers triggering secondary growth resumption in Northern Hemisphere conifers. *Proceedings of the National Academy of Sciences*, *117*(34), 20645-20652.

Hunter, A. F., & Lechowicz, M. J. (1992). Predicting the timing of budburst in temperate trees. *Journal of Applied Ecology*, 597-604.

Innes, J. L. (1994). Climatic sensitivity of temperate forests. *Environmental pollution*, *83*(1-2), 237-243.

Jackson, S. D. (2009). Plant responses to photoperiod. *New Phytologist*, *181*(3), 517-531.

Jiménez, M. N., Navarro, F. B., Sánchez-Miranda, A., & Ripoll, M. A. (2019). Using stem diameter variations to detect and quantify growth and relationships with climatic variables on a gradient of thinned Aleppo pines. *Forest ecology and management*, *442*, 53-62.

Just, M. G., Dale, A. G., Long, L. C., & Frank, S. D. (2019). Urbanization drives unique latitudinal patterns of insect herbivory and tree condition. *Oikos*, *128*(7), 984-993.

Kim, M. S., Richardson, B. A., McDonald, G. I., & Klopfenstein, N. B. (2011). Genetic diversity and structure of western white pine (*Pinus monticola*) in North America: a baseline study for conservation, restoration, and addressing impacts of climate change. *Tree genetics & genomes*, *7*(1), 11-21.

Kramer, K., Leinonen, I., & Loustau, D. (2000). The importance of phenology for the evaluation of impact of climate change on growth of boreal, temperate and Mediterranean forests ecosystems: an overview. *International Journal of Biometeorology*, *44*(2), 67-75.

Law, B. E., Falge, E., Gu, L. V., Baldocchi, D. D., Bakwin, P., Berbigier, P., ... & Wofsy, S. (2002). Environmental controls over carbon dioxide and water vapor exchange of terrestrial vegetation. *Agricultural and Forest Meteorology*, *113*(1-4), 97-120.

Liu, Q., Fu, Y. H., Zeng, Z., Huang, M., Li, X., & Piao, S. (2016). Temperature, precipitation, and insolation effects on autumn vegetation phenology in temperate China. *Global change biology*, *22*(2), 644-655.

Mäkinen, H., Nöjd, P., & Saranpää, P. (2003). Seasonal changes in stem radius and production of new tracheids in Norway spruce. *Tree Physiology*, *23*(14), 959-968.

Mátyás, C., Dostál, J., Beran, F., Čáp, J., Fulín, M., Vejpustková, M., ... & Frýdl, J. (2021). Climatic Sensitivity Profile of *Abies* Species–A Key to Their Future Role in the Adaptive Silviculture of Central-Southeast Europe.

McGarigal, K., & McComb, W. C. (1995). Relationships between landscape structure and breeding birds in the Oregon Coast Range. *Ecological monographs*, *65*(3), 235-260.

McMaster, G. S., & Wilhelm, W. W. (1997). Growing degree-days: one equation, two interpretations. *Agricultural and forest meteorology*, *87*(4), 291-300.

Mildrexler, D. J., Shaw, D. C., & Cohen, W. B. (2019). Short-term climate trends and the Swiss needle cast epidemic in Oregon's public and private coastal forestlands. *Forest Ecology and Management*, *432*, 501-513.

Miller, P., Lanier, W., & Brandt, S. (2001). Using growing degree days to predict plant stages. *Ag/Extension Communications Coordinator, Communications Services, Montana State University-Bozeman, Bozeman, MO*, *59717*(406), 994-2721.

Minore, D. (1990). *Thuja plicata* Donn ex D. Don—western redcedar. *Silvics of North America*, *1*, 590-600.

Niemiera, A. X. (2012). Leyland Cypress, x *Cupressocyparis leylandii*.

Niinemets, Ü. (2010). Responses of forest trees to single and multiple environmental stresses from seedlings to mature plants: past stress history, stress interactions, tolerance and acclimation. *Forest Ecology and management*, *260*(10), 1623-1639.

O'Hara, K. L., York, R. A., & Heald, R. C. (2008). Effect of pruning severity and timing of treatment on epicormic sprout development in giant sequoia. *Forestry*, *81*(1), 103-110.

Oliver, W. W., & Ryker, R. A. (1990). *Pinus ponderosa* Dougl. ex Laws. ponderosa pine. *Silvics of North America*, *1*(654), 413.

Pillsbury, N. H., Reimer, J. L., & Thompson, R. P. (1998). *Tree volume equations for fifteen urban species in California*. Tech. Rep. 7. San Luis Obispo, CA: Urban Forest Ecosystems Institute, California Polytechnic State University.

Pödör, Z., Manninger, M., & Jereb, L. (2014). Application of sigmoid models for growth investigations of forest trees. *Advanced Computational Methods for Knowledge Engineering*, 353-364.

Polgar, C. A., & Primack, R. B. (2011). Leaf-out phenology of temperate woody plants: from trees to ecosystems. *New phytologist*, *191*(4), 926-941.

PRISM Climate Group, Oregon State University, https://prism.oregonstate.edu.

Raddi, P., Danti, R., & Della Rocca, G. (2014). x *Cupressocyparis leylandii*. *Enzyklopädie der Holzgewächse: Handbuch und Atlas der Dendrologie*, 1-17.

Rehfeldt, G. E. (1979). Ecological adaptations in Douglas-fir (*Pseudotsuga menziesii* var. glauca) populations. *Heredity*, *43*(3), 383-397.

Restaino, C. M., Peterson, D. L., & Littell, J. (2016). Increased water deficit decreases Douglas fir growth throughout western US forests. *Proceedings of the National academy of Sciences*, *113*(34), 9557-9562.

Restaino, C. M., Peterson, D. L., & Littell, J. (2016). Increased water deficit decreases Douglas fir growth throughout western US forests. *Proceedings of the National academy of Sciences*, *113*(34), 9557-9562.

Rey, J. M. (1999). Modelling potential evapotranspiration of potential vegetation. *Ecological Modelling*, *123*(2-3), 141-159.

RStudio Team. (2015). *RStudio: Integrated Development Environment for R*. Boston, MA. Retrieved from www.rstudio.com

Rundel, P. W. (1972). Habitat restriction in giant sequoia: the environmental control of grove boundaries. *American Midland Naturalist*, 81-99.

Ruth, R. H., & Harris, A. S. (1973). Western hemlock-Sitka spruce. *Silvicultural Systems*, 5.

SAS Institute Inc. 2013. SAS® 9.4. Cary, NC: SAS Institute Inc.

Soil Survey Staff, Natural Resources Conservation Service, United States Department of Agriculture. Web Soil Survey. Available online.

Spittlehouse, D. L. (2008). Climate Change, impacts, and adaptation scenarios: climate change and forest and range management in British Columbia. BC Min. For. Range, Res. Br., Victoria. *Victoria. BC Tech. Rep*, *45*.

Suarez, M.L, & Kitzberger, T. (2010). Differential effects of climate variability on forest dynamics along a precipitation gradient in northern Patagonia. *Journal of ecology*, *98*(5), 1023-1034.

Suarez, M. L., Villalba, R., Mundo, I. A., & Schroeder, N. (2015). Sensitivity of *Nothofagus dombeyi* tree growth to climate changes along a precipitation gradient in northern Patagonia, Argentina. *Trees*, *29*(4), 1053-1067.

Systat Software. SigmaPlot for Windows, version 14. San Jose: Cranes, 2008. Available at: www. systatsoftware.com

Thorson, T. D., Bryce, S. A., Lammers, D. A., Wood, A. J., Omernik, J. M., Kagan, J., … Comstock, J. A. (Cartographers) (2003). Color poster with map, descriptive text, summary tables, and photographs. [Ecoregions of Oregon]. Reston, VA: U.S. Geological Survey. Retrieved from http://www.epa.gov/ wed/pages/ecoregions/or_eco.htm

Vejpustková, M., & Čihák, T. (2019). Climate response of Douglas fir reveals recently increased sensitivity to drought stress in Central Europe. *Forests*, *10*(2), 97.

Walthall, C. L., Hatfield, J., Backlund, P., Lengnick, L., Marshall, E., Walsh, M., ... & Ziska, L. H. (2013). Climate change and agriculture in the United States: Effects and adaptation.

Weatherspoon, C. P. (1990). Sequoiadendron giganteum (Lindl.) Buchholz Giant Sequoia. *Silvics of North America*, *1*, 552-562.

Weiskittel, A. R., Crookston, N. L., & Radtke, P. J. (2011). Linking climate, gross primary productivity, and site index across forests of the western United States. *Canadian Journal of Forest Research*, *41*(8), 1710-1721.

Wensel, L. C., & Krumland, B. (1983). Volume and taper relationships for redwood, douglas fir, and other conifers in California's North Coast.

Wenny, D. L., Swanson, D. J., & Dumroese, R. K. (2002). The chilling optimum of Idaho and Arizona ponderosa pine buds. *Western Journal of Applied Forestry*, *17*(3), 117-121.

Zhou, X., & Hemstrom, M. A. (2010). Timber volume and aboveground live tree biomass estimations for landscape analyses in the Pacific Northwest. *Gen. Tech. Rep. PNW-GTR-819. Portland, OR: US Department of Agriculture, Forest Service, Pacific Northwest Research Station. 31 p., 819.*

Zianis, D., Muukkonen, P., Mäkipää, R., & Mencuccini, M. (2005). *Biomass and stem volume equations for tree species in Europe*. FI.

Zobel, D. B., Roth, L. F., & Hawk, G. M. (1985). Ecology, pathology, and management of Port-Orford-Cedar (*Chamaecyparis lawsoniana* (General Technical Report 184). Pacific Northwest Forest; Range Experiment Station.

Zobel, D. B., Riley, L., Kitzmiller, J. H., & Sniezko, R. A. (2001). Variation in water relations characteristics of terminal shoots of Port-Orford-cedar (*Chamaecyparis lawsoniana*) seedlings. *Tree physiology*, *21*(11), 743-749.

# 3. Sensitivity of Inter-Annual Growth and Wood Properties to Climate Variability for 11 Conifer Species Across a Gradient in Water Deficit

## 3.1 Introduction

The temperate evergreen forests in the Pacific Northwest (PNW) of the United States contain highly productive and long living stands (Baldocchi et al., 2018). Given that site productivity within this region is most influenced by growing season moisture availability and the monthly temperature range, the expected increase in summer drought and evaporative demand under climate change can be detrimental to the growth and survival of tree species in the PNW (Weiskittel et al., 2011). However, the extent to which species growth and survival are impacted by climate change depends on species sensitivity to climate variability and water deficit.

Tree ring properties, including tree ring widths, latewood widths, latewood percentages, and wood basic density can be used as indicators for species growth response to seasonal and inter-annual climate conditions and ultimately determine differences in species climate sensitivity. Further, latewood percentage and wood basic density can be used as indicators for wood quality, which is relevant in understanding the impact of climate change on the wood structure of valuable timber species. Studying multiple metrics of tree rings and wood properties can provide more comprehensive information on growth response to climate variation and water deficit (Dannenberg et al., 2014).

Our current knowledge of species-specific growth-climate relationships is limited by the lack of empirical studies evaluating the relationship between species growth dynamics and

climate variability across different timescales and contrasting abiotic conditions, such as climate gradients (Suarez and Kitzberger, 2010). Therefore, studying the seasonal and inter-annual growth through tree rings and wood properties of many ecologically and commercially valuable species across a gradient in water deficit and evaluating their relationship with climate variability can contribute to filling this knowledge gap. This knowledge would ultimately help to predict forest response to climate change and help to make more informed management decisions to enhance forest health and productivity.

## 3.2 Literature Review

### 3.2.1 Tree Ring Properties and Climate

Radial growth as reflected by tree ring widths can provide information on the sensitivity of growth to climate variation over time, including changes in annual and seasonal hydroclimate. Differences in seasonal and annual ring growth trends can be due to species-specific wood property and physiological differences as well as differences in external factors, such as climate (Brienen and Zuidema, 2005). Tree rings reflect past climate variation given that cambial processes, including the number of cells formed in the tree ring and cell enlargement, are sensitive to climate and other environmental factors (Dannenberg and Wise, 2016). In general, a wider tree ring reflects a higher growth rate due to a higher rate of cell production within the cambium. The factors that encourage or limit growth, ranging from water availability, temperature, and growing season length, may vary across species, regions, and ecosystems. In temperate forests, wider tree ring widths typically develop during a cooler, moister growing season given that high water availability and low evapotranspiration demand are conducive to

growth (Littell et al., 2008). However, growth may also be benefited by a warmer growing season given that there is sufficient soil water availability (Ettl and Peterson, 1995).

Seasonal climate variation is reflected in the earlywood and latewood ring widths, which can be particularly sensitive to water availability and temperature during different times of the growing season. Earlywood, comprised of large lumen diameters and thin cell walls, is formed early in the growing season and typically accounts for 40-80% of the ring width. Latewood, comprised of narrow lumen diameters and thick cell walls, is formed later in the growing season when growth slows and finally ceases (Aernouts et al., 2018). The formation of latewood in tree rings has been found to increase in response to favorable growing conditions, including greater water supply and less evaporative demand, but is particularly driven by summer rainfall (Hankin et al., 2019; Kennedy, 1961; Zobel and Van Buijtenen, 2012). Considering that summer rainfall makes up only 10% of the total annual rainfall in the PNW, low soil moisture availability during the growing season is agreed to be the major limiting growth factor (Waring and Franklin, 1979).

The timing of the earlywood to latewood transition, which is influenced primarily by reduced soil moisture, is important in determining the percentage of latewood within tree rings (Filipescu et al., 2014). The percentage of latewood that comprises the total tree ring is generally higher under drought conditions (Creber, 1977). In contrast, under favorable conditions such as higher water availability, there is greater radial growth and the percentage of latewood is reduced, although higher moisture availability later in the growing season can also promote the development of latewood (Kennedy, 1961). In conifers, the latewood percentage can be used to determine wood density considering they are strongly and positively related (Filipescu et al., 2014; Warren, 1979).

### 3.2.2 Wood Basic Density, Climate, and Wood Quality

Wood basic density can be used as an indicator for wood quality and suitability for different products. Xylem mechanical strength and xylem transport safety, which related to wood basic density, can also be used as an indicator of tree vulnerability to drought stress (Pratt et al., 2007). A tree responds to drought conditions by closing stomates to decrease transpiration, which can result in reduced growth or mortality due to cavitation and hydraulic failure. During extreme drought events, cavitation may occur in the xylem as a result of higher evaporative demand and reduced soil water availability, which increases water tension in the xylem, develops pockets of air in the tracheids, and ultimately blocks the transportation of water (Hammond et al., 2019; Dalla-Salda, 2009). The stress under drought conditions can be extreme enough to cause hydraulic failure, in which plants do not have access to enough water for survival and may undergo carbon starvation. However, the xylem structure can influence tree vulnerability to cavitation and hydraulic failure. It has been found that thicker cell walls and smaller lumen diameters in xylem tracheids are conducive for maintaining water transport during droughts by allowing for the flow of water to stay intact. Considering these characteristics are associated with wood basic density, variations in this measurement may indicate the extent of tree vulnerability to drought stress (Rathgeber et al., 2006; Dalla-Salda, 2009). Further, it has been found that coastal Douglas-fir trees that have survived extreme drought events tended to have significantly higher ring density as a result of xylem plasticity, further reinforcing the idea that higher density and prompt tree adaptation is associated with reduced vulnerability to droughts (Martinez-Meier et al., 2008; Ruiz Diaz Britez et al., 2014). An understanding of species-specific relationships between climate variation and wood basic density would also contribute to knowledge regarding the ability for trees to sequester and store carbon due to its positive correlation with carbon

accumulation (Nogueira et al., 2005; Flores and Coomes, 2011; Pompa-García and Venegas-González, 2016).

Wood density can also be used as an indicator for wood quality through its strong relationship with valued mechanical properties, including wood strength, stiffness, hardness, workability, and decay resistance (Jozsa and Middleton, 1994; Rathgeber et al., 2006). Mechanical properties can determine the suitability of wood for certain products. For example, strong, high density wood would be ideal for products such as structural timber, laminated veneer, and plywood while low density wood might be more suitable for paper products and pulp (Filipescu et al., 2014). Further, wood basic density can improve the efficiency of wood for energy production given that denser wood contains less moisture (Creber, 1977; Zobel and Van Buijtenen, 2012).

## 3.3 Study Background and Significance

Wood and tree ring properties are important for providing comprehensive information and different perspectives on long term trends in wood formation in response to seasonal and annual climate variability. Further, the relationship between growth and climate can vary significantly between species due to differences in species physiology and climate sensitivity. Therefore, this study focuses on evaluating the wood and tree ring properties of many different commercially and ecologically valuable PNW species in relation to seasonal and annual climate variation across a water deficit gradient. There has been greater demand in determining tree growth and development processes under contrasting environmental conditions, such as climate gradients (Suarez and Kitzberger, 2010). Making tree ring measurements and comparisons across these gradients can provide a comprehensive view on the range of tree growth responses to

climate and therefore contributes to a better understanding of tree sensitivity to changes in future climate variability (Suarez et al., 2015). Considering site productivity within the PNW region is most influenced by growing season moisture availability and the monthly temperature range, conducting this study across a water deficit gradient can provide valuable information on species growth response to these relevant climate factors.

11 native and non-native conifer species were planted in 1996 in three sites across the Oregon Coast Range to the Willamette Valley, with each site representing a contrasting level of water deficit. These species include coastal Douglas-fir (*Pseudotsuga menziesii* (Mirb.) Franco), Port-Orford-cedar (*Chamaecyparis lawsoniana* (A. Murr.) Parl.), Willamette Valley ponderosa pine (*Pinus ponderosa* var. *willamettensis* (Douglas ex P. Lawson and C. Lawson), western white pine *(Pinus monticola* (Douglas ex D. Don) Nutt), western redcedar, giant sequoia (*Sequoiadendron giganteum* (Lindl.) Buchholz), Sitka spruce (*Picea sitchensis* (Bongard) Carriere), a weevil resistant variety of Sitka spruce, western hemlock (*Tsuga heterophylla* (Raf.) Sarg), grand fir (*Abies grandis* (Dougl.) Lindl.), and Leyland cypress (× *Cupressocyparis leylandii* (Hartw.) Bartel and (D. Don) Spach). In the winter of 2021-2022, wood increment cores were extracted from each species plot at each site in order to record measurements of tree ring widths, latewood widths, latewood percentages, and overall wood basic density. Monthly, seasonal, and annual climate measurements were recorded for each site from 1996 to 2021 in order to determine the relationship between species, wood and tree ring properties, and climate variability under different levels of water deficit, which can provide insight on species-specific growth-climate relationships and sensitivity to certain climate conditions.

Given that individual tree response to climate influence their function and effects in forest ecosystems, an understanding of species-specific growth-climate relationships can be used

to predict the impact of climate change on PNW forest health and productivity as well as its ability to provide ecosystem services, such as carbon sequestration (Jin et al., 2021; Millar et al., 2007). It can also be used to inform models for prediction purposes and determine tree species distribution in the PNW under climate change (Mathys et al., 2014). It can further be used to inform management decisions on species selection for reforestation purposes to improve stand resistance and resilience to projected climate changes. This knowledge can also aid in increasing timber production by providing insight on which species to plant on a given site, determining how climate will affect wood quality and carbon sequestration potential for various species, improving the long-term viability of restoration efforts, and minimizing the effect of disturbances associated with climate change on reforested ecosystems. For many of the species included in this study, their overall wood density, radial growth, and latewood percentages and their relationship to climate have not been evaluated in the existing literature.

## 3.4 Research Questions, Objectives, and Hypotheses

The broad goals of this study are to contribute to knowledge for predicting tree species resiliency to projected climate changes and to inform species selection for reforestation efforts in the PNW. Therefore, research questions for this study include: 1) How does species-specific climate sensitivity influence annual radial growth and latewood development in contrasting levels of water deficit for 11 native and non-native conifer species in western Oregon? 2) How does overall wood basic density vary under contrasting levels of water deficit between 11 native and non-native conifer species in western Oregon?

Objectives for this study include: 1) Determine annual and seasonal trends in the growth-climate relationships between the 11 species across the water deficit gradient; 2) identify which

climate variables most influence the annual basal area increment, annual latewood basal area increment, and latewood percentages as well as determine the extent of their influence for the 11 species across the water deficit gradient; and 3) measure and compare overall wood basic density for the 11 species across the water deficit gradient.

Specifically, it is hypothesized that:

Hypothesis 1: The extent to which water deficit limits growth is partially species-dependent, and the annual basal area increment and annual latewood basal area increment tends to become more limited as water availability decreases eastward along the water deficit gradient from the Willamette Valley to the Coast Range for less drought tolerant or drought intolerant species, including grand fir, giant sequoia, western hemlock, Port-Orford-cedar, Sitka spruce, and to a less extent, western redcedar and western white pine, while also showing greater variation in year-to-year measurements due to higher sensitivity to climate variability. Species such as Douglas-fir and Leyland cypress that are adapted to a wider range of conditions tend to be less sensitive to differences in climate conditions and would therefore have decreased annual basal area increment and annual latewood basal area increment eastward across the sites at a lower magnitude compared to the more drought sensitive species, higher measurements in drier sites compared to the more drought sensitive species, and less variation in year-to-year measurements. Species such as Willamette Valley ponderosa pine that are more adapted to drier conditions as indicated by their native range would have less of an increase in annual basal area increment and annual latewood basal area increment moving westward along the water deficit gradient, have lower measurements on sites with higher water availability compared to species adapted to moist conditions, and show greater variation in year-to-year measurements.

Hypothesis 2: Based on the relationships described in hypothesis 1 and given that greater latewood percentages are associated with drought conditions, Douglas-fir and Leyland cypress, which tend to be more drought resistant but also most productive under conditions of higher water availability, would show a slight increase in overall annual latewood percentage eastward across the water deficit gradient while reflecting fewer extreme differences in year-to-year variability. Meanwhile, all other less drought resistant or drought intolerant species, with the exception of Willamette Valley ponderosa pine, would show a more dramatic increase in overall annual latewood percentage eastward across the gradient while reflecting more year-to-year variability. Willamette Valley ponderosa pine, which is adapted to drier environments but still sensitive to water deficit, would instead show less of an increase in overall annual latewood percentage eastward across the gradient while reflecting more year-to-year variability.

Hypothesis 3: Given the positive correlation between latewood percentage and wood basic density, the species and site combinations that were expected to develop high annual latewood percentages as outlined in hypothesis 2 would also develop a higher wood basic density.

## 3.5 Methods

### 3.5.1 Study Design and Starker Forests, Inc Species Trial

This study covers a gradient in climate regimes and water deficit across site locations that range from the central Oregon Coast Range to the foothills of the Willamette Valley. The Oregon Coast Range is a mountain range that runs parallel to the Pacific Ocean and is characterized by having a mild maritime climate with cool, dry summers and mild, wet winters (McGarigal and McComb, 1995). The Oregon Coast Range creates a rain shadow effect that results the

Willamette Valley of Oregon, located on the lee side of the Oregon Coast Range, having comparatively warmer conditions with less rainfall (Omernik and Griffith, n.d.). While western Oregon is considered to be a highly productive area, the distinct climate gradient across the Coast Range and Willamette Valley ecoregions can be used to inform the growth-climate relationships for many commercially and ecologically valuable species.

In 1996, the Starker Forests, Inc Species Trial (SFIST) was established to determine how well 12 different native and non-native conifer species would grow across the range of Starker Forests, Inc's ownership in western Oregon. The purpose of the SFIST was to identify potential alternative timber species considering the expected changes in climate and its associated disturbances may negatively impact the primary crop species, namely Douglas-fir, grown in this region. Three sites, named Huffman, Underhill, and Campbell, were chosen to represent the gradient of water deficit across the company's property from the central Coast Range to the foothills of the Willamette Valley of western Oregon.

The Huffman site has the highest average annual rainfall of 2,000 mm and lowest average annual potential evapotranspiration of 800 mm between the three sites. It is the furthest west of the three sites and is located in in Eddyville, Oregon within the central Oregon Coastal Range. The site has an elevation of 138 meters and consists of soils from the Bohannon-Preacher Complex, which have a udic moisture regime that is characterized by having available water that equals or exceeds the amount of evapotranspiration (NRCS, n.d.). Considering the observed climate and soil characteristics, the Huffman site will represent the wet site for this study and will hereafter be referred to as the Huffman (wet) site.

The Underhill site has the intermediate average annual rainfall of 1,700 mm and an average annual potential evapotranspiration of 850 mm. It is located in Blodgett, Oregon, found

in the eastern side of the Oregon Coast Range between the Huffman and Campbell sites. The site has an elevation of 328 meters and consists of soils from the Preacher-Bohannon-Slickrock complex and the Apt-McDuff complex (NRCS, n.d.). Considering the observed climate and soil characteristics, the Underhill site will represent the intermediate site for this study and will hereafter be referred to as the Underhill (intermediate) site.

The Campbell site has the lowest annual rainfall of 1,300 mm and highest average annual potential evapotranspiration of 940 mm between the three sites. It is the furthest east of the three sites and is located in Corvallis, Oregon in the western Willamette Valley. The site has an elevation of 196 meters and consists of soils from the Dixonville-Gellatly complex and the Philomath series (NRCS, n.d.). Considering the observed climate and soil characteristics, the Campbell site will represent the dry site for this study and will hereafter be referred to as the Campbell (dry) site. Additional information on the SFIST and study sites is included in Chapter 2 pages 41-43.

The species that were initially planted for the SFIST included Port-Orford-cedar (POC), Willamette Valley ponderosa pine (WVPP), giant sequoia (GS), a blister rust resistant variety of western white pine (WWP), Sitka spruce (SSP), a weevil resistant variety of Sitka spruce (WRSP), western redcedar (WRC), western hemlock (WH), Leyland cypress (LC), grand fir (GF), Douglas-fir (DF), and Japanese larch (*Larix kaempferi*). However, Japanese larch will be excluded from this study due to the nearly 100% mortality observed at all three sites.

Before these sites were established for SFIST, the land was forested and managed for commercial timber production. Prior to the start of the study, the sites were cleared of brush and subsoiled and 12, 52 m x 55 m plots were established with each of the 12 species being randomly assigned to a plot. The trees at each site were planted between 1996 and 1998 depending on local

seedling availability, with most trees being planted in 1996. Seedling were grown in a container and planted with a Vexar mesh tube to protect them from ungulate browsing. Seedlings were planted at a 3 m x 3 m spacing. Herbicide was regularly applied during the first two years of growth to reduce the presence of competing vegetation.

In January of 2021, measurement plots were installed within each site. Within the center of each plot, a 30.5 m x 30.5 m measurement plot was established that contained approximately 100 trees consisting of 10 rows of 10 trees. These measurement plots were used to sample trees in this study. Each measurement plot had a surrounding buffer of about 3 to 4 rows to minimize the impact of edge effects in this study. Additional information and figures on the site history and plot structure is included in Chapter 2 pages 44-47.

### 3.5.2 Climate Measurements

Weather stations were installed in a cleared area within 0.3 miles of each site to record half-hourly climate variables, including rainfall (mm), minimum, maximum, and average temperature (°C), relative humidity (%), average and maximum vapor pressure deficit (kPa), and solar radiation (MJ $m^2$) over a one-year period. Estimated daily and monthly climate data since 1996 was collected through the PRISM model (PRISM Climate Group, n.d.). Considering averages provided by PRISM are only an approximation for our study sites, collecting site-specific climate information from the weather stations over the course of one year allowed for the calibration of past PRISM data and improved its accuracy for use in analyses. Calibration was conducted using a linear regression using the recorded weather station data and respective PRISM data during the same time period to determine the correlation coefficient and apply the regression equation for each climate variable at each site.

The cumulative Growing degree days (GDD) were then calculated for every month since 1996 at each site, which was determined by referring to the mean daily temperature and adding the number of degrees above 5°C and below 25°C. If the mean temperature is at or below the 5°C threshold, the GDD for that day would be zero. The GDD for each day in a given month is then summed to determine the monthly GDD. Monthly potential evapotranspiration (PET) values since 1996 were calculated for each site using the temperature-based equation derived from Hamon (1963), which was then used to calculate monthly water deficit and water surplus. This equation accounts for saturated water vapor concentration, mean temperature, and day length to determine PET. Monthly values of the Palmer Drought Severity Index (PDSI) since 1996 were also calculated for each site using the PDSI package in R (R Core Team, 2020. v4.0.5; Zhong et al., 2017. v0.1.3).

Using recorded and derived climate variables allowed for measurements to be determined at the annual, seasonal, and monthly scale from 1996 to 2021 for rainfall (mm), mean, minimum, and maximum temperature (°C), mean and maximum VPD (kPa), relative humidity (%), PET (mm), PDSI, global radiation (MJ $m^2$), and GDD. Additional information on climate measurements is included in Chapter 2 pages 47-51.

### 3.5.3 Wood Increment Core Measurements

The 10 trees per measurement plot that were selected to have dendrometer bands (Chapter 2 page 53) also had wood increment cores extracted from them in March of 2022. The lack of diameter growth measured across all trees with dendrometer bands during the months of January and February of 2022 ensured that the trees had ceased to continue growing, which indicated that the annual tree ring for 2021 was complete. Coring trees that had monthly diameter

growth measurements accounted for over the course of one year would allow for comparisons to be made between the cumulative observed growth and tree ring measurements. Further, the quartile process used to select trees for dendrometer band installation would allow for a representative sample of wood increment cores to be acquired.

Wood cores with a 5.15 mm diameter were extracted using a Haglöf increment borer at breast height (1.37 m). A bark-to-bark core sampling was conducted, which would allow there to be a replicate for each bark-to-pith sample to be used to compare ring measurements and put aside for future research. Openings in the tree as a result of coring were sealed using a water-resistant putty to minimize tree vulnerability to insects and diseases. Cores were stored in large paper straws to protect the cores from physical and water damage. During the same day a given core was extracted, the green mass (g) was measured using a scale and green volume (mL) was measured using a water displacement technique. Following these measurements, the cores were conditioned. The conditioning process involved the cores remaining for two to four weeks in a 20°C, low humidity environment. Following the conditioning process, the dry weight of each core was weighed to allow for the calculation of the wood moisture content (Eckelman, 1997).

$$Moisture\ content\ (\%) = \frac{Green\ weight\ (g) - Dry\ weight\ (g)}{Dry\ weight\ (g)} * 100 \quad (1)$$

The wood basic density (WBD) was calculated using the following formula:

$$Basic\ density\ (\frac{g}{cm^3}) = \frac{dry\ weight\ (g)}{green\ volume\ (cm^3)} \quad (2)$$

The dried cores were then glued to labeled core mounts, ensuring that the core was oriented as it was when removed from the tree, in which the wood fibers are aligned vertically when viewed from the ends of the mount. The cores are pressed down into the mount grooves with a tightly wrapped string, which ensures they are glued securely to the mounts. The mounted

cores were then processed through a belt sander and then hand sanded using an extra fine sanding sponge, which allows for the tree ring boundaries to be more visibly distinct. Once the sanding process has been completed, the WinDENDRO$^{TM}$ program (Regent Instruments Canada Inc.) was utilized to scan cores and measure their total and latewood tree ring widths to the 0.0001 mm.

Considering tree ring widths decrease as trees age due to increasing stem diameter, using raw ring widths in analyses would not be able to clearly reveal environmental impacts on tree growth (Liu et al. 2014). Therefore, standardization techniques can be used to remove the age trend present in tree ring widths to only retain climate and environmental signals. Total and latewood tree ring widths were converted to annual basal area increment (BAI, $cm^2$), which represents total ring area for a given year and accounts for age by including tree stem diameter. The BAI standardization approach represents tree growth better than using tree ring widths (Biondi, 1998). This conversion was conducted using the following formula:

$$BAI = \pi (R_n^2 - R_{n-1}^2) \quad (3)$$

Where:

*BAI* is annual basal area increment; *R* is the tree radius; and *n* is the year associated with a given tree ring.

BAI was calculated from pith to bark and assumes a concentrical distribution of tree rings (Phipps and Whiton, 1988). Latewood basal area increment (LW BAI) takes into account the contribution of the earlywood (EW) to the total radius for a given year. Latewood (LW) percentage was then calculated by dividing the LW BAI by the total BAI for a given year.

### 3.5.4 Statistical Analyses

#### 3.5.4.1 *Wood Basic Density Analysis*

A two-way ANOVA and Tukey's multiple comparisons test were utilized to determine if there was a significant difference in the WBD between species and sites or if the species by site interaction was significant. Tukey's multiple comparisons test was used considering all possible comparisons between more than two groups were being compared, the groups had equal sample sizes, and it avoids the risk of an inflated type 1 error while making multiple comparisons. The ANOVA and Tukey's multiple comparisons test assumptions were checked to ensure that they were met. Normal Q-Q plots of residuals and plots of standardized residuals against fitted values were used to assess model assumptions.

#### 3.5.4.2 *Tree Ring and Climate Analysis*

Time series linear mixed effect models were developed to determine the relationship between climate and the response variables BAI, LW BAI, and LW percentage for the 11 species. Each model contained a site variable that was included as a fixed effect considering site differences are of interest and are constant across all species and individual trees. The basal area for each tree in a given year was also included as fixed effects in all models to account for the variation in tree sizes and the slowing of growth that occurs as trees reach a certain threshold in size. These variables were significant and resulted in a lower model AIC value. Climate variables were included as fixed effects considering climate is of interest and is constant across all individual trees at a given site. Variable selection techniques were employed to determine which climate variables were most important in explaining variation in the response variables. The random effect of individual trees was also included in all models to account for random error

associated with unidentifiable tree-to-tree variation. These models also accounted for autocorrelation that resulted from the longitudinal nature of the data.

An example of a model with the three response variables is provided:

$$sqrtBAI_{ijkt},\ sqrtLWBAI_{ijkt},\ LWp_{ijkt} = \beta_0 + \beta_1 Site + \beta_2 BA_{ijkt} + \beta_3 C_{ijkt}\ \eta_{ij}\ t + cijk + \epsilon_{ijkt}$$

$$1 \leq i \leq 11,\ 1 \leq j \leq 3,\ 1 \leq k \leq 10,\ 1 \leq t \leq 22$$

Where:

$sqrtBAI_{ijkt}$ is the square root of the annual basal area increment, $sqrtLWBAI_{ijkt}$ is the square root of the latewood basal area increment and $LWp_{ijkt}$ is the latewood percentage of the $k^{th}$ tree for $i^{\text{th}}$ species in $j^{th}$ site on $t^{th}$ year; $\beta_1 Site$ is the fixed effect on the response for $j^{th}$ site; $\beta_2 BA_{ijkt}$ is the basal area of $the\ k^{th}$ tree for $i^{\text{th}}$ species in $j^{th}$ site on $t^{th}$ year; $\beta_3 C_{ijkt}$ is the fixed effect of a climate variable on the response for $i^{\text{th}}$ species in $j^{th}$ site on $t^{th}$ year; $c_{ijk} \sim Normal(0, \sigma^2_{\text{tree}})$ is the random effect of the $ijk^{th}$ tree; and $\epsilon_{ijkt} \sim Normal(0, \Sigma)$ where $\Sigma$ is defined following an AR(1) structure.

The model assumptions were checked to ensure that they were met. The assumptions of a linear mixed model include: 1) observations are independent at each configuration of explanatory variables; 2) the response variable follows a gaussian distribution; and 3) subpopulations share equal variance.

The independence assumption was initially not met for all models, although species were randomly assigned to plots and the trees from which wood increment cores were extracted were randomly selected using a stratified random sampling approach. Considering this longitudinal dataset had autocorrelation, an AR(1) structure was applied to all models considering first-order autoregression was present, in which current values were correlated with the immediately

preceding value. Adding AR(1) removed the presence of autocorrelation, lowered the model AIC values, and allowed for the independence assumption to be met. To check the normality and equal variance assumption, a Normal Q-Q plot of residuals and a standardized residuals vs fitted plot were used.

The independence and normality assumptions were met for all models with BAI and LW BAI response variables and all assumptions were met for models with a LW percentage response variable. However, the standardized residuals vs fitted plots for all models with a BAI and latewood BAI response variable revealed data points with a funnel-shaped distribution, indicating that heteroscedasticity was present. To address the issue of unequal variance in the models, transformations of the response variable were compared. The square root transformation was most effective in removing heteroscedasticity and resulted in the most consistently random residual plots. To compare model performances between the original response variables and transformed response variables, the Furnival's index was used and confirmed improved model performances using the transformed response variables.

To determine which climate variables best explain growth for each species for a given response variable, all possible climate variables that would be biologically meaningful were considered and tested. These include the annual averages, spring and summer averages, and monthly averages from April to October for the mean, minimum, and maximum temperature (°C), mean and maximum VPD (kPa), relative humidity (%), PET (mm), and PDSI. These also include annual sums, spring and summer sums, and monthly sums of rainfall (mm), global radiation (MJ $m^2$), and GDD. There was a total of 120 climate variables tested.

The Variance Inflation Factor (VIF) was first tested using R (R core Team, 2020. v4.0.5.) to determine if there is multicollinearity present in this climate dataset. All linearly dependent

variables and those with a VIF greater than 10 were removed from the dataset considering a high VIF indicates high correlation with other variables (Vittinghoff et al., 2006).

The LASSO and stepwise variable selection methods were then applied to all remaining climate variables. LASSO, or Least Absolute Shrinkage and Selection Operator, uses a penalty function to shrink many regression coefficients to zero, implying that those predictor variables were not significant (Tibshirani, 1996). Further, considering this method does not exclusively use p-values for variable selection, it has a low Type 1 error risk. The stepwise variable selection method successively adds and removes potential predictor variables while testing for statistical significance and comparing AIC values. Different forms of this method, including forward and backward selection, were also tested. Climate variables consistently being reported as non-significant using all four methods were then removed. The remaining climate variables were then filtered for each species-specific model by checking the P-value, adjusted $r^2$, model AIC, VIF, and whether the sign of each estimate is biologically realistic.

#### 3.5.4.3 *Time Series Analysis*

A time series analysis was conducted using the Proc Mixed procedure in SAS Studio 3.8 software (SAS Institute, Cary NC). A time series analysis needed to be used due to the longitudinal nature of the response variables. The linear mixed model that was used accounted for the random effect of individual trees over time. The VC covariance structure was included considering it resulted in the lowest BIC compared to other tested covariance structures. A type 3 ANOVA test for fixed effects was used to determine if there were significant differences in responsible variables between species, sites, and years or if interactions between these variables were significant. BAI, LW BAI, and LW percentage across species, sites, and years were

compared via Least Squares Means (LSM). Given that many comparisons were being made, the Tukey-Kramer test was used to avoids the risk of an inflated type 1 error.

This analysis was conducted based on four, five-year interval averages for annual BAI, LW BAI, and LW percentage to simplify and better compare trends across species, sites, and time. Intervals include 2001-2006, 2007-2011, 2012-2016, and 2017-2021, and will be referred to by the last year listed in each interval.

## 3.6 Results

### 3.6.1 Weather from 1996-2021

The Huffman (wet), Underhill (intermediate), and Campbell (dry) sites are located along a gradient in climate conditions ranging from the central Oregon Coast Range to the foothills of the Willamette Valley in western Oregon. The primary climate variables of interest that differentiate the three sites include variables that impact levels of water deficit, including rainfall, PET, PDSI, and maximum VPD. Average climate conditions from 1996 until 2021 for the three sites are presented in table 3.1.

| **Average Climate Conditions Across Sites (1996-2021)** | | | |
|---|---|---|---|
| **Climate** | **Huffman (Wet)** | **Underhill (Intermediate)** | **Campbell (Dry)** |
| Rainfall (mm) | 1976 | 1786 | 1314 |
| PET (mm) | 856 | 915 | 941 |
| PDSI | 0.68 | -0.07 | -0.10 |
| Maximum VPD (kPa) | 0.85 | 1.02 | 1.12 |
| Maximum Temperature (°C) | 15.5 | 15.7 | 16.9 |
| Average Temperature (°C) | 9.7 | 10.7 | 11 |
| Minimum Temperature (°C) | 5.7 | 5.4 | 5.2 |
| Relative Humidity (%) | 82.9 | 72.6 | 71.5 |
| Radiation (MJ $m^2$ $month^{-1}$) | 390 | 396 | 398 |
| GDD | 2050 | 2143 | 2243 |

Table 3.1: Average climate variables from 1996-2021 for the Huffman (wet), Underhill (intermediate), and Campbell (dry) sites, including rainfall (mm), PET (mm), PDSI, maximum VPD (kPa), maximum, average, and minimum temperature (°C), radiation (MJ $m^2$ $month^{-1}$), and GDD.

#### 3.6.1.1 *Water Balance*

Average annual rainfall was significantly different across sites (one-way ANOVA, $P < 0.0001$). Average annual rainfall was significantly higher at the Huffman (wet) and Underhill (intermediate) sites than at the Campbell (dry) site. There was also a significant difference in PET across sites (one-way ANOVA, $P < 0.0001$). PET was significantly higher at the Campbell (dry) site than at the Huffman (wet) and Underhill (intermediate) sites.

The 1996 to 2021 annual water balance at each site was determined from the difference between average monthly rainfall and average monthly PET (Figure 3.2). At the Campbell (dry) site, the period of water deficit began in early April and lasted until mid-September, which was the longest among the three sites. The Campbell (dry) site also had the highest water deficit peak in July of 135.7 mm and lowest peak water surplus in December of 216.4 mm among all sites. At both the Underhill (intermediate) and Huffman (wet) sites, the period of water deficit lasted from early May until early September. The peak water deficit in July at these two sites were also similar and averaged 117.6 mm. However, Huffman (wet) site had the higher peak water surplus of 315.49 mm in December compared to the Underhill (intermediate) site, which had peak water surplus in December of 288.76 mm.

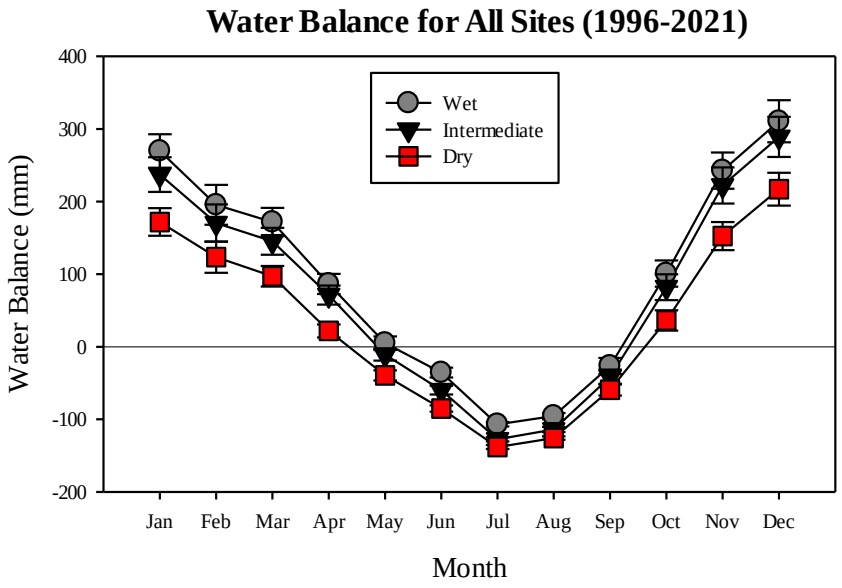


Figure 3.1: Average monthly water balance from 1996 to 2021 for the Huffman (wet), Underhill (intermediate), and Campbell (dry) sites with error bars representing standard error. Periods of water surplus are indicated by measurements above the line at zero while periods of water deficit are indicated by measurements below the line at zero.

#### 3.6.1.2 *Vapor Pressure Deficit*

2021 maximum VPD was significantly different across sites (one-way ANOVA, $P < 0.0001$). 2021 maximum VPD was significantly higher at the Campbell (dry) site than at the Huffman (wet) and Underhill (intermediate) sites. The maximum VPD for the Campbell (dry) site was typically higher throughout the year compared to the other sites and had the highest average peak in August at 2.55 kPa. The maximum VPD for the Huffman (wet) site was typically lower throughout the year compared to the other sites and had the lowest average peak in August at 1.77 kPa while the Underhill (intermediate) site had an average peak in August of 2.15 kPa (Figure 3.2).

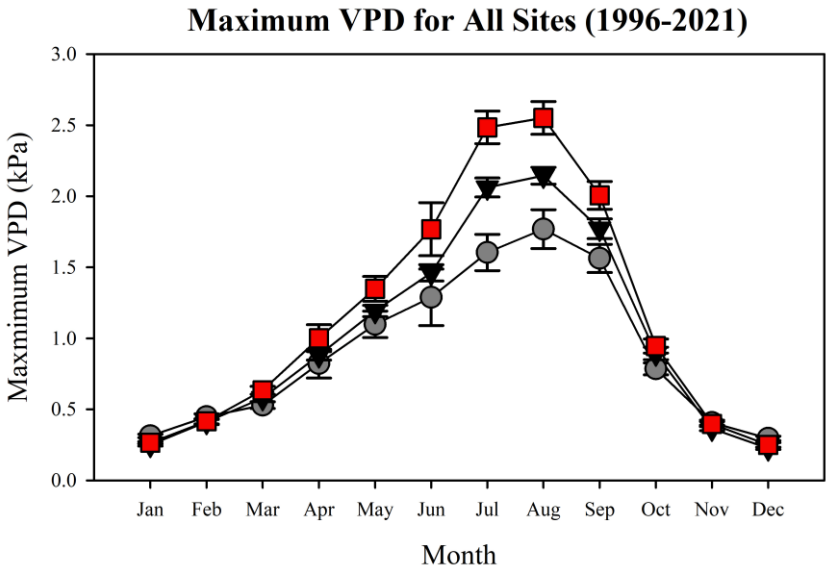


Figure 3.2: Average of maximum VPD (kPa) from 1996 to 2021 for the Huffman (wet), Underhill (intermediate), and Campbell (dry) sites, including average of monthly maximum VPD (kPa) with error bars representing standard error.

#### 3.6.1.3 *Palmer Drought Severity Index*

There was not a significant difference in mean annual PDSI between 1996 and 2021 for the three sites (one-way ANOVA, $P = 0.913$). There were similar trends in mean annual PDSI between sites over time. In general, the period between 1996 and 1998-1999 was consistently wet for all sites, followed by alternating years of droughty and wet conditions. The most severe droughts that have affected the three sites occurred during 2001, 2014, and 2016. While there were periods of fluctuation in PDSI across the years, its extent varied across sites; the Campbell (dry) site tended to have more intense droughts and less wet conditions compared to the Huffman (wet) site (Figure 3.3).

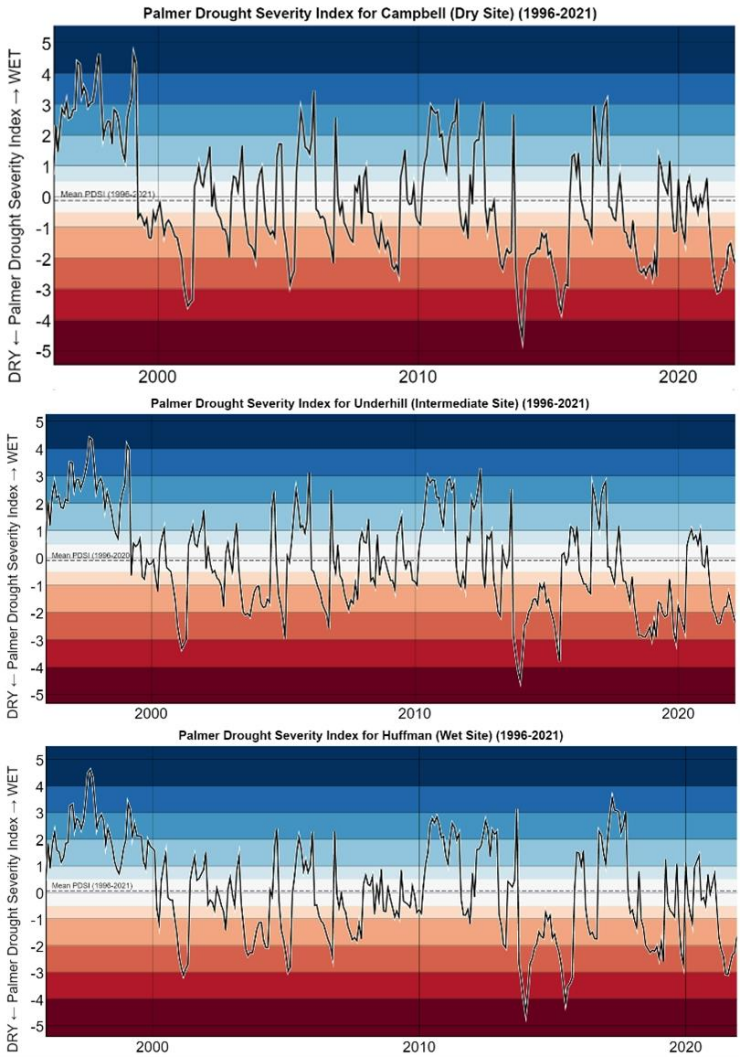


| PDSI Classifications | | |
|---|---|---|
| 4.0 or more | Extremely wet | |
| 3.0 to 3.99 | Very wet | |
| 2.0 to 2.99 | Moderately wet | |
| 1.0 to 1.99 | Slightly wet | |
| 0.5 to 0.99 | Incipient wet spell | |
| 0.49 to -0.49 | Near normal | |
| -0.5 to -0.99 | Incipient dry spell | |
| -1.0 to -1.99 | Mild drought | |
| -2.0 to -2.99 | Moderate drought | |
| -3.0 to -3.99 | Severe drought | |
| -4.0 or less | Extreme drought | |

Figure 3.3: Monthly PDSI from 1996 to 2021 for the Huffman (wet), Underhill (intermediate), and Campbell (dry) sites.

## 3.6.2 Annual Basal Area Increment

### 3.6.2.1 *Trends in Annual Basal Area Increment*

Annual BAIs from 1998-2007 until 2021 for each species across the three sites are shown in figure 3.4. For the majority of species, with the exception of WWP, annual BAI at the Huffman (wet) site had dramatically surpassed the annual BAI at the Underhill (intermediate) and Campbell (dry) sites until the early to mid 2010's. Up until the early to mid 2010's, the

Campbell (dry) site typically the lowest annual BAI, with the execption of LC and WVPP. After the early to mid 2010's, for many of these species, annual BAI at the Huffman (wet) site declined while annual BAI at the Underhill (intermediate) and Campbell (dry) site appear to have matched or surpassed growth at the Huffman (wet) site. This was especially apparent for WRC and WRSP, in which annual BAI at the Underhill (intermediate) site dramatically surpassed growth at the other two sites. In contrast, annual BAI for WWP appeared relatively consistent across sites over the years and had typically increased until the late 2010's.

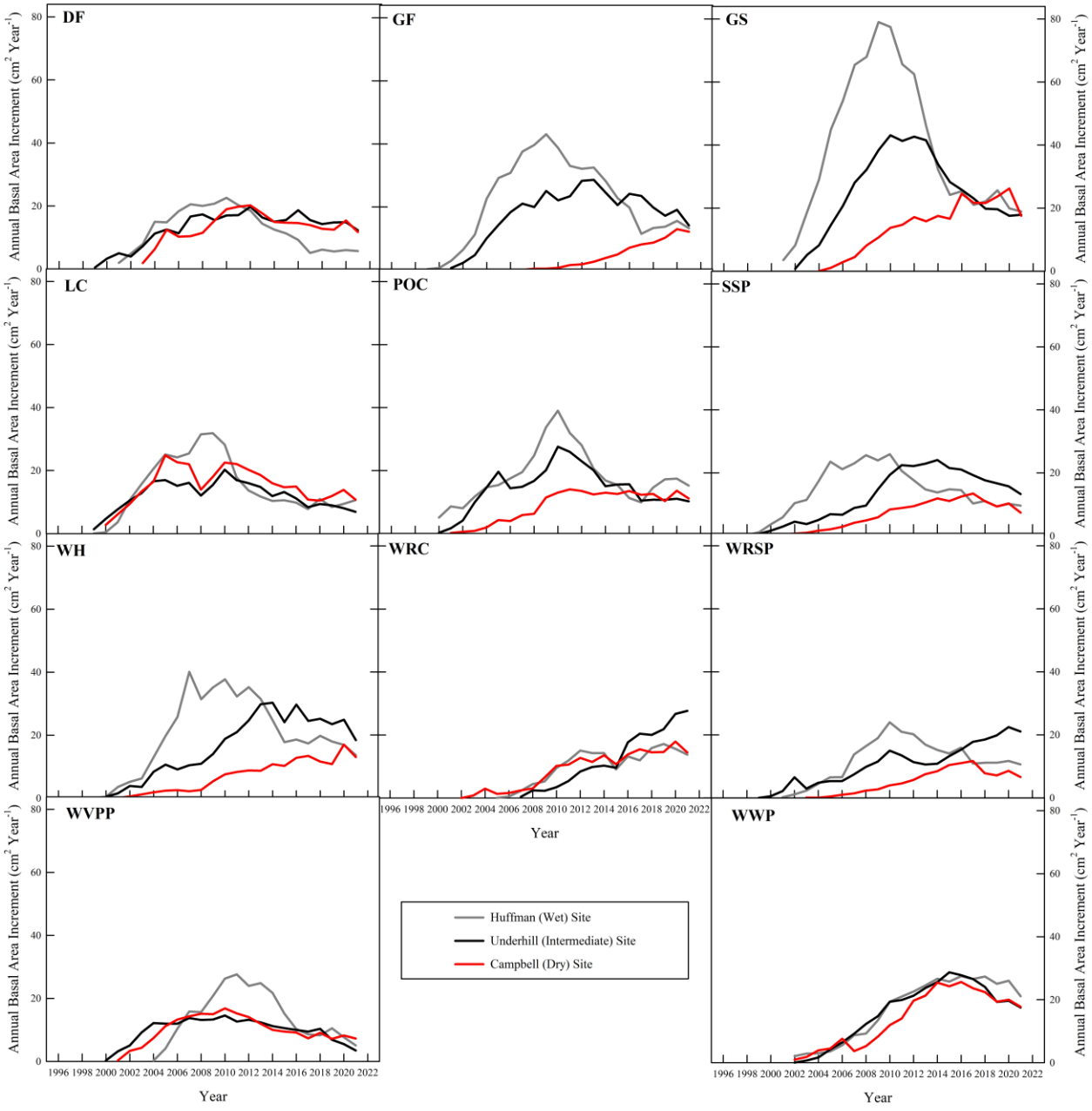


Figure 3.4: Annual BAI ($cm^2\,Year^{-1}$) from 1998-2007 until 2021 for each species across the Huffman (wet), Underhill (intermediate), and Campbell (dry) sites.

The time series analysis revealed that species, sites, years, and all interactions between them were significant for annual BAI (Table 3.2). Given that the species by site by year interaction was significant, the pattern of BAI was significantly different between species and sites during different years. In general, GS at the Huffman (wet) and Underhill (intermediate) sites as well as GF and WH at the Huffman (wet) site tended to have a significantly higher BAI compared to the greatest number of species and site combinations, particularly in the late 2000's to early 2010's. The annual BAI for GS at the Huffman (wet) site was especially high during the late 2000's, in which it was significantly higher than other species and site combinations by 33.374 to 73.329 $cm^2$. Trends in annual BAI for each of the five-year intervals are shown in figure _.

| Source | BAI |
|---|---|
| Species | <0.0001 * |
| Site | <0.0001 * |
| Species*Site | <0.0001 * |
| Year | <0.0001 * |
| Species*Year | <0.0001 * |
| Site*year | <0.0001 * |
| Species*Site*Year | <0.0001 * |

Table 3.2: P-values associated with BAI for species, sites, years, and all possible interactions (three-way repeated measures ANOVA). Significant P-values, where $P < 0.05$, are indicated with an asterisk (*).

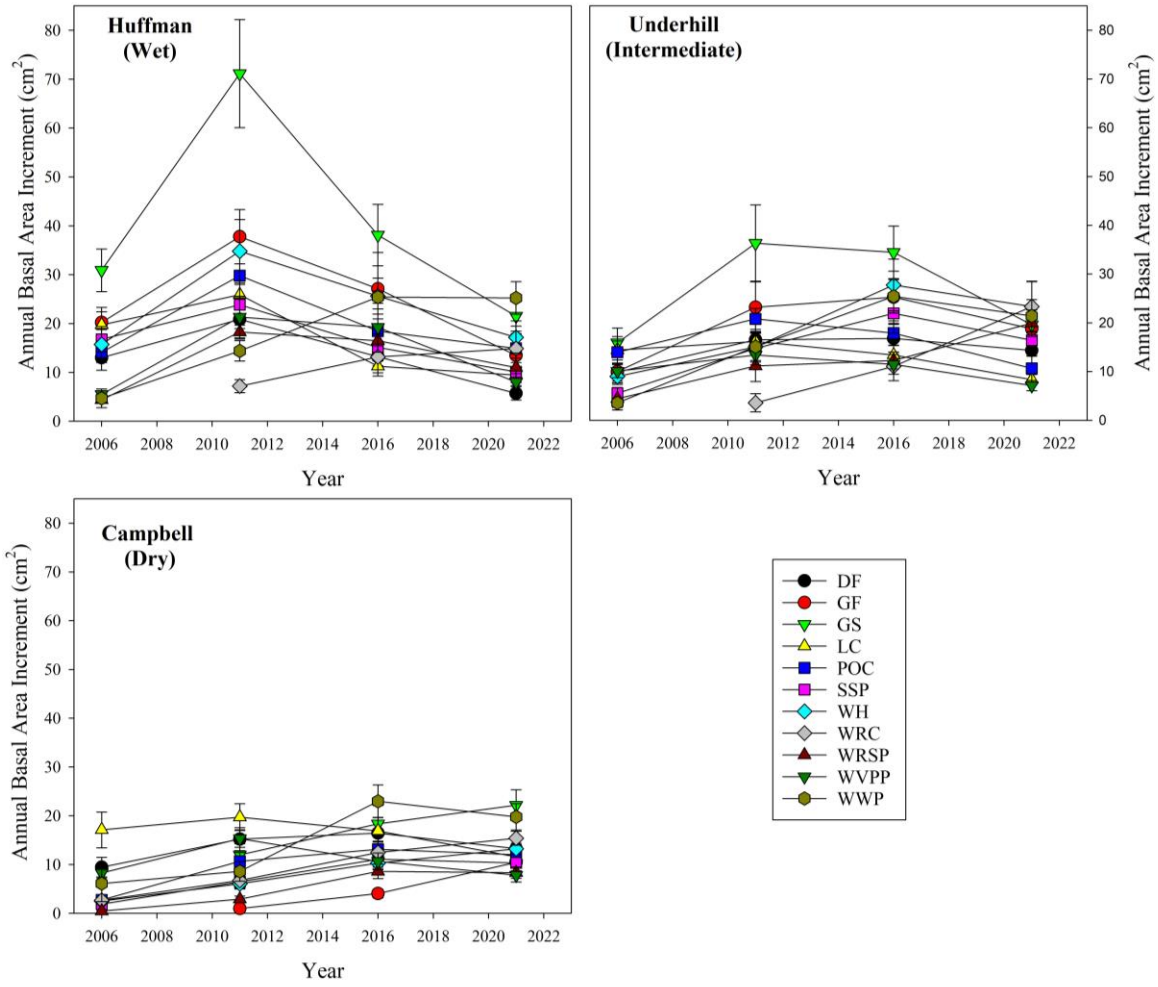


Figure 3.5: Average of annual BAI ($cm^2$ $Year^{-1}$) from five-year intervals (2001-2006, 2007-2011, 2012-2016, and 2017-2021) for all species at the Huffman (wet), Underhill (intermediate), and Campbell (dry) sites.

### 3.6.2.2 *Annual Basal Area Increment and Climate*

Spring rainfall was determined to be the climate variable that was significantly related to annual BAI $cm^2$ across the largest number of species and was characterized as having a positive relationship with annual BAI (table When comparing among these species, spring rainfall had the largest impact on annual BAI for GS as indicated by having the largest coefficient, followed by WH, WVPP, LC, and POC. Mean VPD in May was the second most frequently appearing climate variable across all species, and was negatively related to annual BAI. When comparing

among these species, mean VPPD in May had the largest impact on annual BAI for POC, followed by WRSP, SSP, and WVPP. Graphs of spring rainfall and mean May VPD from 1996 to 2021 are shown in the appendix ( Figures S.3.1 and S.3.2). July rainfall, April GDD, summer GDD, and annual maximum VPD were also significant for multiple species, with all but the annual maximum VPD having a positive relationship with annual BAI.

Four climate variables had a significant effect on the annual BAI for GF, which was the greatest number across all species, followed by DF, WRC, and WVPP, which each had three influential climate variables. GS, LC, POC, SSP, WH, and WRSP each had two significant climate variables, while WWP was only strongly influenced by one climate variable.

In general, DF was the only species in which its annual BAI was exclusively driven by summer water supply. The annual BAI of GS, POC, SSP, and WRSP was driven by water supply and conditions that affect evaporative demand, the annual BAI of LC, WH, and WRC was driven by water supply and conditions affecting growing season length, and the annual BAI of GF and WVPP was driven by water supply and conditions that affect evaporative demand and growing season length. In contrast, the annual BAI for WWP was exclusively driven by conditions that affect growing season length and was not significantly influenced by climate factors related to water availability. Species-specific annual BAI models, values describing model fit, and parameter estimates and standard errors associated with climate variables are listed in the appendix (Table S.3.1).

| Annual Basal Area Increment | | |
|---|---|---|
| **Climate Variables** | **Species** | **Parameter Estimate** |
| Annual Rainfall (mm) | DF | 0.0003545 |
| Spring Rainfall (mm) | GS | 0.0013537 |
| | LC | 0.0007703 |
| | POC | 0.0005002 |
| | WH | 0.0012839 |
| | WVPP | 0.0011267 |
| April Rainfall (mm) | WRC | 0.0014635 |
| July Rainfall (mm) | DF | 0.020655 |
| | SSP | 0.0026745 |
| | WRSP | 0.0029655 |
| August Rainfall (mm) | DF | 0.0093792 |
| Annual PDSI | GF | 0.0472874 |
| Annual Maximum VPD (kPa) | GF | -0.2901791 |
| | GS | -0.3531398 |
| May Mean VPD (kPa) | POC | -1.0865974 |
| | SSP | -0.8130418 |
| | WRSP | -0.8685165 |
| | WVPP | -0.6372394 |
| Annual Minimum Temperature (°C) | LC | 0.1212692 |
| May Minimum Temperature (°C) | GF | 0.1009278 |
| July Minimum Temperature (°C) | GF | 0.1014889 |
| Summer GDD | WRC | 0.0004261 |
| | WWP | 0.0004765 |
| April GDD | WVPP | 0.0015975 |

Table _: The climate variables and associated parameter estimates that were included in each species-specific annual BAI model. All parameter estimates associated with climate variables were significant ($P < 0.05$).

## 3.6.3 Annual Latewood Basal Area Increment

### 3.6.3.1 *Trends in Annual Latewood Basal Area Increment*

Annual LW BAI since 1998-2007 until 2021 for each species across the three sites are shown in figure 3.6. Similar to the trend in annual BAI for GF, GS, POC, SSP, WH, and WVPP, annual LW BAI for these species at the Huffman (wet) site had dramatically surpassed the the LW BAI at the Huffman (wet) and Underhill (intermediate) sites until the early to mid 2010's. Up until the early to mid 2010's, the Campbell (dry) site typically the lowest annual LW BAI. After the early to mid 2010's, for many of these species, annual BAI at the Huffman (wet) site declined while annual BAI at the Underhill (intermediate) and/or Campbell (dry) site matched or

surpassed growth at the Huffman (wet) site. In contast, annual LW BAI for LC at the Campbell (dry) site typically suprassed the LW BAI for LC at the other two sites. Similar to annual BAI, annual LW BAI for WRC and WWP were typically similar across sites and steadily increased with time.

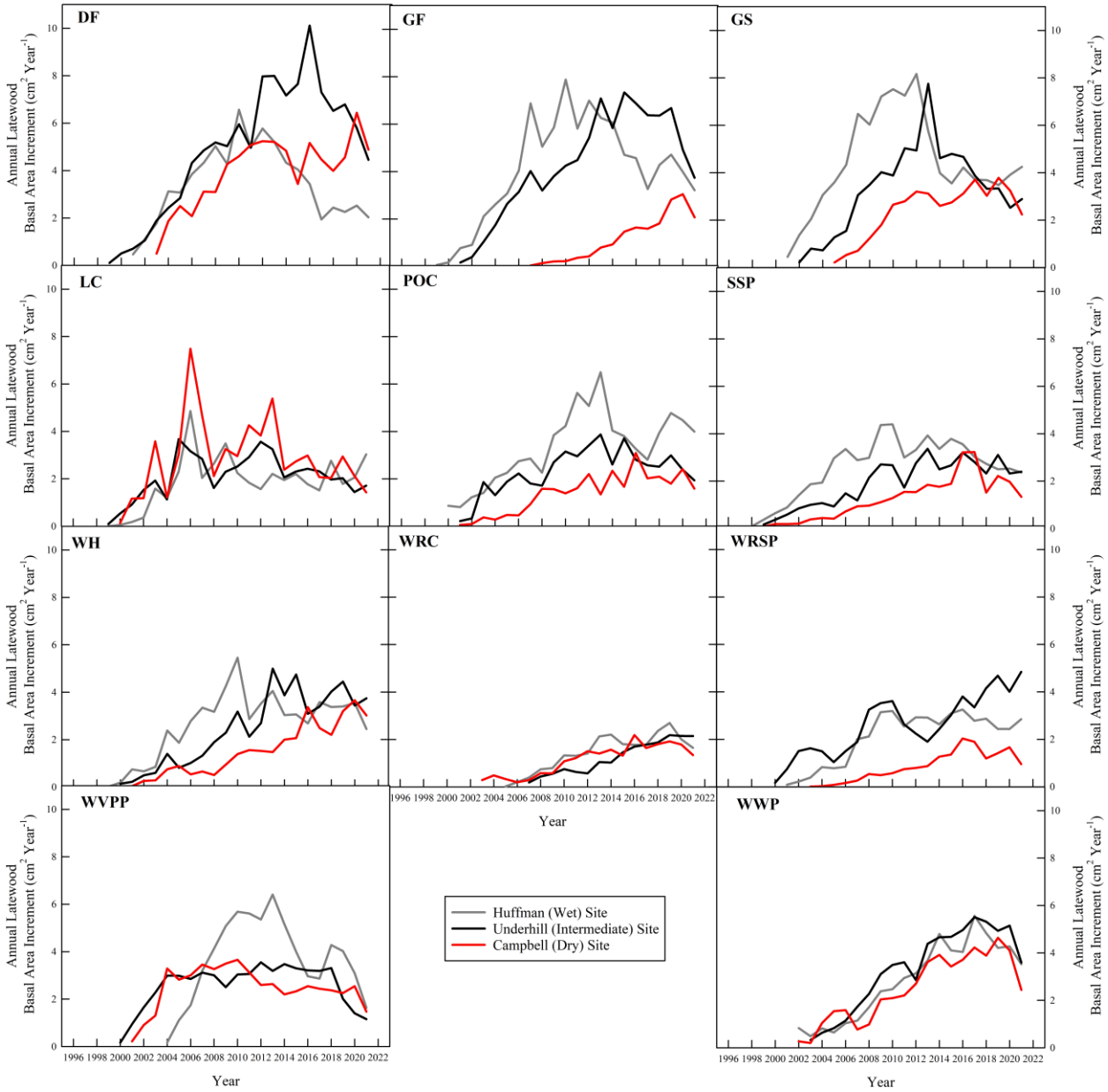


Figure 3.6: Annual LW BAI (cm$^2$ Year$^{-1}$) from 1998-2007 until 2021 for each species across the Huffman (wet), Underhill (intermediate), and Campbell (dry) sites.

The time series analysis revealed that species, sites, years, and all interactions between them were significant for LW BAI (Table 3.4). Given that the species by site by year interaction was significant, the pattern of LW BAI was significantly different between species and sites in different years. In general, DF at the Underhill (intermediate) site, GF at the Underhill (intermediate) and Huffman (wet) sites, and GS at the Huffman (wet) site tended to have a significantly higher LW BAI compared to the greatest number of species and site combinations, particularly in the late 2000's to early 2010's. DF in particular tended to have a high LW BAI in the early 2010's, which was significantly higher than many other species and site combinations by 3.891 to 7.16 $cm^2$. Trends in annual LW BAI for each of the five-year intervals are shown in figure 3.7.

| Source | LW BAI |
|---|---|
| Species | <0.0001 * |
| Site | <0.0001 * |
| Species*Site | 0.0008 * |
| Year | <0.0001 * |
| Species*Year | <0.0001 * |
| Site*Year | <0.0001 * |
| Species*Site*Year | <0.0001 * |

Table _: P-values associated with latewood basal area increment (LW BAI) for species, sites, years, and all possible interactions (three-way repeated measures ANOVA). Significant P-values, where $P < 0.05$, are indicated with an asterisk (*).

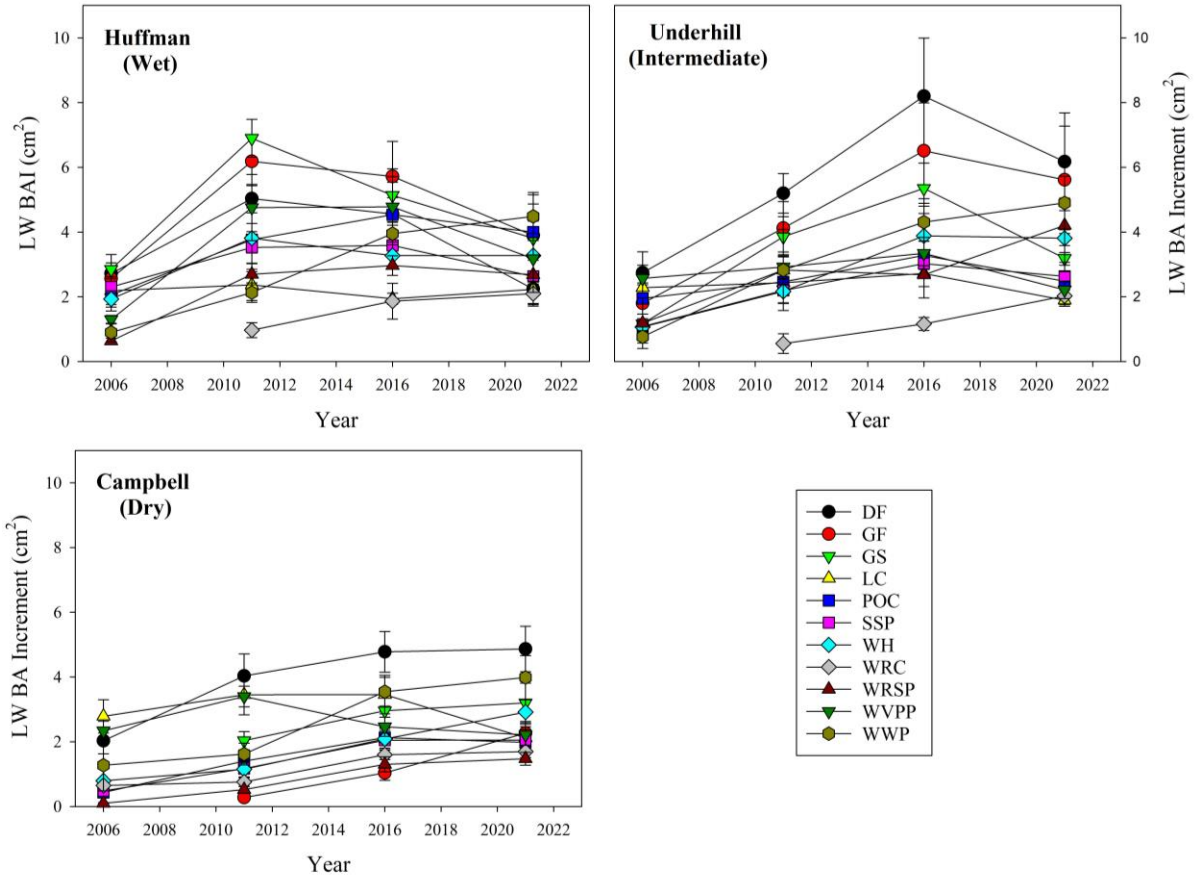


Figure 3.7: Average of annual LW BAI ($cm^2$ $Year^{-1}$) from five-year intervals (2001-2006, 2007-2011, 2012-2016, and 2017-2021) for all species at the Huffman (wet), Underhill (intermediate), and Campbell (dry) sites.

### 3.6.3.2 *Annual Latewood Basal Area Increment and Climate*

Summer rainfall was determined to be the climate variable that was significantly related to annual LW BAI ($cm^2$ $year^{-1}$) across the largest number of species and was characterized as having a positive relationship with annual BAI (table 3.5). When comparing among these species, summer rainfall had the largest impact on annual LW BAI for WH as indicated by having the largest coefficient, followed by SSP, WRC, DF, GF, POC, and GS. Annual maximum VPD was the second most frequently appearing climate variable across all species, and was instead negatively related to annual LW BAI. When comparing among these species,

annual maximum VPD had the largest impact on annual LW BAI for WRC, followed by WVPP, GF, DF, GS, and SSP. Graphs of summer rainfall and annual maximum VPD from 1996 to 2021 are shown in the appendix (Figures S.3.3 and S.3.4). Annual rainfall, spring rainfall, April rainfall, August rainfall, July minimum temperature, summer GDD, and April GDD were also significant for multiple species, with all having a positive relationship with annual LW BAI.

The annual LW BAI for WRC was influenced by seven climate variables, which was the greatest number across all species, followed by DF and GF, which each had four influential climate variables. SSP and WH each at three signifiant variables. Gs, LC, POC, WRSP, and WVPP each had two significant climate variables. WWP was only strongly influenced by the summer GDD.

In general, POC and WRSP were the only species in which its annual LW BAI was exclusively driven by water supply. The annual LW BAI of GS, LC, SSP, and WVPP was driven by water supply and conditions that affect evaporative demand, the annual LW BAI of WH was driven by water supply and conditions that affect growing season length, and the annual LW BAI of DF, GF, and WRC was driven by water supply, conditions that affect evaporative demand, and growing season length. In contrast, the annual LW BAI for WWP was exclusively driven by conditions that affect growing season length and was not significantly influenced by climate factors related to water availability.

Of the 14 total climate variables that were significant across all models, there were 11 climate variables that were included in both the annual BAI species-specific models and the annual LW BAI species-specific models. The exceptions include annual PDSI and the minimum temperature in May, which were only included in the annual BAI species-specific models, and summer rainfall and mean monthly radiation, which were only included in the annual LW BAI

species-specific models. Further, climate variables related to VPD had a negative coefficient across all models while all other climate variables had a postive coefficient across all models. Species-specific annual LW BAI models, values describing model fit, and parameter estimates and standard errors associated with climate variables are listed in the appendix (Table S.3.2).

| **Latewood Basal Area Increment** | | |
|---|---|---|
| **Climate Variables** | **Species** | **Parameter Estimates** |
| Annual Rainfall (mm) | DF | 0.0001852 |
| | SSP | 0.0001469 |
| Spring Rainfall (mm) | WH | 0.0005316 |
| Summer Rainfall (mm) | DF | 0.0007901 |
| | GF | 0.00077373 |
| | GS | 0.0006111 |
| | POC | 0.0006631 |
| | SSP | 0.0009017 |
| | WH | 0.0011717 |
| | WRC | 0.0011717 |
| April Rainfall (mm) | GF | 0.00061128 |
| | WRC | 0.001581 |
| July Rainfall (mm) | LC | 0.0074324 |
| | POC | 0.0034888 |
| | WRSP | 0.0019959 |
| August Rainfall (mm) | WRSP | 0.0018003 |
| | WVPP | 0.0029628 |
| Annual Maximum VPD (kPa) | DF | -0.2664699 |
| | DF | -0.2664699 |
| | GS | -0.1913911 |
| | SSP | -0.1009787 |
| | WRC | -0.459168 |
| | WVPP | -0.2922751 |
| May Mean VPD (kPa) | WRC | -0.2922751 |
| July mean VPD (kPa) | LC | -0.4561882 |
| Annual Minimum Temperature (°C) | WH | 0.0741518 |
| July Minimum Temperature (°C) | GF | 0.08487594 |
| Summer GDD | WRC | 0.001714 |
| | WWP | 0.00059655 |
| April GDD | DF | 0.0020617 |
| | WRC | 0.006454 |
| Mean Monthly Radiation (MJ m² month$^{-1}$) | WRC | 0.030857 |

Table 3.5: The climate variables and associated parameter estimates that were included in each species-specific annual LW BAI model. All parameter estimates associated with climate variables were significant ($P < 0.05$).

### 3.6.4 Annual Latewood Percentage

#### 3.6.4.1 *Trends in Annual Latewood Percentage*

Annual LW percentage since 1998-2007 until 2021 for each species across the three sites are shown in figure 3.8. In general, there were no consistent trends in annual LW percentage across sites over the years given that this measurement often fluctuated at different rates. However, annual LW percentage at the Campbell (dry) site tended to either decrease or remain consistent over time for the majority of species, and large increases in annual LW percentage were observed in a few years during the 2000's. Annual latewood percentage at the Huffman (wet) and Underhill (intermediate) sites tended to increase or remain consistent over time for the majority of species, with large increases being observed in the late 2000's and late 2010's.

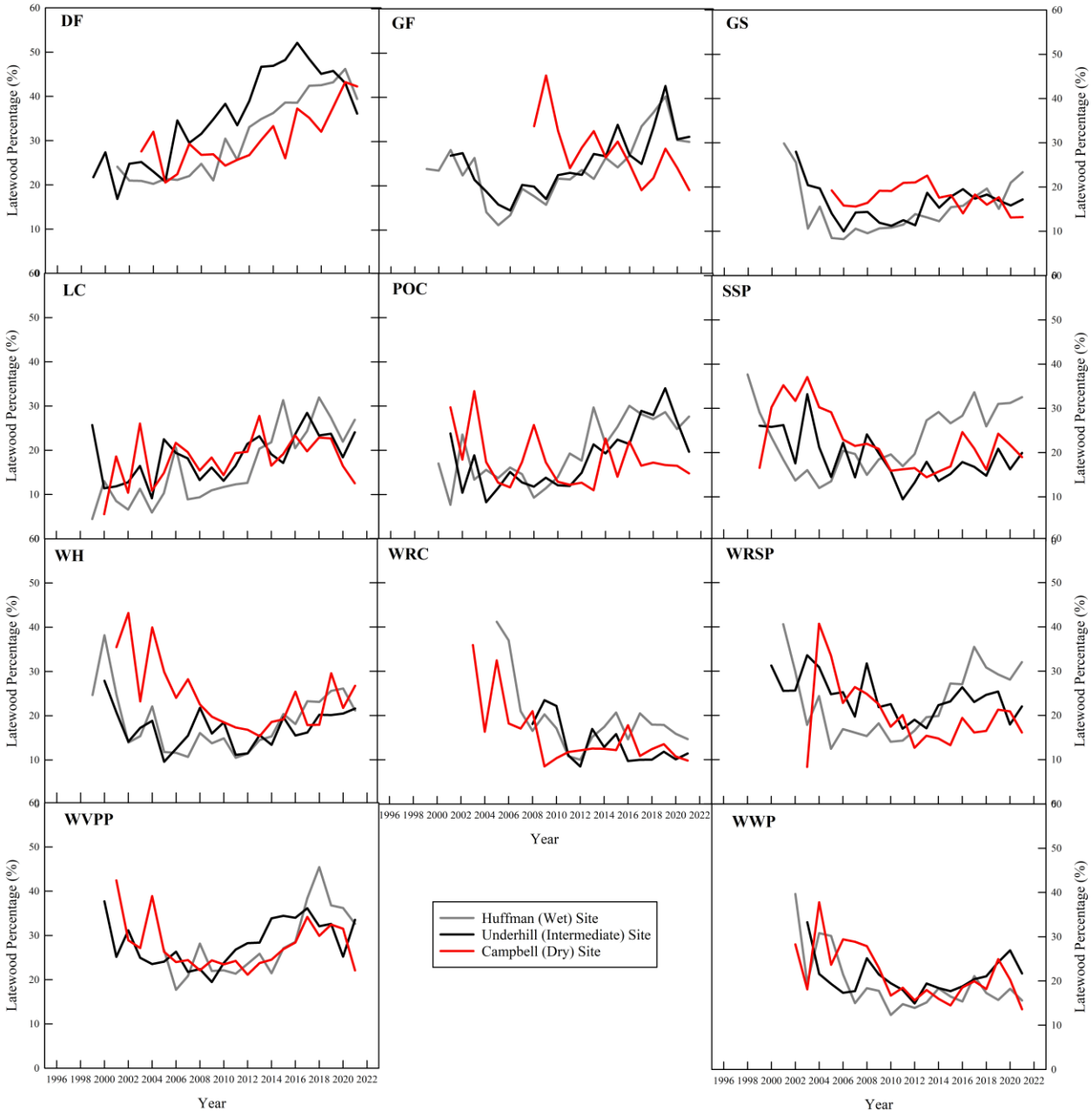


Figure 3.8: Annual LW percentage (%) from 1998-2007 until 2021 for each species across the Huffman (wet), Underhill (intermediate), and Campbell (dry) sites.

The time series analysis revealed that species, years, and all interactions between species, sites, and years were significant for LW percentage (Table 3.6). Given that the species by site by year interaction was significant, the pattern of LW percentage was significantly different

between species and sites in different years. In general, DF and GF at all sites and WVPP at the Huffman (wet) and Underhill (intermediate) sites had a higher LW percentage compared to the greatest number of species and site combinations, particularly in the 2010's. The LW percentage for DF at the Underhill (intermediate) site in the ate 2010's was particularly high considering it was significantly higher than many species and site combinations by 17.02 to 32.84%. Trends in annual LW percentage for each of the five-year intervals are shown in figure 3.9.

| Source | LW Percentage |
|---|---|
| Species | <0.0001 * |
| Site | 0.2886 |
| Species*Site | 0.0063 * |
| Year | <0.0001 * |
| Species*Year | <0.0001 * |
| Site*year | <0.0001 * |
| Species*Site*Year | <0.0001 * |

Table 3.6: P-values associated with latewood (LW) percentage for species, sites, years, and all possible interactions (three-way repeated measures ANOVA). Significant P-values, where $P < 0.05$, are indicated with an asterisk (*).

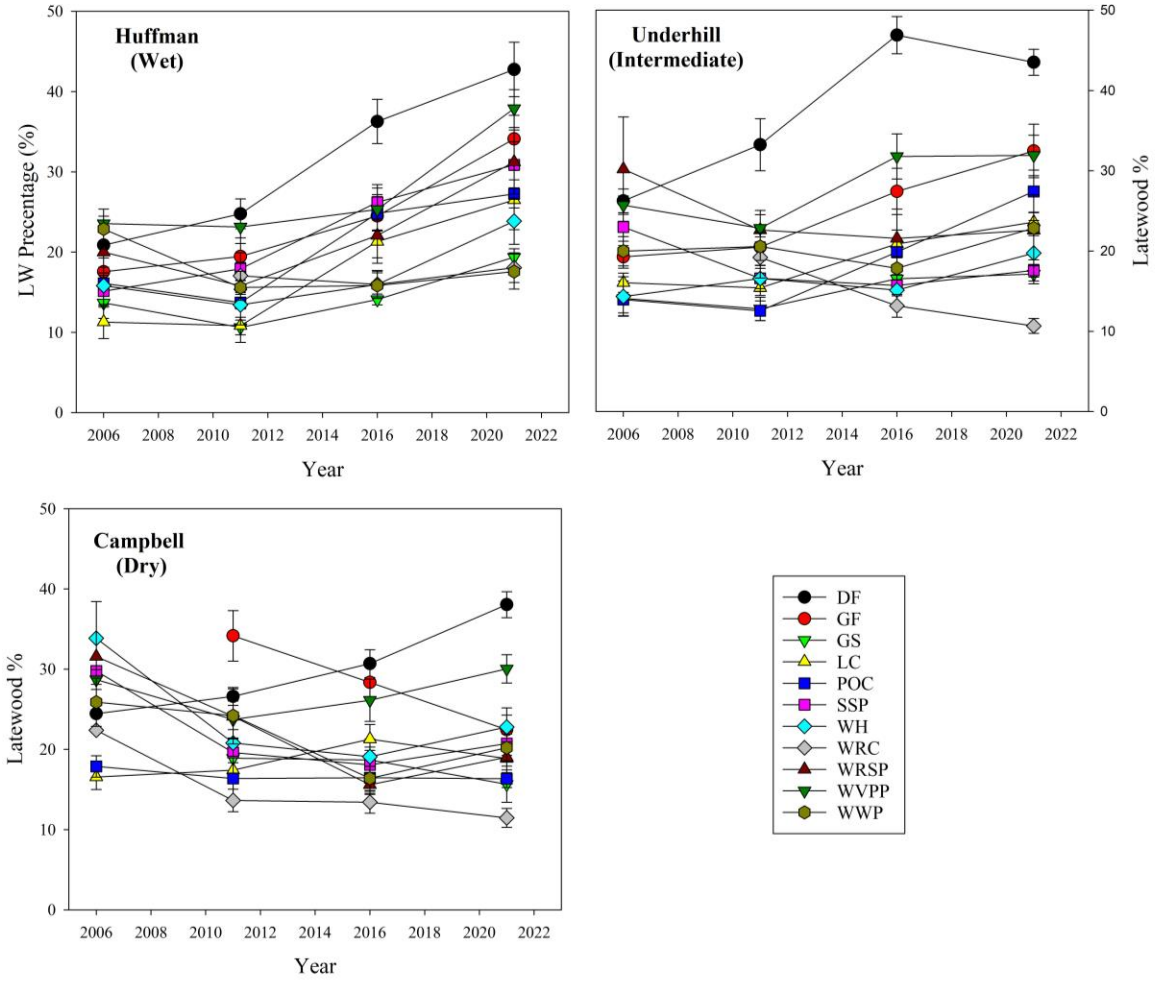


Figure 3.9: Average of annual LW percentage (%) from five-year intervals (2001-2006, 2007-20011, 2012-2016, and 2017-2021) for all species at the Huffman (wet), Underhill (intermediate), and Campbell (dry) sites.

### 3.6.4.1 *Annual Latewood Percentage and Climate*

August rainfall was determined to be the climate variable that was significantly related to annual LW percentage across the largest number of species and was characterized as typically having a positive relationship with annual LW percentage (table _). When comparing among these species, August rainfall had the largest impact on annual LW percentage for WRC as

indicated by having the largest coefficient, followed by WH, WRSP, WWP, and GS (Table 3.7). August rainfall appeared to have a negative correlation with LC and POC.

Annual rainfall was the second most frequently appearing climate variable across all species, and was typically negatively related to annual LW percentage. When comparing among these species, annual rainfall had the largest impact on annual LW BAI for WWP, followed by SSP, GF, and GF. Annual rainfall appeared to be postively related to annual LW percentage for DF. Graphs of August rainfall and annual rainfall from 1996 to 2021 are shown in the appendix (Figures S.3.5 and S.3.6). Mean May VPD, summer rainfall, April rainfall, annual PDSI, spring rainfall, and annual relative humidity were also significant for multiple species. The first four climate variables listed were positively related with annual LW percentage while the last two climate variables were negatively related with annual LW percentage. However, a few contradictions were present: GS, SSP, and WWP had a positive annual PDSI value and a negative annual rainfall value. LC and POC had a positive summer rainfall value but a negative August rainfall value as well as a negative spring rainfall value but a positive April rainfall value.

The annual LW percentage for GS, LC, POC, and WWP were influenced by four climate variables, which was the greatest number across all species, followed by SSP, which had three influential climate variables. DF, WH, WRC, and WRSP each had two signifiant climate variables. The annual LW percentage for GF was only strongly influenced by the annual rainfall while WVPP was only strongly infleunced by July rainfall.

In general, the annual LW percentage for DF, GF, GS, LC, POC, WRC, and WVPP were exclusively driven by water supply while the annual LW percentage of SSP, WH, and WWP were driven by water supply and conditions affecting evaportative demand. Unlike annual BAI

and annual LW BAI, annual LW percentage was not driven by conditions that affect growing season length for any species.

Of the 10 total climate variables that were significant across all LW BAI models, there were eight climate variables that overlapped with the annual BAI models. The exceptions include annual, May, and July minimum temperature as well as summer and April GDD, which were only included in the annual BAI models, while summer rainfall and annual relative humidity were only included in the annual LW percentage models. There were also eight climate variables that overlapped with the annual LW percentage models. The exceptions include mean July VPD, radiation, summer and April GDD, and annual and July minimum temperature, which were only included in the annual LW BAI models, while annual PDSI was only included in the annual LW percentage models.

Further, climate variables related to VPD had a negative coefficient across the annual BAI and LW BAI models, but was positive for the annual LW percentage models. All other climate variables had a postive coefficient across the annual BAI and LW BAI models while climate variables related to annual and early growing season water supply were typically negative for the annual LW BAI models. Species-specific annual LW percentage models, values describing model fit, and parameter estimates and standard errors associated with climate variables are listed in the appendix (S.3.3).

| Annual Latewood Percentage | | |
|---|---|---|
| **Climate Variables** | **Species** | **Parameter Estimates** |
| Annual Precipitation (mm) | DF | 0.004313 |
| | GF | -0.002232 |
| | GS | -0.002826 |
| | SSP | -0.002959 |
| | WWP | -0.005704 |
| Spring Precipitation (mm) | GS | -0.012198 |
| | LC | -0.029973 |
| | POC | -0.027461 |
| Summer Precipitation (mm) | DF | 0.022865 |
| | LC | 0.02875 |
| | POC | 0.03323 |
| April Precipitation (mm) | LC | 0.02982 |
| | POC | 0.029892 |
| July Precipitation (mm) | WVPP | -0.091894 |
| August Precipitation (mm) | GS | 0.036373 |
| | LC | -0.166881 |
| | POC | -0.118666 |
| | WH | 0.092083 |
| | WRC | 0.12152 |
| | WRSP | 0.08415 |
| | WWP | 0.081965 |
| Annual PDSI | GS | 0.76897 |
| | SSP | 1.331994 |
| | WWP | 1.584779 |
| Annual Maximum VPD (kPa) | WH | 2.554468 |
| May Mean VPD (kPa) | SSP | 24.214492 |
| | WWP | 17.836496 |
| Annual Relative Humidity (%) | WRC | -0.31994 |
| | WRSP | -0.4417 |

Table 3.7: The climate variables and associated parameter estimates that were included in each species-specific annual LW percentage model. All parameter estimates associated with climate variables were significant ($P < 0.05$).

### 3.6.5 Wood Basic Density

There was a strong species by site interaction for WBD (two-way ANOVA, $P < 0.0001$). LC at the Campbell (dry) site showed higher WBD compared to the majority of species and site combinations. In contrast, WVPP at the Huffman (wet) site showed lower WBD compared to a few other species and site combinations.

The WBD of LC at the Campbell (dry) site was significantly higher by 0.208 to 0.379 g $cm^{-3}$ than 25 other site and species combinations, with combinations involving all sites and the

majority of species. WVPP at the Huffman (wet) site was significantly lower by 0.242 to 0.251 g $cm^{-3}$ than three other site and species combinations. All other significant differences in WBD are demonstrated in table _.

| Wood Basic Density (g $cm^{-3}$) Across Species and Sites | | | | |
|---|---|---|---|---|
| **Species** | **Site** | **Wood Basic Density (g $cm^{-3}$)** | **SE** | |
| DF | Wet | 0.511 | 0.0271 | bcd |
| | Intermediate | 0.556 | 0.0257 | abcd |
| | Dry | 0.471 | 0.0257 | bcd |
| GF | Wet | 0.466 | 0.0311 | bcd |
| | Intermediate | 0.563 | 0.0311 | abcd |
| | Dry | 0.626 | 0.0311 | ab |
| GS | Wet | 0.444 | 0.0334 | bcd |
| | Intermediate | 0.478 | 0.0334 | bcd |
| | Dry | 0.411 | 0.0334 | cd |
| LC | Wet | 0.489 | 0.0534 | bcd |
| | Intermediate | 0.534 | 0.0478 | bcd |
| | Dry | 0.754 | 0.0478 | a |
| POC | Wet | 0.617 | 0.0271 | ab |
| | Intermediate | 0.480 | 0.0271 | bcd |
| | Dry | - | - | - |
| SSP | Wet | 0.499 | 0.0276 | bcd |
| | Intermediate | 0.540 | 0.0291 | bcd |
| | Dry | 0.525 | 0.0276 | bcd |
| WH | Wet | 0.477 | 0.0653 | bcd |
| | Intermediate | 0.562 | 0.0653 | abcd |
| | Dry | 0.610 | 0.0653 | bcd |
| WRC | Wet | 0.427 | 0.0474 | bcd |
| | Intermediate | 0.441 | 0.0474 | bcd |
| | Dry | 0.572 | 0.0474 | abcd |
| WRSP | Wet | 0.492 | 0.0327 | bcd |
| | Intermediate | 0.528 | 0.0327 | bcd |
| | Dry | 0.480 | 0.0327 | bcd |
| WVPP | Wet | 0.375 | 0.0234 | d |
| | Intermediate | 0.479 | 0.0234 | bcd |
| | Dry | 0.546 | 0.0234 | bcd |
| WWP | Wet | 0.442 | 0.0213 | bcd |
| | Intermediate | 0.439 | 0.0213 | bcd |
| | Dry | 0.482 | 0.0213 | bcd |

Table _: Mean and standard error (SE) of wood basic density (g $cm^{-3}$) for each species across the Huffman (wet), Underhill (intermediate), and Campbell (dry) sites acquired from wood increment cores extracted in the winter of 2022.

## 3.7 Discussion

### 3.7.1 Annual Basal Area Increment

When evaluating species' responses to environmental gradients, less sensitive species growing on more favorable sites, such as those with greater water availability and less evaporative demand, tend to have less of a tree ring response to climate variability while more sensitive species on limiting sites, such as those with a higher water deficit, would have stronger responses to climate variability (Fritts, 1976; Abrams et al., 1998). With this consideration, I hypothesized that species such as DF and LC, which tend to be more drought resistant but also more productive under conditions of higher water availability, would show a slight decline in overall annual BAI eastward across the water deficit gradient with less extreme differences in year-to-year variability. Meanwhile, less drought resistant species such as GF, GS, POC, SSP, WRSP, WH, WRC, and WWP were expected to show a more dramatic decline in overall annual BAI eastward across the water deficit gradient and greater year-to-year variability in BAI associated with more sensitive responses to interannual climate variability. WVPP, which is adapted to drier environments but still sensitive to water deficit, was expected to show less of an increase in overall annual BAI westward across the gradient while reflecting more year-to-year variability than DF or LC.

My results only partially support these hypotheses. The Huffman (wet) site had the highest overall annual BAI while the Campbell (dry) site had the lowest overall annual BAI for the majority of species, but only until the early to mid-2010's, after which the annual BAI at the Huffman (wet) site tended to decline or was surpassed by the two over sites, suggesting rapid initial growth at the wettest site but less extreme differences in growth between all sites in recent years. Further, in addition to DF and LC, WRC and WWP showed reduced year-to-year variability in BAI across sites. Although it has been reported that the growth of these species is limited by water deficit, they are both very adaptive and are capable of surviving under a wide

range of conditions, which may explain their relatively consistent annual BAIs over my study period (Grossnickle and Russell, 2006; Antos et al., 2016; Graham, 1990).

The decline in annual BAI at the wettest site in recent years for many species was concurrent with a high frequency of drought years as indicated by low annual PDSI values. There may be a few explanations for this observed trend. Due to the larger tree sizes at the Huffman (wet) site, competition for resources may be occurring, resulting in the slowing of growth or altered growth response to climate (Ettinger and HilleRisLambers 2013; Carnwath and Nelson 2016). The trees at the Huffman (wet) site may have also become acclimated to the wetter conditions typical of these sites up to the early 2010's and the prolonged and extreme drought events in recent years may have disproportionally impacted the tree growth responses at this site. This idea is supported by previous work showing that tree growth sensitivity to climate has the potential to change over time as a result of climate variability and long periods of cool and wet or warm and dry conditions (Carrer and Urbinati 2006, Hayles et al. 2007, Olivar et al. 2015).

My results also suggest that the pattern of annual BAI was significantly different between species and between sites at different times. In particular, GS at the Huffman (wet) and Underhill (intermediate) sites as well as GF and WH at the Huffman (wet) site tended to have a significantly higher annual BAI compared to many other species and site combinations, particularly in the late 2000's to early 2010's, which were dominated by wetter years with positive PDSI values and a few years with less extreme water deficit conditions. This finding is consistent with previous work suggesting that water deficit tends to be the most limiting growth factor in the PNW (Grier and Running, 1977; Bréda et al., 2006). Therefore, years in which water deficit is less extreme or in which there is sufficient water availability can promote the

growth of particularly sensitive species. Further, GS at the Huffman (wet) site showed the largest increases in annual BAI during this time. These trends reflect the known ecology of GS, GF, and WH.

The finding that the annual BAI for GS was primarily influenced by spring rainfall and maximum VPD is consistent with previous work suggesting that GS growing in the low elevation sites of the PNW are primarily limited by growing season water deficit and secondarily by higher summer temperatures (Rundel, 1972). Although GS in this study was planted outside of its native range, it was highly productive in the wetter and milder climates of the western Oregon Coast Range, while the lower water availability and higher evaporative demand at the Campbell (dry) site in the Willamette Valley foothills resulted in an annual BAI that was not different than any other site and species combinations over time. This trend was also found by Hughes and Brown (1992), in which tree ring indices reflected very low GS growth during drought events. Further, the exceptional growth at the two wetter sites reflects other GS observations in the literature, in which GS trees, which attain the largest recorded volumes of any known tree species, tend to show rapid growth after their initial establishment and can quickly outgrow all associated species (Weatherspoon, 1990).

WH tends to thrive in cool and moist maritime climates and is highly sensitive to extended summer drought conditions, which is consistent with its high annual BAI at the wettest site (Harris, 1990; Ruth and Harris, 1973). My results also indicate that the annual BAI for WH was influenced by spring rainfall and early growing season GDD, which is similar to what was found by Kuser and Ching (1980) and Ruth and Harris (1973), where the growth of WH was primarily driven by water availability and spring temperatures, but limited by extended droughts and very high temperatures. GF is considered to be moderately drought tolerant and grows best

under cool, moist conditions, which is consistent with its high annual BAI at the wettest site (Foiles, 1959; Mátyás et al., 2021). These results are also consistent with Weller (2018), in which mean annual increment for GF was primarily driven by soil hydrology. However, the results of this study indicate that annual BAI for GF was also influenced by maximum VPD, suggesting that the lower water availability and higher evaporative demand that is expected under climate change would limit the growth of GF despite the warmer temperatures that had the potential to benefit its growth.

These significant interactions suggest that GS, GF, and WH tend to have very high growth rates under conditions of high water availability, as indicated by the high annual BAI in response to the conditions at the wettest sites during years with little to no drought. However, given that an increase in growing season water deficit is expected due to climate change in the PNW (Dannenberg and Wise, 2016), the growth potential of these species may become increasingly limited moving forward, which can reduce forest productivity and impact ecosystem services such as timber production and carbon sequestration (Latta et al., 2010).

The species-specific time series models revealed that species differed in which aspects of climate most influence their annual BAI, which can be used to determine the possible effects of climate change on the growth of these species. Although the annual BAI of DF was exclusively driven by growing season water supply, which is projected to decrease as a result of climate change, its relative consistency in overall annual BAI across sites suggests that the growth DF may only become slightly limited in areas where more frequent and severe droughts are expected. In contrast, the annual BAIs of GS, POC, SSP, and WRSP were correlated with variables associated with both water supply and evaporative demand, suggesting that these species may be more sensitive to climate change since both higher temperatures and reduced

growing season rainfall are projected to increase water deficits moving forward (Peterson et al., 2014). The annual BAI of LC, WH, and WRC was driven by water supply and conditions affecting growing season length while the annual BAI of GF and WVPP was driven by water supply, evaporative demand, and growing season length. Although longer growing seasons as a result of warmer early spring temperatures and later frosts in the autumn are expected, it may not result in increased productivity due to increased water deficit (Barber et al., 2000; Bernal et al., 2011). Therefore, these species, particularly GF and WVPP, may not benefit from extended growing seasons as a result of their sensitivity to water deficit, which is expected to increase as a result of climate change. In contrast, the annual BAI for WWP was exclusively driven by growing season length and was not significantly influenced by climate factors related to water availability. This finding was surprising considering it has been reported that WWP is primarily limited by water balance, although it can survive across a large range of precipitation (Wellner, 1962). However, given that its annual BAI across sites tended to be very similar, WWP may not be as sensitive to differences in water deficit between the sites as GS, POC, SSP, and WRSP. While increased water deficit under climate change may still limit the growth of WWP, my results suggest that it may benefit from lengthening growing seasons more than any other species in this study.

Most species had greater BAI on the wettest site than on the driest site, supporting findings from existing literature, which suggest that water deficit tends to be the most limiting growth factor in the PNW (Grier and Running, 1977; Bréda et al., 2006). In addition, tree ring measurement values, such as annual BAI, can change in response to climate variation, with some species exhibiting more sensitivity than others depending on whether site conditions are favorable or limiting to growth (Fritts, 1976; Creber, 1977). However, results showing a

significant site by species by time interaction, as well as the very high annual BAI for many species at the wettest site until the early to mid-2010's, after which annual BAI sharply declined, also suggested that species growth sensitivity may vary over time in response to an increase in climate variability regardless of mean site conditions. This supports the study presented by Thornton et al. (2014) that not accounting for climate variability and only considering changes in mean climate when making climate change projections can significantly underestimate the impact of climate change on tree growth. Therefore, despite many species benefiting from the increase in water availability at the Huffman (wet) site, sensitive species may still be vulnerable to the increase in climate variability that is expected to occur under climate change in the form of more frequent and extreme drought events, which was observed for many species in recent years. Further, the primary effects of climate that influence tree rings include growing season rainfall and temperature (Creber, 1977), which is mostly supported by this study, although the climate variables that most influenced growth was often species-specific and included a combination of variables related to water supply, evaporative demand, and growing season length.

### 3.7.2 Annual Latewood Basal Area Increment

The formation of LW in tree rings, which typically develops from July until the end of the growing season, has been found to increase in response to favorable growing conditions, including lower water deficit, but is particularly driven by summer rainfall (Hankin et al., 2019; Kennedy, 1961; Zobel and Van Buijtenen, 2012). As a result, I hypothesized that LW BAI trends across species and sites would parallel expected changes in total BAI.

The expected trends as outlined in the hypothesis were somewhat supported by the results of this study. The trends observed for annual LW BAI across sites over time were similar to

those for annual BAI, with the wettest site and driest site having the highest and lowest annual LW BAI, respectively, until the early to mid-2010's. Similar to annual BAI, annual LW BAI for WRC and WWP also had minimal year-to-year variability across sites. These similarities are reasonable given that LW contributes to the total BAI and are both benefited by increased water availability. Similar to annual BAI, the observed decrease in annual LW BAI in recent years may also be a result of competition or an increase in growth-climate sensitivity on trees adapted to the wetter conditions at the Huffman (wet) site due to the prolonged and extreme drought conditions.

The results indicate that the species by site by time interaction was significant for annual LW BAI, which suggests that the pattern for annual LW BAI was significantly different between species and between sites at different times Specifically, DF at the Underhill (intermediate) site, GF at the Underhill (intermediate) and Huffman (wet) sites, and GS at the Huffman (wet) site tended to have a significantly higher LW BAI compared to the greatest number of species and site combinations, particularly in the late 2000's to early 2010's. GS at Underhill (intermediate) site in the late 2000's to early 2010's had a significantly higher annual BAI but not annual LW BAI compared to other species and site combinations, but GS at the Huffman (wet) site was significantly higher for both annual BAI and LW BAI. This suggests that although GS tends to have narrow LW widths and a low LW percentage compared to many other species (Piirto, 1985), the conditions that allowed the exceptionally high annual BAI at the wettest site also resulted in a larger LW BAI, while the water availability at the Underhill (intermediate) and Campbell (dry) sites may have not been high enough for a significantly larger annual LW BAI.

WH at the Huffman (wet) site in the late 2000's to early 2010's had a significantly higher annual BAI but not annual LW BAI compared to other species and site combinations. DF at the Underhill (intermediate) site in the late 2000's to early 2010's had a significantly higher annual

LW BAI but not annual BAI compared to other species and site combinations This suggests that the growth of WH is driven primarily by early growing season conditions while the opposite is true for DF. These significant interactions also suggest that GS, GF, and DF tend to have very high growth rates near the end of the growing season under conditions of higher water availability, as indicated by the high annual LW BAI in response to the conditions at the wetter sites during years with little to no drought. This is also justified by the finding that larger LW sections develop from trees in sites with long periods of rainfall late in the growing season (Kennedy, 1961; Gourley, 2016). However, given that an increase in growing season drought conditions is expected due to climate change in the PNW (Dannenberg and Wise, 2016), which would reduce the development of LW that contributes to the total BAI of a tree, the growth potential of these species may become increasingly limited moving forward.

The species-specific time series models revealed that species differed in which aspects of climate most influence their annual LW BAI, which can be used to determine the possible effects of climate change on the growth of these species. The annual LW BAIs for the majority of species were influenced by summer rainfall and maximum VPD, which supports the general consensus that greater water availability during the summer can extend the time in which LW is developing while higher water deficits can limit the development of LW (Zobel and Van Buijtenen, 2012).

Given that the annual LW BAIs of POC and WRSP were exclusively driven by variables affecting growing season water supply, which is projected to decrease as a result of climate change, their summer growth may become limited in areas where more frequent and severe droughts are expected. The annual LW BAIs of GS, LC, SSP, and WVPP were driven by variables affecting both water supply and evaporative demand. This could suggest that LW

growth in these species may become very sensitive to conditions under climate change considering that both higher temperatures and reduced growing season rainfall are expected to contribute to more extreme water deficits moving forward (Peterson et al., 2014). The annual LW BAIs of DF, GF, and WRC were driven by variables associated with water supply, evaporative demand, and growing season length while the annual LW BAI of WH was driven by variables associated with water supply and growing season length. Although extended growing seasons as a result of later frosts in the autumn are expected under climate change, it may not result in increased productivity due to increased water deficit (Barber et al., 2000; Bernal et al., 2011). Therefore, the growth of these species later in the growing season, particularly DF, GF, and WRC, may not benefit from extended growing seasons as a result of their sensitivity to water deficit. Similar to the unexpected findings for annual BAI, the annual LW BAI for WWP was similar across sites and exclusively driven by growing season length, further suggesting that WWP may not be as sensitive to differences in water deficit between the sites. While increased water deficit under climate change may still limit the growth of WWP, it may benefit from the longer growing season more than all other species in this study. For all species except for WWP, the influence of water supply on growth continued throughout the growing season as it was positively associated with annual BAI and annual LW BAI. Therefore, the reduction in growing season water availability that is projected under climate change has the potential to reduce the growth of these species given drought conditions would be able to limit wood production throughout the entire growing season.

Similar to annual BAI, my LW BAI findings support the existing literature suggesting that tree ring measurement values, such an annual LW BAI, can change in response to climate variation, which some species exhibiting more sensitivity than others depending on site

conditions and whether they are favorable or limiting to growth (Fritts, 1976; Creber, 1977). The similar trends between annual BAI and annual LW BAI confirm the relationship between these two measurements. Favorable conditions, such as greater water availability, lower evaporative demand, and longer growing seasons can benefit both measurements, although conditions later in the growing season tend to have a greater influence in annual LW BAI. Further, the primary effects of climate that influence LW include summer rainfall, summer temperatures and the length of the growing season (Zobel and Van Buijtenen, 2012; Wang et al., 2000), which is mostly supported by this study, although the climate variables that most influenced LW were often species-specific and included a combination of variables related to water supply, evaporative demand, and growing season length. The same type of climate conditions influenced both the annual BAI and annual LW BAI of GS, SSP, GF, WH, and WWP while the annual LW BAI for all other species were influenced by different conditions. Therefore, projected intra-annual climate variability must be considered for these species given that they are sensitive to different conditions over the course of the growing season (Creber, 1977).

### 3.7.3 Annual Latewood Percentage

The percentage of LW is of interest in forestry and wood products industries in part because a greater amount of LW is associated with higher wood density, which can influence the quality of wood and its potential use for different products (Creber, 1977; Smith et al., 1966).In conifers, the percentage of LW that comprises the annual BAI is generally higher under drought conditions given that the transition from EW formation to LW formation is triggered primarily by reduced soil moisture; drought conditions can therefore limit EW development (Creber, 1977; Domec and Gartner, 2002). In contrast, under favorable conditions such as higher water availability, EW formation continues further into the growing season and the percentage of LW

is reduced, although higher moisture availability later in the growing season can also promote the development of LW (Kennedy, 1961). With this consideration, it was hypothesized that species such as DF and LC, which tend to be more drought resistant but also most productive under conditions of higher water availability, would show a slight increase in overall annual LW percentage eastward across the water deficit gradient while reflecting fewer extreme differences in year-to-year variability. Meanwhile, all other less drought resistant or drought intolerant species, including GF, GS, POC, SSP, WRSP, WH, WRC, and WWP, were expected to show a more dramatic increase in overall annual LW percentage eastward across the gradient while reflecting more year-to-year variability. WVPP, which is adapted to drier environments but still sensitive to water deficit, would instead show less of an increase in overall annual LW percentage eastward across the gradient while reflecting more year-to-year variability than DF or LC.

The expected trends as outlined in the hypothesis were somewhat supported by the results of this study. Although the driest site tended to have high annual LW percentages during the initial years of growth, the Underhill (intermediate) and Huffman (wet) sites tended to have higher annual LW percentages than the dry site in recent years when drought conditions were more frequent across all sites. Coupled with our annual BAI results, this suggests that conditions promoting high rates of annual BAI were generally associated with lower LW percentages in the species we examined. This conclusion is consistent with a literature review by Zobel and Van Buijtenen (2012), that found favorable and wetter conditions promote greater BAI and development of EW while reducing LW percentage, while droughty conditions result in reduced BAI and the initiation of LW formation earlier in the growing season. Further, annual LW percentage at all three sites in this study tended to increase sharply during drought years, as

indicated by a low annual PDSI value. This year-to-year variability for annual LW percentage may also be a result of LW development tending to be more sensitive to climate than EW development (Zobel and Van Buijtenen, 2012), resulting in sharp increases and decreases in annual LW percentage in response to drought conditions.

Differences in LW percentages among species did vary across sites and years, suggesting differential responses to interactions between site and climate variability among species. In particular, DF and GF at all sites and WVPP at the Huffman (wet) and Underhill (intermediate) sites had a higher LW percentage compared to the greatest number of species and site combinations, particularly in the 2010's. The 2010's consisted of many extreme drought years as reflected by the very low annual PDSI values, which suppresses growth and results in a larger development of LW (Kennedy, 1961). While similar to annual LW BAI, these results included all sites for DF and GF and included WVPP instead of GS. This suggests that the large annual LW BAI for GS was a product of the high overall growth rates of the trees rather than a result of a large LW percentage, which makes sense given that GS has a lower LW percentage compared to many other species (Piirto, 1985). For WVPP at the Huffman (wet) and Underhill (intermediate) sites, which had a decrease in annual BAI during the 2010's and an increase in annual LW BAI, the larger annual LW percentage was likely a result of reduced growth and wetter summer conditions at the two wetter sites. Further, annual LW percentage was exclusively driven by July rainfall, which supports the finding of Howe (1968) that greater water availability later in the growing season resulted in an increase in the amount of LW for ponderosa pine. This trend also applied to DF, which was also driven by summer rainfall and supports the finding of Gourley (2016) that LW growth for DF was most influenced by the amount of summer rainfall. In the 2010's, GF had a decrease in annual BAI, suggesting that LW production started earlier in

the growing season, resulting in a larger percentage of LW. This trend is supported by the findings of Kraus and Spurr (1961) that LW production can begin earlier in the year during dry conditions. Given that all sites for DF and GF were significant in this interaction, regardless of the differences in water deficit at each site, the proportionally larger development of LW for these species is likely sensitive to any reduction in rainfall from drought events as reflected by annual PDSI values.

The species-specific time series models revealed that species differed in which aspects of climate most influence their annual LW percentage, which can be used to determine the possible effects of climate change on the growth and wood properties of these species given that LW percentage can be associated with reduced growth but is positively correlated with wood density and wood strength (Kennedy, 1961; Smith et al., 1966). The annual LW percentage for the majority of species was positively related to summer rainfall but negatively related to annual rainfall, which supports the general consensus that high water availability throughout the year can promote the development of EW and delay LW development, while greater water availability during the summer can extend the time in which LW is developing (Zobel and Van Buijtenen, 2012). Given that growing season rainfall is expected to decrease under climate change (add reference), my results suggest that an increase in annual LW percentage as a result of the earlier formation of LW is likely.

In general, the annual LW percentage for DF, GF, GS, LC, POC, WRC, and WVPP were exclusively driven by variables affecting water supply while the annual LW percentage of SSP, WH, and WWP were driven by variables affecting water supply and evaporative demand, suggesting that the development of LW relative to EW may be very sensitive to conditions under climate change, particularly SSP, WH, and WWP, considering they are affected by water deficit,

which is expected to become more extreme as a result of higher temperatures and reduced rainfall during the growing season (Peterson et al., 2014). Unlike annual BAI and annual LW BAI, annual LW percentage was not driven by conditions that affect growing season length for any species, further reinforcing the importance of water deficit in influencing annual LW percentage.

### 3.7.4 Wood Basic Density

A high WBD is known to be associated with a high LW percentage given that LW is denser than EW (Creber, 1977; Zobel and Van Buijtenen, 2012). As a result, I hypothesized that species and site combinations that were expected to develop high annual LW percentages would also develop a higher WBD. My results partially supported this hypothesis. Most species tended to have a higher WBD at the driest site and a lower WBD at the wettest site, which is consistent with the general trends in LW percentage up to 2010's and supports the general consensus that the percentage of LW, which relates to WBD, is generally higher under drought conditions (Creber, 1977; Domec and Gartner, 2002). However, the variability in year-to-year annual LW percentage also resulted in unclear trends with WBD, which was derived from the entire core rather than from individual years. Therefore, the relationship between LW percentage and WBD is difficult to evaluate directly from my results. Further, other factors such as the wall thickness of LW cells, which can vary among and between species, can significantly impact WBD regardless of LW percentage, which may explain why trends in density and LW percentage were not entirely consistent with one another (Besley, 1964; Zobel and Van Buijtenen, 2012).

The species by site interaction was significant for WBD. In particular, LC at the Campbell (dry) site showed higher WBD compared to the majority of other species and site

combinations while WVPP at the Huffman (wet) site showed lower WBD compared to a few species and site combinations. Both of these results were surprising given that LC was not involved with the significant interactions related to annual LW percentage despite its WBD being significantly higher than most other species and site combinations while WVPP at the wettest site was found to have a significantly higher annual LW percentage in the late 2010's compared to other combinations, which would have suggested a higher WBD instead.

Although the wood properties of LC are not covered extensively in the literature, LC is reported to typically have a moderate density of 0.415 g cm−3 (Haslett et al., 1985), which is much lower than the WBD observed for LC across all sites in this study, particularly in the Underhill (intermediate) and Campbell (dry) sites where LC had a WBD of 0.534 and 0.754 g cm−3, respectively. LC's high WBD values at the drier sites in this study may suggest that the density of LC wood is particularly responsive to droughty conditions. The dramatic increase in WBD at the driest site for LC suggests that may be less vulnerable to drought stress and cavitation, which consistent with reports that LC is highly drought tolerant and capable of adapting to many different environments, more so than most other species in this study (Raddi et al., 2014; Niemiera, 2012). Thicker cell walls and smaller lumen diameters in xylem tracheids, which are associated with higher WBD, can better maintain water transport during droughts by reducing vulnerability to cavitation (Rathgeber et al., 2006; Dalla-Salda, 2009). Further, it has been found that trees that have survived extreme drought events tended to have significantly higher ring density as a result of xylem plasticity, which also reinforces the idea that higher WBD and prompt tree adaptation is associated with reduced vulnerability to droughts (Martinez-Meier et al., 2008; Ruiz Diaz Britez et al., 2014). Linkages between high drought resistance and higher WBD may also explain why LC had the second highest total BAI at the driest site. Given

the relationship between WBD and wood quality, as well as the consistency in total BAI across sites for LC, my results suggest that LC may be particularly well-suited to provide both high quality wood and relatively high rates of growth under conditions of lower water availability.

Although WVPP at the wettest site was found to have a significantly higher annual LW percentage in the late 2010's compared to other combinations, its annual LW percentage for WVPP at this site prior to the late 2010's was low and the first annual ring values at DBH height developed a few years later than most other combinations, which may have resulted in a reduced amount of overall LW and an overall reduction of WBD. Further, as mentioned by Besley (1964), other characteristics such as cell characteristics and chemical deposits can affect WBD regardless of LW percentage. WVPP at this site also had a WBD of 0.375 g $cm^{-3}$, which was lower than other published values for WVPP and is considered a low density among all pines (Zobel and Burley, 2004). Bouffier et al. (2003) reported that this variety of ponderosa pine tends to be denser than ponderosa pine, with a WBD of 0.48 g $cm^{-3}$, which is similar to what was found for WVPP at the Underhill (intermediate) site, while a higher density was found at the driest site. Given the relationship between WBD and quality, and given that WVPP had the lowest total BAI at the Huffman (wet) site, WVPP under very wet conditions results in both a lower quality wood and in reduced growth.

The significant interaction between species and sites suggests that WBD can depend on the sensitivity of different species to climate variability. More drought tolerant species such as LC may be able to adapt to drier conditions as a result of climate change through its development of WBD. Species that are not adapted to their environments, such as WVPP at the wettest site as reflected by its very low total BAI, may produce a minimal amount of both EW and LW, reducing the total WBD regardless of annual LW percentage. As mentioned previously, although

these results suggest that there is a negative correlation between rainfall and WBD, resulting in an increase in WBD as a result of climate change, high inter-annual and intra-annual variability also has the potential to adversely affect wood quality (Olivar et al., 2015).

## 3.8 Conclusion

This study focused on examining the variation in inter-annual growth and wood properties, including LW percentage and WBD, for 25-year-old stands involving 11 different species across sites with contrasting levels of water deficit in western Oregon in order to determine differences in species growth-climate sensitivity and the relationship between climate and wood properties for different species.

It was found that while most hypotheses were somewhat supported and results confirmed that the extent to which water deficit limits growth is dependent on species growth sensitivity, there can be considerable differences in species growth sensitivity over time in response to an increase in water deficits regardless of mean site conditions. Dramatic drops in the annual BAIs of GS, GF, and WH at our wettest site during a droughty period from the 2010's to early 2020's highlight the importance of considering projected climate variability in addition to projected mean site conditions in order to fully account for its potential impact on growth and wood properties. Further, the climate variables that most influenced BAI and intra-annual wood development were often species-specific and included a combination of variables related to water supply, evaporative demand, and growing season length, which are all expected to shift to varying extents as a result of climate change.

Trends in annual BAI, annual LW BAI, and annual LW percentage across sites and over time suggest that growth and wood properties are very sensitive to climate variability, making it

more challenging to predict the effects of climate change on these characteristics. However, an understanding of the relationship between climate variables and intra-annual wood development, and how these relationships differ between species under different levels of water deficit, can inform the response of growth and wood properties to projected climate changes.

Further research can be done on ring-specific density, which can provide more information on the relationship between climate variability and density of different species under different levels of water deficit. Research can also be done on comparing intrinsic water use efficiency during particularly droughty and wet years. The measurements of inter-annual growth as derived from tree rings and wood properties will also be conducted regularly to determine the impact of water deficit throughout the rotation age of these species.

## 3.9 References

Aernouts, J., Gonzalez-Benecke, C. A., & Schimleck, L. R. (2018). Effects of Vegetation Management on Wood Properties and Plant Water Relations of Four Conifer Species in the Pacific Northwest of the USA. *Forests*, *9*(6), 323.

Abrams, M. D., Ruffner, C. M., & Morgan, T. A. (1998). Tree-ring responses to drought across species and contrasting sites in the ridge and valley of central Pennsylvania. *Forest Science*, *44*(4), 550-558.

Andreu, L., Gutierrez, E., Macias, M., Ribas, M., Bosch, O., & Camarero, J. J. (2007). Climate increases regional tree-growth variability in Iberian pine forests. *Global Change Biology*, *13*(4), 804-815.

Antos, J. A., Filipescu, C. N., & Negrave, R. W. (2016). Ecology of western redcedar (*Thuja plicata*): Implications for management of a high-value multiple-use resource. *Forest Ecology and Management*, *375*, 211-222.

Baldocchi, D., Chu, H., & Reichstein, M. (2018). Inter-annual variability of net and gross ecosystem carbon fluxes: A review. *Agricultural and Forest Meteorology*, *249*, 520-533.

Barber, V. A., Juday, G. P., & Finney, B. P. (2000). Reduced growth of Alaskan white spruce in the twentieth century from temperature-induced drought stress. *Nature*, *405*(6787), 668-673.

Barnett, J. R., & Jeronimidis, G. (Eds.). (2003). Wood quality and its biological basis.

Bernal, M., Estiarte, M., & Peñuelas, J. (2011). Drought advances spring growth phenology of the Mediterranean shrub Erica multiflora. *Plant Biology*, *13*(2), 252-257.

Besley, L (1964). The significance of fiber geometry and distribution in assessing pulpwood quality. *Thppi 47(11): 183A-184B*

Biondi, F. (1998). Removing the tree-ring width biological trend using expected basal area increment. *Fort Valley Experimental Forest—A Century of Research 1908–2008*, 124-131.

Blasing, T. J., & Fritts, H. C. (1976). Reconstructing past climatic anomalies in the North Pacific and western North America from tree-ring data. *Quaternary Research*, *6*(4), 563-579.

Bouffier, L. A., Gartner, B. L., & Domec, J. C. (2003). Wood density and hydraulic properties of ponderosa pine from the Willamette valley vs. the Cascade mountains. *Wood and Fiber Science*, *35*(2).

Bréda, N., Huc, R., Granier, A., & Dreyer, E. (2006). Temperate forest trees and stands under severe drought: a review of ecophysiological responses, adaptation processes and long-term consequences. *Annals of Forest Science*, *63*(6), 625-644.

Brienen, R. J., & Zuidema, P. A. (2005). Relating tree growth to rainfall in Bolivian rain forests: a test for six species using tree ring analysis. *Oecologia*, *146*(1), 1-12.

Brix, H. (1972). Nitrogen fertilization and water effects on photosynthesis and earlywood–latewood production in Douglas-fir. *Canadian Journal of Forest Research*, *2*(4), 467-478.

Carnwath, G. C., & Nelson, C. R. (2016). The effect of competition on responses to drought and interannual climate variability of a dominant conifer tree of western North America. *Journal of Ecology*, *104*(5), 1421-1431.

Carrer, M., & Urbinati, C. (2006). Long-term change in the sensitivity of tree-ring growth to climate forcing in Larix decidua. *New Phytologist*, *170*(4), 861-872.

Creber, G. T. (1977). Tree rings: a natural data-storage system. *Biological Reviews*, *52*(3), 349-381.

Dalla-Salda, G., Martinez-Meier, A., Cochard, H., & Rozenberg, P. (2009). Variation of wood density and hydraulic properties of Douglas-fir (Pseudotsuga menziesii (Mirb.) Franco) clones related to a heat and drought wave in France. *Forest Ecology and Management*, *257*(1), 182-189.

Dannenberg, M. P., & Wise, E. K. (2016). Seasonal climate signals from multiple tree ring metrics: A case study of Pinus ponderosa in the upper Columbia River Basin. *Journal of Geophysical Research: Biogeosciences*, *121*(4), 1178-1189.

Dannenberg, M., Wise, E. K., & Keung, J. H. (2014, December). Seasonal Climate Signals in Multiple Tree-Ring Parameters: A Pilot Study of Pinus ponderosa in the Columbia River Basin. In *AGU Fall Meeting Abstracts* (Vol. 2014, pp. PP43B-1485).

Domec, J. C., & Gartner, B. L. (2002). How do water transport and water storage differ in coniferous earlywood and latewood?. *Journal of Experimental Botany*, *53*(379), 2369-2379.

Eckelman, C. A. (1997). *Wood moisture calculations*. Purdue University, Department of Forestry & Natural Resources.

Ettinger, A. K., & HilleRisLambers, J. (2013). Climate isn't everything: competitive interactions and variation by life stage will also affect range shifts in a warming world. *American Journal of Botany*, *100*(7), 1344-1355.

Ettl, G. J., & Peterson, D. L. (1995). Extreme climate and variation in tree growth: individualistic response in subalpine fir (*Abies lasiocarpa*). *Global Change Biology*, *1*(3), 231-241.

Filipescu, C. N., Lowell, E. C., Koppenaal, R., & Mitchell, A. K. (2014). Modeling regional and climatic variation of wood density and ring width in intensively managed Douglas-fir. *Canadian journal of forest research*, *44*(3), 220-229.

Flores, O., & Coomes, D. A. (2011). Estimating the wood density of species for carbon stock assessments. *Methods in Ecology and Evolution*, *2*(2), 214-220.

Foiles, M. W. (1959). Silvics of grand fir. *Misc. Pub. No. 21. Ogden, UT: US Department of Agriculture, Forest Service, Intermountain Forest and Range Experiment Station.*

Gourley, D. M. (2016). Impact of Climate and Disturbance on the Formation of Earlywood and Latewood in Douglas-fir at the Salal Fields Study Site.

Graham, R. T. (1990). *Pinus monticola* Dougl. ex D. Don western white pine. *Silvics of North America*, *1*, 385-394.

Grier, C. G., & Running, S. W. (1977). Leaf area of mature northwestern coniferous forests: relation to site water balance. *Ecology*, *58*(4), 893-899.

Grossnickle, S. C., & Russell, J. H. (2006). Yellow-cedar and western redcedar ecophysiological response to fall, winter and early spring temperature conditions. *Annals of Forest Science*, *63*(1), 1-8.

Hammond, W. M., Yu, K., Wilson, L. A., Will, R. E., Anderegg, W. R., & Adams, H. D. (2019). Dead or dying? Quantifying the point of no return from hydraulic failure in drought-induced tree mortality. *New Phytologist*, *223*(4), 1834-1843.

Hamon, W. R. (1963). Computation of direct runoff amounts from storm rainfall. *Int. Assoc. Sci. Hydrol. Publ.*, *63*, 52-62.

Hankin, L. E., Higuera, P. E., Davis, K. T., & Dobrowski, S. Z. (2019). Impacts of growing-season climate on tree growth and post-fire regeneration in ponderosa pine and Douglas-fir forests. *Ecosphere*, *10*(4), e02679.

Harris, A. S. (1990). *Picea sitchensis* (Bong.) Carr. Sitka spruce. *Silvics of North America; Burns, RM, Honkala, BH, Eds*, 260-267.

Haslett, A.N., Williams, D.H. and Kinninmonth, J.A. 1985. Drying of major cypress species grown in New Zeal

Howe, J. P. (1968). Influence of irrigation on ponderosa pine. *Forest Prod. J*, *18*(1), 84-93.

Hughes, M. K., & Brown, P. M. (1992). Drought frequency in central California since 101 BC recorded in giant sequoia tree rings. *Climate dynamics*, *6*(3), 161-167.

Jin, Y., Li, J., Bai, X., Zhao, Y., Cui, D., & Chen, Z. (2021). High temperatures constrain latewood formation in *Larix gmelinii* xylem in boreal forests. *Global Ecology and Conservation*, *30*, e01767.

Jozsa, L. A., & Middleton, G. R. (1994). A discussion of wood quality attributes and their practical implications.

Kennedy, R. W. (1961). Variation and periodicity of summerwood in some second-growth Douglas-fir. *Tappi*, *44*, 161-166.

Kraus, J. F., & Spurr, S. H. (1961). Relationship of Soil Moisture to the Springwood-Summerwood Transition in Southern Michigan Red Fine. *Journal of Forestry*, *59*(7), 510-511.

Kuser, J. E., & Ching, K. K. (1980). Provenance variation in phenology and cold hardiness of western hemlock seedlings. *Forest Science*, *26*(3), 463-470.

Lachenbruch, B., Johnson, G. R., Downes, G. M., & Evans, R. (2010). Relationships of density, microfibril angle, and sound velocity with stiffness and strength in mature wood of Douglas-fir. *Canadian Journal of Forest Research*, *40*(1), 55-64.

Latta, G., Temesgen, H., Adams, D., & Barrett, T. (2010). Analysis of potential impacts of climate change on forests of the United States Pacific Northwest. *Forest Ecology and Management*, *259*(4), 720-729.

Littell, J. S., Peterson, D. L., & Tjoelker, M. (2008). Douglas-fir growth in mountain ecosystems: water limits tree growth from stand to region. *Ecological Monographs*, *78*(3), 349-368.

Martinez-Meier, A., Sanchez, L., Pastorino, M., Gallo, L., & Rozenberg, P. (2008). What is hot in tree rings? The wood density of surviving Douglas-firs to the 2003 drought and heat wave. *Forest Ecology and Management*, *256*(4), 837-843.

Mathys, A., Coops, N. C., & Waring, R. H. (2014). Soil water availability effects on the distribution of 20 tree species in western North America. *Forest Ecology and Management*, *313*, 144-152.

Mátyás, C., Dostál, J., Beran, F., Čáp, J., Fulín, M., Vejpustková, M., ... & Frýdl, J. (2021). Climatic Sensitivity Profile of Abies Species–A Key to Their Future Role in the Adaptive Silviculture of Central-Southeast Eu-rope.

McGarigal, K., & McComb, W. C. (1995). Relationships between landscape structure and breeding birds in the Oregon Coast Range. *Ecological monographs*, *65*(3), 235-260.

Millar, C. I., Stephenson, N. L., & Stephens, S. L. (2007). Climate change and forests of the future: managing in the face of uncertainty. *Ecological applications*, *17*(8), 2145-2151.

Niemiera, A. X. (2012). Leyland Cypress, x *Cupressocyparis leylandii*.

Nogueira, E. M., Nelson, B. W., & Fearnside, P. M. (2005). Wood density in dense forest in central Amazonia, Brazil. *Forest Ecology and Management*, *208*(1-3), 261-286.

Olivar Agresta, J., Bogino, S. M., Spiecker, H., & Bravo Oviedo, F. (2015). Changes in climate-growth relationships and IADF formation over time of pine species (*Pinus halepensis*, *P. pinaster and P. sylvestris*) in Mediterranean environments. *Forest Systems*, *24*(1), 1-9.

Omernik, J. M., & Griffith, G. E. Ecoregions of Oregon.

Peterson, D. W., Kerns, B. K., & Dodson, E. K. (2014). Climate change effects on vegetation in the Pacific Northwest: A review and synthesis of the scientific literature and simulation model

projections. *Gen. Tech. Rep. PNWGTR-900. Portland, OR: US Department of Agriculture, Forest Service, Pacific Northwest Research Station. 183 p., 900.*

Phipps, R. L., & Whiton, J. C. (1988). Decline in long-term growth trends of white oak. *Canadian Journal of Forest Research*, *18*(1), 24-32.

Piirto, D. D. (1985). Wood of giant sequoia: properties and unique characteristics. In *Proceedings of the workshop on management of giant sequoia* (p. 19).

Pompa-García, M., & Venegas-González, A. (2016). Temporal variation of wood density and carbon in two elevational sites of Pinus cooperi in relation to climate response in northern Mexico. *PLoS One*, *11*(6), e0156782.

Pratt, R. B., Jacobsen, A. L., Ewers, F. W., & Davis, S. D. (2007). Relationships among xylem transport, biomechanics and storage in stems and roots of nine *Rhamnaceae* species of the California chaparral. *New phytologist*, *174*(4), 787-798.

PRISM Climate Group, Oregon State University, https://prism.oregonstate.edu.

Raddi, P., Danti, R., & Della Rocca, G. (2014). x *Cupressocyparis leylandii*. *Enzyklopädie der Holzgewächse: Handbuch und Atlas der Dendrologie*, 1-17.

Rathgeber, C. B., Decoux, V., & Leban, J. M. (2006). Linking intra-tree-ring wood density variations and tracheid anatomical characteristics in Douglas fir (*Pseudotsuga menziesii* (Mirb.) Franco). *Annals of Forest Science*, *63*(7), 699-706.

RStudio Team. (2015). *RStudio: Integrated Development Environment for R*. Boston, MA. Retrieved from www.rstudio.com

Ruiz Diaz Britez, M., Sergent, A. S., Martinez Meier, A., Bréda, N., & Rozenberg, P. (2014). Wood density proxies of adaptive traits linked with resistance to drought in Douglas fir (*Pseudotsuga menziesii* (Mirb.) Franco). *Trees*, *28*(5), 1289-1304.

Rundel, P. W. (1972). Habitat restriction in giant sequoia: the environmental control of grove boundaries. *American Midland Naturalist*, 81-99.

Ruth, R. H., & Harris, A. S. (1973). Western hemlock-Sitka spruce. *Silvicultural Systems*, 5.

SAS Institute Inc. 2013. SAS® 9.4. Cary, NC: SAS Institute Inc.

Smith, J. H. G., Heger, L., & Hejjas, J. (1966). Patterns in Growth of Earlywood, Latewood, and Percentage Latewood Determined by Complete Analysis of 18 Douglas-fir Trees. *Canadian Journal of Botany*, *44*(4), 453-466.

Soil Survey Staff, Natural Resources Conservation Service, United States Department of Agriculture. Official Soil Series Descriptions. Available online.

Suarez, M.L., & Kitzberger, T. (2010). Differential effects of climate variability on forest dynamics along a precipitation gradient in northern Patagonia. *Journal of ecology*, *98*(5), 1023-1034.

Suarez, M. L., Villalba, R., Mundo, I. A., & Schroeder, N. (2015). Sensitivity of *Nothofagus dombeyi* tree growth to climate changes along a precipitation gradient in northern Patagonia, Argentina. *Trees*, *29*(4), 1053-1067.

Thornton, P. K., Ericksen, P. J., Herrero, M., & Challinor, A. J. (2014). Climate variability and vulnerability to climate change: a review. *Global change biology*, *20*(11), 3313-3328.

Tibshirani, R. (1996). Regression shrinkage and selection via the lasso. *Journal of the Royal Statistical Society: Series B (Methodological)*, *58*(1), 267-288.

Vittinghoff, E., Glidden, D. V., Shiboski, S. C., & McCulloch, C. E. (2006). Regression methods in biostatistics: linear, logistic, survival, and repeated measures models.

Wang, L., Payette, S., & Bégin, Y. (2000). A quantitative definition of light rings in black spruce (Picea mariana) at the arctic treeline in northern Québec, Canada. *Arctic, Antarctic, and Alpine Research*, *32*(3), 324-330.

Waring, R. H., & Franklin, J. F. (1979). Evergreen Coniferous Forests of the Pacific Northwest: Massive long-lived conifers dominating these forests are adapted to a winter-wet, summer-dry environment. *Science*, *204*(4400), 1380-1386.

Warren, W. G. (1979). The contribution of earlywood and latewood specific gravities to overall wood specific gravity. *Wood and Fiber Science*, 127-135.

Weatherspoon, C. P. (1990). *Sequoiadendron giganteum* (Lindl.) Buchholz Giant Sequoia. *Silvics of North America*, *1*, 552-562.

Weiskittel, A. R., Crookston, N. L., & Radtke, P. J. (2011). Linking climate, gross primary productivity, and site index across forests of the western United States. *Canadian Journal of Forest Research*, *41*(8), 1710-1721.

Wellner, C. A. (1962). Silvics of western white pine. *Misc. Pub. No. 26. Ogden, UT: US Department of Agriculture, Forest Service, Intermountain Forest and Range Experiment Station. 24 p.*

Zobel, B. J., & Van Buijtenen, J. P. (2012). *Wood variation: its causes and control*. Springer-Verlag.

# 4. Conclusions

## 4.1 Summary of Findings

In chapter 2, we determined that the first hypothesis regarding trends in tree size, survival, and intra-annual radial growth across the water deficit gradient as it relates to species drought sensitivity was mostly true. We determined that the second hypothesis regarding the relationship between species drought sensitivity and growing season length across the water deficit gradient was not fully supported by the results of this study. It was found that tree size and survival at 25 years old for GS, WH, SSP, WRSP, GF, POC, and WWP declined progressively under higher levels of water deficit, and had declined dramatically at the driest site, indicating low drought resistance. However, POC and WWP had more similar tree sizes between the Huffman (wet) and Underhill (intermediate) sites than the other listed species. DF and LC followed a similar trend with less extreme differences across sites, while WVPP and WRC tended to have their largest tree sizes and highest survival at the driest site. It was also found that temperature was a major driver of seasonal growth initiation and cessation.

WVPP at the Huffman (wet) and Underhill (intermediate) site and LC at the Underhill (intermediate) and Campbell (dry) sites initiated growth significantly later than many other species and site combinations. WVPP at the Underhill (intermediate) and Campbell (dry) sites, LC at the Huffman (wet) and Underhill (intermediate) sites, and GS at the Underhill (intermediate) sites had a significantly later date of growth cessation than other species and site combinations. Species type was significant in determining the length of the growing season rather than water deficit while seasonal CBAI was typically driven by differences in water deficit. GS and WWP at the Huffman (wet) site tended to have a significantly higher CBAI than

the majority of species and site combinations while GS had a significantly longer growing season than the majority of species and site combinations

In chapter 3, we determined that all four hypotheses regarding the relationship between species drought resistance under different levels of water deficit and annual BAI, annual LW BAI, annual LW percentage, and WBD were all partially supported by the results for this study. The site by species by time interaction was significant for all response variables, except for WBD which was measured from full tree cores rather than on an inter-annual basis. GS at the Huffman (wet) and Underhill (intermediate) sites as well as GF and WH at the Huffman (wet) site had a significantly higher annual BAI compared to many other species and site combinations, particularly in the late 2000's to early 2010's. DF at the Underhill (intermediate) site, GF at the Underhill (intermediate) and Huffman (wet) sites, and GS at the Huffman (wet) site had a significantly higher LW BAI compared to the greatest number of species and site combinations, particularly in the late 2000's to early 2010's. DF and GF at all sites and WVPP at the Huffman (wet) and Underhill (intermediate) sites had a significantly higher LW percentage compared to the greatest number of species and site combinations, particularly in the 2010's.

The wettest site had the highest overall annual BAI and annual LW BAI while the driest site had the lowest overall annual BAI and annual LW BAI for the majority of species, but only until the early to mid-2010's, after which growth at the wettest site tended to decline or was surpassed by the two over sites, suggesting rapid initial growth at the wettest site but less extreme differences in growth between all sites in recent years due to competition and/or prolonged drought conditions. The opposite of these trends was true for annual LW percentage, which tended to be highest at the driest site and lowest and the wettest site, until the early to mid-2010's. WBD tended to be highest on the driest site and lowest on the wettest site, although the

site by species interaction was significant. LC at the Campbell (dry) site had a significantly higher WBD compared to the majority of other species and site combinations while WVPP at the Huffman (wet) site had a significantly lower WBD compared to a few species and site combinations

## 4.2 Management Implications

This study has shown that species differ in the extent to which they are sensitive to water deficit and climate variability on the seasonal, inter-annual, and cumulative scale. While water deficit was the primary factor influencing growth on all time scales and wood properties, species also differed in the extent to which they were sensitive to climate variables such as water supply, evaporative demand, and growing season length.

The results of this study suggest that reforestation efforts for sensitive species such as GS, WH, SSP, WRSP, GF, POC, and WWP should be particularly mindful of the areas that are expected to have lower growing season moisture, higher evaporative demand, and more frequent and intense droughts as a result of climate change. This consideration should also, to a lesser extent, be made for more drought resistant species such as DF and LC while reforestation efforts for WRC and WVPP should instead be mindful of areas where extreme droughts are expected given their observed resistance to water deficit. Further, this study can help to inform where proactive management is required across species ranges and prioritize the management of forests that are expected to become the most vulnerable as a result of climate change. It can also inform where species are predicted to expand their range and inform assisted migration efforts depending on the projected climate changes at a given site and on the sensitivity of a given species.

DF is considered one of the most valuable timber species in the PNW and has proven to be very drought resistant, which would be beneficial for maintaining productivity under projected changes in climate. However Swiss needle cast (SNC) has become a significant threat to the growth of DF, particularly in the plantations across the Oregon Coast Range (Mildrexler et al., 2019). The results indicate that WH, GF, and GS had greater productivity than DF at the Huffman (wet) site, which is located in the central Oregon Coast Range. Therefore, these may be potential alternative species for reforestation and timber production in areas of the Oregon Coast Range that are prone to SNC.

The results of chapter 3 also emphasize that, even when species are adapted to and thriving in sites that typically have moist conditions, increased climate variability and prolonged periods of unusually warm and dry conditions can affect the growth sensitivity of species. Therefore, reforestation efforts and management across a species' range much also be mindful of the projected increase in climate variability and drought conditions, which has the potential to influence the growth of species regardless of the extent to which they are sensitive to drought conditions and what the mean climate conditions are at a particular site.

When considering the effect of climate on wood properties, an increase in water deficit typically resulted in an increase in annual LW percentage and WBD at the expense of radial growth production, with the exception of LC. However, sites that are projected to have an increase in climate variability can negatively affect wood quality or at the very least, make it difficult to predict wood qualities.

In contrast to other measurements involved with this study, growing season phenology for each species was not significantly influenced by water deficit but rather by temperature. However, in areas where the projection of warmer temperatures would allow for a longer

growing season, it is important to be mindful of the extent to which water deficit will also increase given that it could limit the potential productivity that the longer growing season may have offered. An understanding of these conditions on a given site paired with the appropriate species as determined by its sensitivity to water deficit can improve the success of reforestation efforts. Further, considering the relationship reported between climate variables and the timing of growth initiation, particularly for WVPP and LC which were significantly different than all other species, can be used to determine the timing of activities such as planting, fertilizer application, and herbicide application depending on the projected climate at a given site. The timing of these activities on a given site must also take into consideration that growth initiation for most species was driven by forcing, which will increase as a result of warming spring temperatures under climate change.

The results in this study, which evaluate the growth-climate relationships of different species on various timescales as well as the impact of climate and water deficit on wood properties, can also be used to better inform growth models to determine how forests will respond to projected climate changes and determine which species to plant in a given area in order to prevent drought stress and vulnerability to disturbance, increase timber production, and enhance carbon sequestration. It can also be used to improve the quality of wood production.

## 4.3 Future Directions

The structure of this study can allow for further exploration of the relationship between species and forest composition, water deficit, and climate variability. Further research can be done on the intra-annual growth and growing season phenology across different years to determine the impact of inter-annual climate variability. Differences water use or soil moisture

dynamics across species and sites could also be investigated to better understand the full impact of water deficit on forests comprised of these species. The measurements of cumulative tree size and survival as well as inter-annual growth as derived from tree rings and wood properties will also be collected regularly to determine the impact of water deficit throughout the rotation age of these species. Additionally, further research can be done on ring-specific density, which can provide more information on the relationship between climate variability and wood density of different species under different levels of water deficit, as well as on comparing intrinsic water use efficiency during particularly droughty and wet years.

## 4.4 References

Mildrexler, D. J., Shaw, D. C., & Cohen, W. B. (2019). Short-term climate trends and the Swiss needle cast epidemic in Oregon's public and private coastal forestlands. *Forest Ecology and Management, 432*, 501-513.

# 5. Appendix

S.2. The volume equations and species-specific coefficients used in chapter 2, as well as their associated reference, are listed below:

Where: *DBHin* is DBH in inches; *HTft* is height in feet; *DBH* is DBH in centimeters; *HT* is height in meters; and *Age* is age in years.

Gonzalez-Benecke (et al. 2018):

$$DF = 0.00899 * (DBHin^{1.9448}) * (HTft^{0.7154}) * (Age^{-0.0473})$$

$$GF = 0.01740 * (DBHin^{1.9930}) * (HTft^{0.6589}) * (Age^{-0.2499})$$

$$WH = 0.00681 * (DBHin^{1.9757}) * (HTft^{0.8061}) * (Age^{-0.1123})$$

$$WRC = 0.01960 * (DBHin^{1.9403}) * (HTft^{0.6847}) * (Age^{-0.2911})$$

Wensel & Krumland (1983):

$$DF = 0.0007938 * (DBHin^{1.590}) * (HTft^{1.436})$$

$$GS = 0.0007903 * (DBHin^{1.792}) * (HTft^{1.282})$$

$$SSP = 0.0005621 * (DBHin^{1.648}) * (HTft^{1.473})$$

$$WRSP = 0.0005621 * (DBHin^{1.648}) * (HTft^{1.473})$$

$$WH = 0.0005621 * (DBHin^{1.648}) * (HTft^{1.473})$$

$$GF = 0.0005621 * (DBHin^{1.648}) * (HTft^{1.473})$$

Zhou & Hemstrom (2010):

$$DF = 10^{-3.21809 + 0.04948 * \log(HTft) * \log(DBHin) - 0.15664 * (\log(DBHin))^2 + 2.02132 * \log(DBHin) + 1.63408 * \log(HTft) - 0.16185 * (\log(HTft))^2}$$

$$GF = 10^{-2.575642 + 1.806775 * \log(DBHin) + 1.094665 * \log(HTft)}$$

$$SSP = 10^{-2.700574 + 1.754171 * \log(DBHin) + 1.164531 * \log(HTft)}$$

$$WH = 10^{-2.72170 + 2.00857 * \log(DBHin) + 1.08620 * \log(HTft) - 0.00568 * DBHin}$$

$$WRC = 10^{-2.379642 + 1.6823 * \log(DBHin) + 1.039712 * \log(HTft)}$$

$$WRSP = 10^{-2.700574 + 1.754171 * \log(DBHin) + 1.164531 * \log(HTft)}$$

$$WVPP = 10^{-2.729937 + 1.909478 * \log(DBHin) + 1.085681 * \log(HTft)}$$

Zianis et al. (2005):

$$POC = \frac{DBH^{1.85298} * HT^{0.86717} * e^{-2.33706}}{28.317}$$

Pillsbury et al. (1998):

$$LC = 0.005764 * (DBHin^{2.260353}) * (HTft^{0.630129})$$

| Annual Basal Area Increment | | | | | | | |
|---|---|---|---|---|---|---|---|
| **Species** | **Models** | **Climate Parameter** | **Parameter Estimate** | **SE** | **$R^2_{GLMM}$** | **RMSE** | **CV** |
| DF | $sqrtBAI_{kt} = \beta_0 + \beta_1 Site + \beta_2 BA_{jkt} + \beta_3 P_{jt} + \beta_4 JulyP_{jt} + \beta_5 AugP_{jt} + \eta_{ij} t + c_{jk} + \varepsilon_{jkt}$ | P | 0.0003545 | 0.0000618 | 0.269 | 1.305 | 0.608 |
| | | JulyP | 0.020655 | 0.0018216 | | | |
| | | AugP | 0.0093792 | 0.0012377 | | | |
| GF | $sqrtBAI_{kt} = \beta_0 + \beta_1 Site + \beta_2 BA_{jkt} + \beta_3 PDSI_{jt} + \beta_4 VPDmax_{jt} + \beta_5 MayTmin_{jt} + \beta_6 JulyTmin_{jt} + \eta_{ij} t + c_{jk} + \varepsilon_{jkt}$ | PDSI | 0.0472874 | 0.0235803 | 0.334 | 2.152 | 0.951 |
| | | VPDmax | -0.2901791 | 0.1093596 | | | |
| | | MayTmin | 0.1009278 | 0.0359377 | | | |
| | | JulyTmin | 0.1014889 | 0.0339638 | | | |
| GS | $sqrtBAI_{kt} = \beta_0 + \beta_1 Site + \beta_2 BA_{jkt} + \beta_3 SpringP_{jt} + \beta_4 VPDmax_{jt} + \eta_{ij} t + c_{jk} + \varepsilon_{jkt}$ | SpringP | 0.0013537 | 0.0004573 | 0.250 | 2.025 | 0.774 |
| | | VPDmax | -0.3531398 | 0.145156 | | | |
| LC | $sqrtBAI_{kt} = \beta_0 + \beta_1 Site + \beta_2 BA_{jkt} + \beta_3 Tmin_{jt} + \beta_4 SpringP_{jt} + \eta_{ij} t + c_{jk} + \varepsilon_{jkt}$ | Tmin | 0.1212692 | 0.0524017 | 0.163 | 1.309 | 0.671 |
| | | SpringP | 0.0007703 | 0.0003345 | | | |
| POC | $sqrtBAI_{kt} = \beta_0 + \beta_1 Site + \beta_2 BA_{jkt} + \beta_3 SpringP_{jt} + \beta_4 MayVPDmean_{jt} + \eta_{ij} t + c_{jk} + \varepsilon_{jkt}$ | SpringP | 0.0005002 | 0.0002891 | 0.235 | 1.243 | 0.611 |
| | | MayVPDmean | -1.0865974 | 0.2936729 | | | |
| SSP | $sqrtBAI_{kt} = \beta_0 + \beta_1 Site + \beta_2 BA_{jkt} + \beta_3 JulyP_{jt} + \beta_4 MayVPDmean_{jt} + \eta_{ij} t + c_{jk} + \varepsilon_{jkt}$ | JulyP | 0.0026745 | 0.0014025 | 0.335 | 1.314 | 0.731 |
| | | MayVPDmean | -0.8130418 | 0.2097432 | | | |
| WH | $sqrtBAI_{kt} = \beta_0 + \beta_1 Site + \beta_2 BA_{jkt} + \beta_3 SpringP_{jt} + \beta_4 AprilGDD_{jt} + \eta_{ij} t + c_{jk} + \varepsilon_{jkt}$ | SpringP | 0.0012839 | 0.0003245 | 0.303 | 1.585 | 0.736 |
| | | AprilGDD | 0.0031121 | 0.0008925 | | | |
| WRC | $sqrtBAI_{kt} = \beta_0 + \beta_1 Site + \beta_2 BA_{jkt} + \beta_3 AprilP_{jt} + \beta_4 SummerGDD_{jt} + \beta_5 AprilGDD_{jt} + \eta_{ij} t + c_{jk} + \varepsilon_{ikt}$ | AprilP | 0.0014635 | 0.0007155 | 0.533 | 0.907 | 0.483 |
| | | SummerGDD | 0.0004261 | 0.0002249 | | | |
| | | AprilGDD | 0.0035826 | 0.001321 | | | |
| WRSP | $sqrtBAI_{kt} = \beta_0 + \beta_1 Site + \beta_2 BA_{jkt} + \beta_3 JulyP_{jt} + \beta_4 MayVPDmean_{jt} + \eta_{ij} t + c_{jk} + \varepsilon_{jkt}$ | JulyP | 0.0029655 | 0.0016821 | 0.492 | 1.487 | 0.781 |
| | | MayVPDmean | -0.8685165 | 0.2929892 | | | |
| WVPP | $sqrtBAI_{kt} = \beta_0 + \beta_1 Site + \beta_2 BA_{jkt} + \beta_3 SpringP_{jt} + \beta_4 MayVPDmean_{jt} + \beta_5 AprilGDD_{jt} + \eta_{ij} t + c_{jk} + \varepsilon_{ikt}$ | SpringP | 0.0011267 | 0.0003093 | 0.218 | 1.230 | 0.718 |
| | | MayVPDmean | -0.6372394 | 0.3037032 | | | |
| | | AprilGDD | 0.0015975 | 0.0007654 | | | |
| WWP | $sqrtBAI_{kt} = \beta_0 + \beta_1 Site + \beta_2 BA_{jkt} + \beta_3 SummerGDD_{jt} + \eta_{ij} t + c_{jk} + \varepsilon_{jkt}$ | SummerGDD | 0.0004765 | 0.0002584 | 0.389 | 1.278 | 0.517 |

Poudel et al. (2019):

$$DF = e^{(-9.5504 + 1.7420 * \log(DBH) + 1.0212 * \log HT)} * 35.315$$

$$GF = e^{(-9.1826 + 1.5459 * \log(DBH) + 1.1730 * \log HT)} * 35.315$$

$$GS = e^{(-10.7638 + 2.0497 * \log(DBH) + 0.9477 * \log HT)} * 35.315$$

$$SSP = e^{(-10.1366 + 1.8640 * \log(DBH) + 1.0835 * \log HT)} * 35.315$$

$$WH = e^{(-9.9763 + 1.9583 * \log(DBH) + 0.9254 * \log HT)} * 35.315$$

$$WRC = e^{(-9.5468 + 2.0363 * \log(DBH) + 0.6601 * \log HT)} * 35.315$$

$$WRSP = e^{(-10.1366 + 1.8640 * \log(DBH) + 1.0835 * \log HT)} * 35.315$$

$$WVPP = e^{(-10.5808 + 2.1110 * \log(DBH) + 0.9126 * \log HT)} * 35.315$$

$$WWP = e^{(-9.5997 + 1.4028 * \log(DBH) + 1.4115 * \log HT)} * 35.315$$

Table S.3.1: Species-specific models for BAI ($cm^2$ $year^{-1}$), where: $sqrtBAI_{jkt}$ for each species is the square root of the annual BAI of the $k^{th}$ tree in $j^{th}$ site on $t^{th}$ year; $\beta_1$Site is the fixed effect on the response for $j^{th}$ site; $\beta_2 BA_{ijkt}$ is the basal area of the $k^{th}$ tree in $j^{th}$ site on $t^{th}$ year; $\beta_4$ through $\beta_6$ is the fixed effect of climate variables on the response in $j^{th}$ site on $t^{th}$ year; $c_{jk} \sim Normal(0, \sigma^2_{tree})$ is the random effect of the $jk^{th}$ tree; and $\epsilon_{jkt} \sim Normal(0, \Sigma)$ where $\Sigma$ is defined following an AR(1) structure.

P: annual precipitation (mm); SpringP: spring precipitation (mm); AprilP: April precipitation (mm); JulyP: July precipitation (mm); AugustP: August precipitation (mm); PDSI: annual PDSI value; VPDmax: annual maximum VPD (kPa); MayVPDmean: mean of May VPD (kPa); Tmin: annual minimum temperature (C°); MayTmin: May minimum temperature (C°); JulyTmin: July minimum temperature (C°); SummerGDD: summer Growing Degree days; and AprilGDD: April Growing Degree days. All parameter estimates associated with climate variables were significant ($P < 0.05$).

SE: standard error; $R^2_{GLMM}$: Conditional coefficient of determination for generalized mixed-effect models, which interpreted as the variation explained by the entire model (Nakagawa & Schielzeth, 2013); RMSE: root mean square error (mm); and CV: coefficient of determination.

| **Annual LW basal Area Increment** | | | | | | | |
|---|---|---|---|---|---|---|---|
| **Species** | **Model** | **Parameter** | **Parameter Estimate** | **SE** | **$R^2_{GLMM}$** | **RMSE** | **CV% OG** |
| DF | $sqrtLWBAI_{kt} = \beta_0 + \beta_1 Site + \beta_2 BA_{jkt} + \beta_3 SummerP_{jt} + \beta_4 P_{jt} + \beta_5 VPDmax_{jt} + \beta_6 AprilGDD_{jt} + \eta_{ij} t + c_{jk} + \varepsilon_{jkt}$ | SummerP | 0.0007901 | 0.00028091 | 0.366 | 2.559 | 0.544 |
| | | P | 0.0001852 | 0.00005312 | | | |
| | | VPDmax | -0.2664699 | 0.06941426 | | | |
| | | AprilGDD | 0.0020617 | 0.00055206 | | | |
| GF | $sqrtLWBAI_{kt} = \beta_0 + \beta_1 Site + \beta_2 BA_{jkt} + \beta_3 SummerP_{jt} + \beta_4 AprilP_{jt} + \beta_5 JulyTmin_{jt} + \beta_6 VPDmax_{jt} + \eta_{ij} t + c_{jk} + \varepsilon_{jkt}$ | SummerP | 0.00077373 | 0.00021931 | 0.378 | 2.969 | 0.755 |
| | | AprilP | 0.00061128 | 0.00028432 | | | |
| | | JulyTmin | 0.08487594 | 0.02089192 | | | |
| | | VPDmax | -0.2726941 | 0.06884206 | | | |
| GS | $sqrtLWBAI_{kt} = \beta_0 + \beta_1 Site + \beta_2 BA_{jkt} + \beta_3 SummerP_{jt} + \beta_4 VPDmax_{jt} + \eta_{ij} t + c_{jk} + \varepsilon_{jkt}$ | SummerP | 0.0006111 | 0.00025639 | 0.191 | 2.402 | 0.641 |
| | | VPDmax | -0.1913911 | 0.07009608 | | | |
| LC | $sqrtLWBAI_{kt} = \beta_0 + \beta_1 Site + \beta_2 BA_{jkt} + \beta_3 VPDmeanJuly_{jt} + \beta_4 JulyP_{jt} + \eta_{ij} t + c_{jk} + \varepsilon_{jkt}$ | VPDmeanJuly | -0.4561882 | 0.16177538 | 0.235 | 1.711 | 0.712 |
| | | JulyP | 0.0074324 | 0.00252357 | | | |
| POC | $sqrtLWBAI_{kt} = \beta_0 + \beta_1 Site + \beta_2 BA_{jkt} + \beta_3 SummerP_{jt} + \beta_4 JulyP_{jt} + \eta_{ij} t + c_{jk} + \varepsilon_{jkt}$ | SummerP | 0.0006631 | 0.00029794 | 0.557 | 1.593 | 0.594 |
| | | JulyP | 0.0034888 | 0.00161945 | | | |
| SSP | $sqrtLWBAI_{kt} = \beta_0 + \beta_1 Site + \beta_2 BA_{jkt} + \beta_3 SummerP_{jt} + \beta_4 P_{jt} + \beta_5 VPDmax_{jt} + \eta_{ij} t + c_{jk} + \varepsilon_{jkt}$ | SummerP | 0.0009017 | 0.00023452 | 0.456 | 1.253 | 0.602 |
| | | P | 0.0001469 | 0.00004404 | | | |
| | | VPDmax | -0.1009787 | 0.05092215 | | | |
| WH | $sqrtLWBAI_{kt} = \beta_0 + \beta_1 Site + \beta_2 BA_{jkt} + \beta_3 SummerP_{jt} + \beta_4 SpringP_{jt} + \beta_5 Tmin_{jt} + \eta_{ij} t + c_{jk} + \varepsilon_{jkt}$ | SummerP | 0.0011717 | 0.00025362 | 0.359 | 1.758 | 0.617 |
| | | SpringP | 0.0005316 | 0.00021849 | | | |
| | | Tmin | 0.0741518 | 0.03712871 | | | |
| WRC | $sqrtLWBAI_{kt} = \beta_0 + \beta_1 Site + \beta_2 BA_{jkt} + \beta_3 SummerP_{jt} + \beta_4 AprilGDD_{jt} + \beta_5 VPDmax_{jt} + \beta_6 AprilP_{jt} + \beta_7 VPDmeanMay_{jt} + \beta_8 RAD_{jt} + \beta_9 ummerGDD_{jt} + \eta_{ij} t + c_{jk} + \varepsilon_{jkt}$ | SummerP | 0.000797 | 0.000235 | 0.582 | 0.809 | 0.538 |
| | | AprilGDD | 0.006454 | 0.0009317 | | | |
| | | VPDmax | -0.459168 | 0.1134382 | | | |
| | | AprilP | 0.001581 | 0.0003164 | | | |
| | | VPDmeanMay | -1.46338 | 0.3021203 | | | |
| | | RAD | 0.030857 | 0.0051882 | | | |
| | | SummerGDD | 0.001714 | 0.0002864 | | | |
| WRSP | $sqrtLWBAI_{kt} = \beta_0 + \beta_1 Site + \beta_2 BA_{jkt} + \beta_3 JulyP_{it} + \beta_4 AugP_{it} + \eta_{ij} t + c_{jk} + \varepsilon_{jkt}$ | JulyP | 0.0019959 | 0.00109563 | 0.686 | 1.352 | 0.603 |
| | | AugustP | 0.0018003 | 0.00077003 | | | |
| WVPP | $sqrtLWBAI_{kt} = \beta_0 + \beta_1 Site + \beta_2 BA_{jkt} + \beta_3 VPDmax_{jt} + \beta_4 AugP_{jt} + \eta_{ij} t + c_{jk} + \varepsilon_{jkt}$ | VPDmax | -0.2922751 | 0.06242276 | 0.311 | 1.861 | 0.598 |
| | | AugustP | 0.0029628 | 0.00102827 | | | |

| | | | | | | | |
|---|---|---|---|---|---|---|---|
| WWP | $sqrtLWBAI_{kt}$ = $\beta_0 + \beta_1 Site + \beta_2 BA_{jkt} + \beta_3 SummerGDD_{jt} + + \eta_{ij}t + c_{jk} + \varepsilon_{jkt}$ | SummerGDD | 0.00059655 | 0.00014818 | 0.423 | 1.875 | 0.570 |

Table S.3.2: Species-specific models for LW BAI ($cm^2\ year^{-1}$), where: $sqrtLWBAI_{jkt}$ for each species is the square root of the annual LW basal area increment of the $k^{th}$ tree in $j^{th}$ site on $t^{th}$ year; $\beta_1$Site is the fixed effect on the response for $j^{th}$ site; $\beta_2 BA_{ijkt}$ is the basal area of the $k^{th}$ tree in $j^{th}$ site on $t^{th}$ year; $\beta_4$ through $\beta_8$ is the fixed effect of climate variables on the response in $j^{th}$ site on $t^{th}$ year; $c_{jk} \sim Normal(0, \sigma^2_{tree})$ is the random effect of the $jk^{th}$ tree; and $\epsilon_{jkt} \sim Normal(0, \Sigma)$ where $\Sigma$ is defined following an AR(1) structure.

P: annual precipitation (mm); SpringP: spring precipitation (mm); SummerP: summer precipitation (mm); AprilP: April precipitation (mm); JulyP: July precipitation (mm); AugustP: August precipitation (mm); VPDmax: annual maximum VPD (kPa); MayVPDmean: mean of May VPD (kPa); JulyVPDmean: mean of July VPD(kPa); Tmin: annual minimum temperature (C°); JulyTmin: July minimum temperature (C°); JulyTmin: July minimum temperature (C°); SummerGDD: summer Growing Degree days; AprilGDD: April Growing Degree days; and RAD: mean radiation (MJ/m²/month). All parameter estimates associated with climate variables were significant ($P < 0.05$).

SE: standard error; $R^2_{GLMM}$: Conditional coefficient of determination for generalized mixed-effect models, which interpreted as the variation explained by the entire model (Nakagawa & Schielzeth, 2013); RMSE: root mean square error (mm); and CV: coefficient of determination.

| **Annual LW Percentage** | | | | | | | |
|---|---|---|---|---|---|---|---|
| **Species** | **Model** | **Parameter** | **Parameter Estimate** | **SE** | **$R^2_{GLMM}$** | **RMSE** | **CV** |
| DF | $LW_{jkt}$ = $\beta_0 + \beta_1 Site + \beta_2 BA_{jkt} + \beta_3 SummerP_{jt} + \beta_4 P_{jt} + \eta_{ij}t + c_{jk} + \varepsilon_{jkt}$ | SummerP | 0.022865 | 0.0064459 | 0.531 | 9.364 | 0.277 |
| | | P | 0.004313 | 0.001237 | | | |
| GF | $GFLW_{jkt}$ = $\beta_0 + \beta_1 Site + \beta_2 BA_{jkt} + \beta_3 P_{jt} + \eta_{ij}t + c_{jk} + \varepsilon_{jkt}$ | P | -0.002232 | 0.001131 | 0.048 | 11.738 | 0.469 |
| GS | $LW_{jkt}$ = $\beta_0 + \beta_1 Site + \beta_2 BA_{jkt} + \beta_3 P_{jkt} + \beta_4 PDSI_{jt} + \beta_5 SpringP_{jt} + \beta_6 AugP_{jt} + \eta_{ij}t + c_{jk} + \varepsilon_{jkt}$ | P | -0.002826 | 0.0011304 | 0.126 | 7.046 | 0.450 |
| | | PDSI | 0.76897 | 0.3900844 | | | |
| | | SpringP | -0.012198 | 0.0045691 | | | |
| | | AugP | 0.036373 | 0.0169568 | | | |
| LC | $LW_{jkt}$ = $\beta_0 + \beta_1 Site + \beta_2 BA_{jkt} + \beta_3 SpringP_{jt} + \beta_4 AprilP_{jt} + \beta_5 SummerP_{jt} + \beta_6 AugP_{jt} + \eta_{ij}t + c_{jk} + \varepsilon_{jkt}$ | SpringP | -0.029973 | 0.008763 | 0.118 | 10.530 | 0.568 |
| | | AprilP | 0.02982 | 0.0116138 | | | |
| | | SummerP | 0.02875 | 0.009319 | | | |
| | | AugP | -0.166881 | 0.031556 | | | |
| POC | $LW_{jkt}$ = $\beta_0 + \beta_1 Site + \beta_2 BA_{jkt} + \beta_3 SpringP_{jt} + \beta_4 AprilP_{jt} + \beta_5 SummerP_{jt} + \beta_6 AugP_{jt} + \eta_{ij}t + c_{jk} + \varepsilon_{jkt}$ | SpringP | -0.027461 | 0.0077795 | 0.283 | 9.587 | 0.512 |
| | | AprilP | 0.029892 | 0.0104952 | | | |
| | | SummerP | 0.03323 | 0.0080963 | | | |
| | | AugP | -0.118666 | 0.0296833 | | | |
| SSP | $LW_{jkt}$ = $\beta_0 + \beta_1 Site + \beta_2 BA_{jkt} + \beta_3 P_{jkt} + \beta_4 PDSI_{jt} + \beta_5 VPDmeanMay_{jt} + \eta_{ij}t + c_{jk} + \varepsilon_{jkt}$ | P | -0.002959 | 0.001612 | 0.135 | 9.623 | 0.461 |
| | | PDSI | 1.331994 | 0.498196 | | | |
| | | VPDmeanMay | 24.214492 | 5.282926 | | | |
| WH | $LW_{jkt}$ = $\beta_0 + \beta_1 Site + \beta_2 BA_{jkt} + \beta_3 AugP_{jt} + \beta_4 VPDmax_{jt} + \eta_{ij}t + c_{jk} + \varepsilon_{jkt}$ | AugP | 0.092083 | 0.0203038 | 0.376 | 7.545 | 0.420 |
| | | VPDmax | 2.554468 | 1.1447343 | | | |
| WRC | $LW_{jkt}$ = $\beta_0 + \beta_1 Site + \beta_2 BA_{jkt} + \beta_3 P_{jkt} + \beta_4 AugP_{jt} + \beta_5 RH_{jt} + \eta_{ij}t + c_{jk} + \varepsilon_{jkt}$ | AugP | 0.12152 | 0.037264 | 0.174 | 7.264 | 0.509 |
| | | RH | -0.31994 | 0.158698 | | | |
| WRSP | $LW_{jkt}$ = $\beta_0 + \beta_1 Site + \beta_2 BA_{jkt} + \beta_3 AugP_{jt} + \beta_4 RH_{jt} + \eta_{ij}t + c_{jk} + \varepsilon_{jkt}$ | AugP | 0.08415 | 0.02666 | 0.133 | 11.987 | 0.551 |
| | | RH | -0.4417 | 0.222231 | | | |
| WVPP | $LW_{jkt}$ = $\beta_0 + \beta_1 Site + \beta_2 BA_{jkt} + \beta_3 JulyP_{jt} + \eta_{ij}t + c_{jk} + \varepsilon_{jkt}$ | JulyP | -0.091894 | 0.0358379 | 0.085 | 10.089 | 0.367 |
| WWP | | P | -0.005704 | 0.002137 | | | |

| | | | | | | | |
|---|---|---|---|---|---|---|---|
| | $LW_{jkt}$ = $\beta_0 + \beta_1 Site + \beta_2 BA_{ikt} + \beta_3 P_{ikt} + \beta_4 PDSI_{it} + \beta_5 AugP_{jt} + \beta_6 VPDmeanMay_{jt} + \eta_{lj}t + c_{jk} + \varepsilon_{jkt}$ | PDSI | 1.584779 | 0.600533 | 0.081 | 9.132 | 0.468 |
| | | AugP | 0.081965 | 0.03095 | | | |
| | | VPDmeanMay | 17.836496 | 7.519011 | | | |

Table _: Species-specific models for annual LW percentage (%), where: $LW_{jkt}$ for each species is the annual LW percentage of the $k^{th}$ tree in $j^{th}$ site on $t^{th}$ year; $\beta_1$Site is the fixed effect on the response for $j^{th}$ site; $\beta_2 BA_{ijkt}$ is the basal area of the $k^{th}$ tree in $j^{th}$ site on $t^{th}$ year; $\beta_3$ through $\beta_6$ is the fixed effect of climate variables on the response in $j^{th}$ site on $t^{th}$ year; $c_{jk} \sim Normal(0, \sigma^2_{tree})$ is the random effect of the jk$^{th}$ tree; and $\epsilon_{jkt} \sim Normal(0, \Sigma)$ where $\Sigma$ is defined following an AR(1) structure.

P: annual precipitation (mm); SpringP: spring precipitation (mm); SummerP: summer precipitation (mm); AprilP: April precipitation (mm); JulyP: July precipitation (mm); AugustP: August precipitation (mm); VPDmax: annual maximum VPD (kPa); MayVPDmean: mean of May VPD (kPa); and RH: annual relative humidity (%). All parameter estimates associated with climate variables were significant ($P < 0.05$).

SE: standard error; $R^2_{GLMM}$: Conditional coefficient of determination for generalized mixed-effect models, which interpreted as the variation explained by the entire model (Nakagawa & Schielzeth, 2013); RMSE: root mean square error (mm); and CV: coefficient of determination.

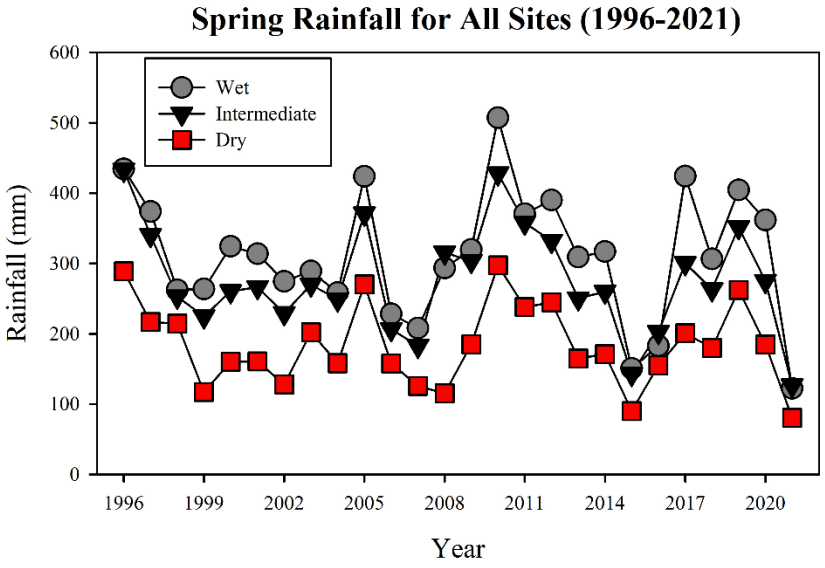


Figure S.3.1: Sum of spring rainfall (mm) from 1996 to 2021 for the Huffman (wet), Underhill (intermediate), and Campbell (dry) sites.

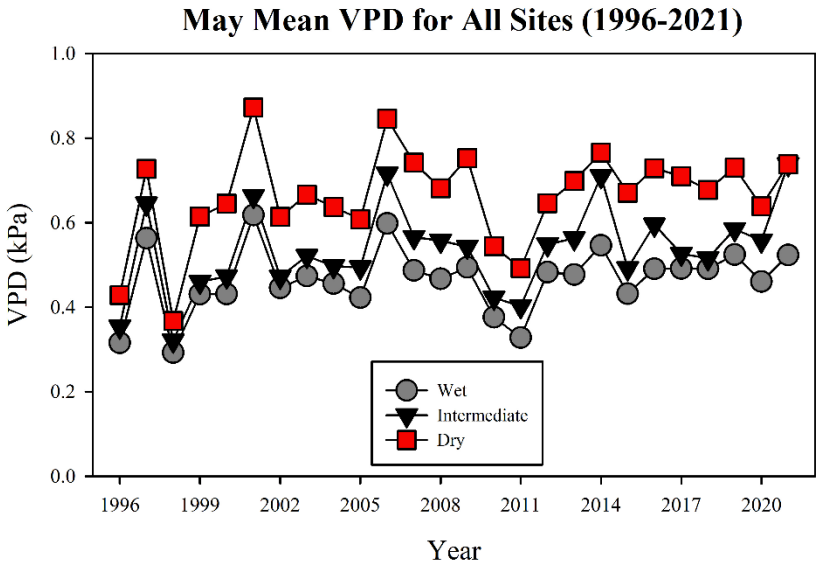


Figure S.3.2: Average of May VPD (kPa) from 1996 to 2021 for the Huffman (wet), Underhill (intermediate), and Campbell (dry) sites.

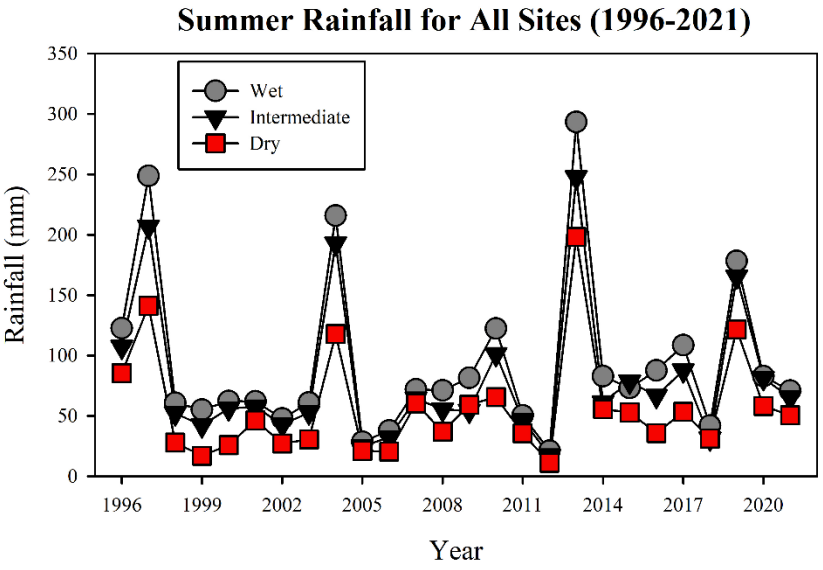


Figure S.3.3: Sum of summer rainfall (mm) from 1996 to 2021 for the Huffman (wet), Underhill (intermediate), and Campbell (dry) sites.

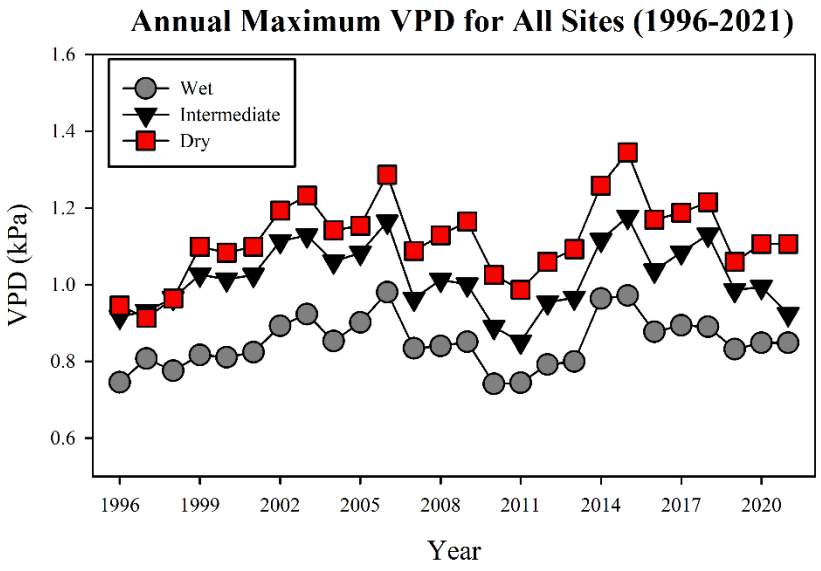


Figure S.3.4: Annual maximum VPD (kPa) from 1996 to 2021 for the Huffman (wet), Underhill (intermediate), and Campbell (dry) sites.

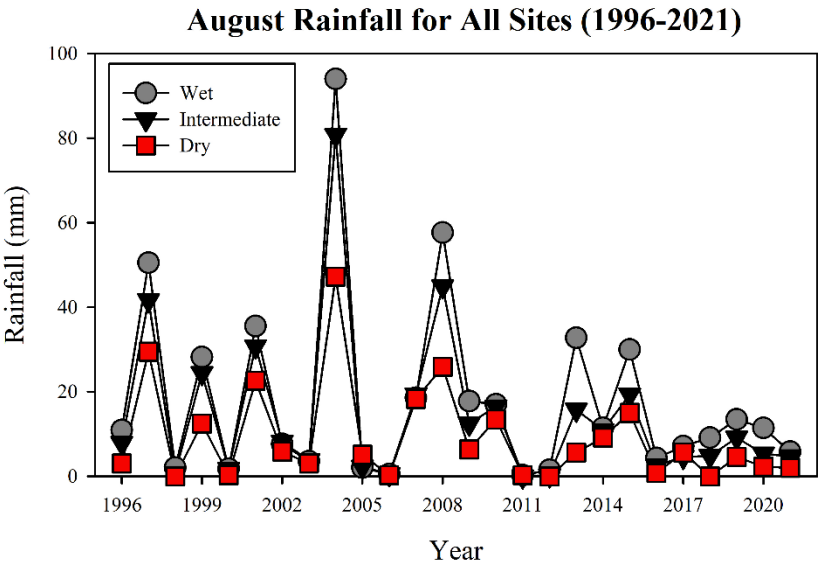


Figure S.3.5: Sum of August rainfall (mm) from 1996 to 2021 for the Huffman (wet), Underhill (intermediate), and Campbell (dry) sites.

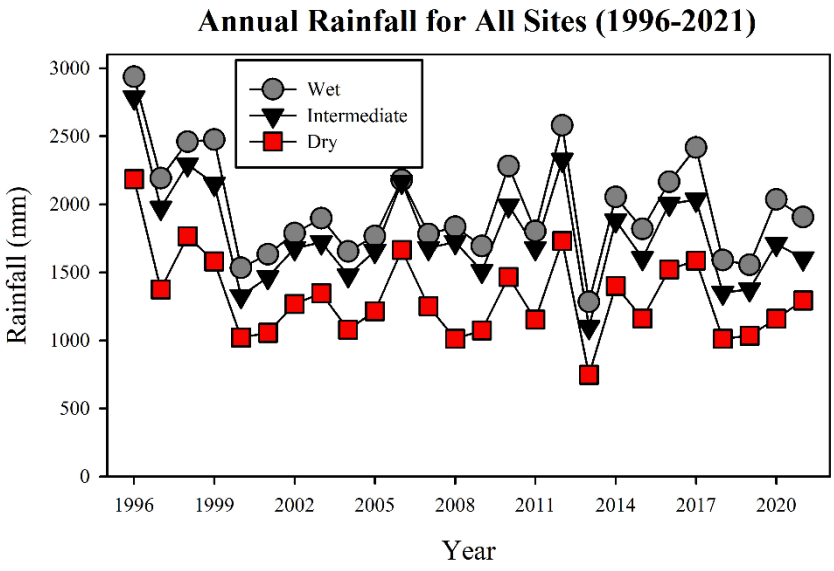


Figure S.3.6: Sum of annual rainfall (mm) from 1996 to 2021 for the Huffman (wet), Underhill (intermediate), and Campbell (dry) sites.